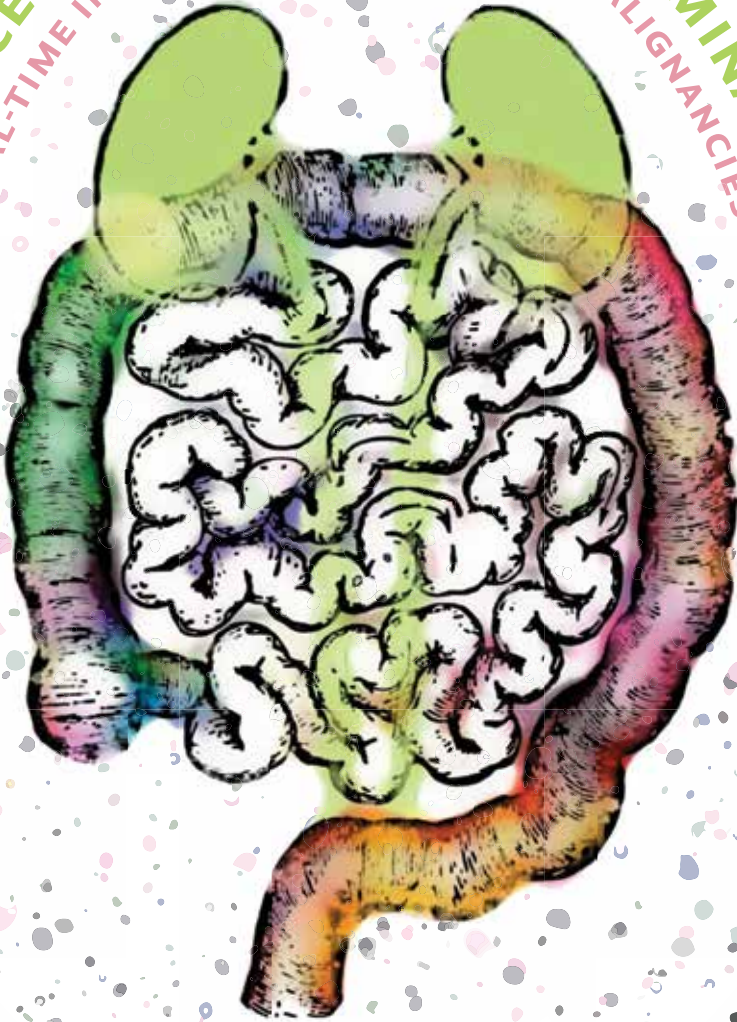
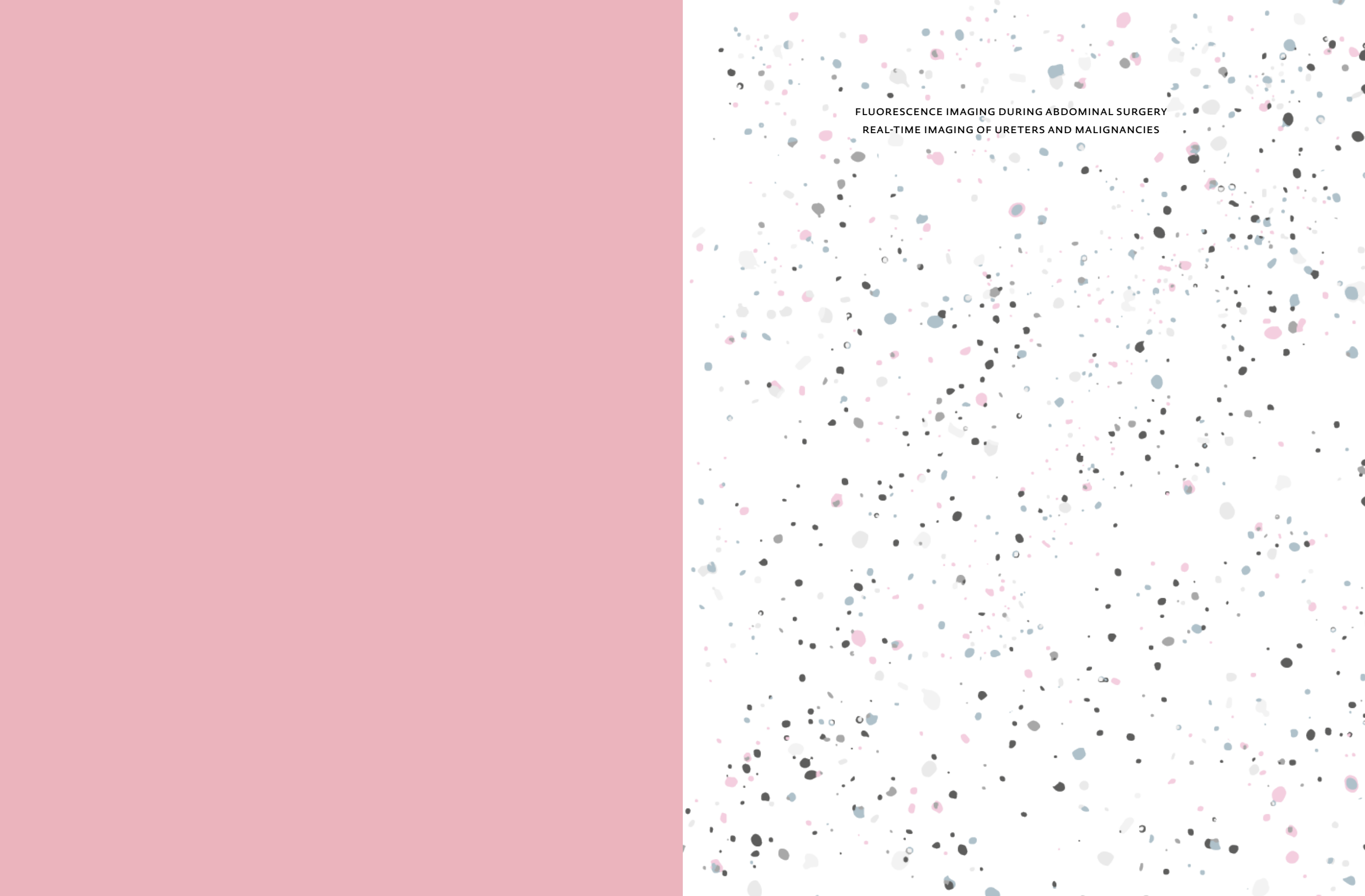


FLUORESCENCE IMAGING DURING ABDOMINAL SURGERY  
REAL-TIME IMAGING OF URETERS AND MALIGNANCIES



Kim Samita de Valk



FLUORESCENCE IMAGING DURING ABDOMINAL SURGERY  
REAL-TIME IMAGING OF URETERS AND MALIGNANCIES

This thesis is dedicated to my parents.  
For their endless love, support and encouragement.

# **FLUORESCENCE IMAGING DURING ABDOMINAL SURGERY**

## **REAL-TIME IMAGING OF URETERS AND MALIGNANCIES**

© K.S. de Valk

### DESIGN

Caroline de Lint, Voorburg (caro@delint.nl)

### COVER IMAGE

Marja de Valk-Terhoeve

### FINANCIAL SUPPORT

The publication of this thesis was financially supported by the foundation  
Centre for Human Drug Research (CHDR), Leiden, the Netherlands

*All rights reserved. No part from this thesis may be reproduced, distributed or transmitted  
in any form or by any means, without prior written permission of the author.*

### PROEFSCHRIFT

ter verkrijging van de graad van doctor  
aan de Universiteit Leiden, op gezag van  
rector magnificus prof.dr.ir. H. Bijl,  
volgens besluit van het college voor promoties  
te verdedigen op dinsdag 1 juni 2021  
klokke 15:00 uur

### DOOR

Kim Samita de Valk  
geboren te Bangkok, Thailand in 1989


PROMOTOR  
Prof. dr. J. Burggraaf

CO-PROMOTOR  
Dr. A.L. Vahrmeijer

LEDEN PROMOTIECOMMISSIE  
Prof. dr. L.F. de Geus-Oei  
Prof. dr. C. Verhoef (*Erasmus Medisch Centrum, Rotterdam*)  
Dr. P.G. Doornebosch (*IJsselland Ziekenhuis, Capelle a/d IJssel*)

Chapter I	Introduction and thesis outline	7
<b>PART 1      CLINICAL TRANSLATION OF ZWITTERIONIC AGENTS</b>		
Chapter II	The clinical translation of novel near-infrared fluorophores for fluorescence guided surgery	15
Chapter III	A zwitterionic near-infrared fluorophore for real-time ureter identification during laparoscopic abdominopelvic surgery	25
Chapter IV	First-in-human assessment of CRGD-ZW800-1, a zwitterionic, integrin-targeted, near-infrared fluorescent peptide in colon carcinoma	41
<b>PART 2      FLUORESCENCE IMAGING WITH SGM-101</b>		
Chapter V	Dose-finding study of a CEA-targeting agent, SGM-101, for intraoperative fluorescence imaging of primary and recurrent colorectal cancer	65
Chapter VI	Carcinoembryonic antigen-specific, fluorescent image-guided cytoreductive surgery with hyperthermic intraperitoneal chemotherapy for metastatic colorectal cancer	85
Chapter VII	The quantification of the pharmacokinetic and pharmacodynamic properties of SGM-101 in colorectal and pancreatic patients in a phase I/II study	93
<b>PART 3      SUMMARY AND APPENDICES</b>		
Chapter VIII	Summary and discussion	109
Chapter IX	Dutch summary (Nederlandse samenvatting)	117
	Curriculum Vitae	123
	List of publications	124





Chapter I

**INTRODUCTION AND  
THESIS OUTLINE**

## NEAR-INFRARED FLUORESCENCE IMAGING

Cancer is one of the leading causes of death worldwide.<sup>1-3</sup> Despite significant expansion and improvement of treatment options, surgery remains the cornerstone treatment for solid cancers. However, there are many complexities to tumor resections that require further evaluation and/or improvement. Oncologic surgeons rely on visual and palpatory assessments to guide themselves during resections for complete tumor removal. However, the infiltrative nature of cancerous tissue or the implementation of neoadjuvant treatment, such as chemoradiotherapy, can make the differentiation between cancerous and normal tissue more challenging.<sup>4</sup> The lack of adequate differentiation can therefore lead to complicated or incomplete tumor resections, resulting in residual tumor cells at the resection margins, consequently leading to disease recurrence.<sup>6</sup> Additionally, morbidity after surgery can also depend on the extent of damage to vital structures, such as nerves, ureters and bile ducts. The use of minimal invasive surgery (i.e. laparoscopic and robotic) has increased over the years, which has proven to decrease morbidity rates, yet iatrogenic damage sometimes remains inevitable.<sup>5</sup> On the other hand, minimal invasive techniques have also formed new surgical challenges, due to the absence of tactile feedback and limitations in the field of view. Therefore, improving the visual feedback in minimal invasive procedures with near-infrared (NIR) light can offer a solution. Fluorescence guided surgery is an ideal tool to assist surgeons in delineating cancerous tissue and detect vital structures in real-time, to help improve oncological surgical outcomes and the preservation of vital structures.

The use of NIR light (wavelength 700-900 nm) during surgery is particularly interesting as it has a penetration depth up to 1 cm with minimal autofluorescence. In order to enable the use of fluorescence during surgery, two external sources are needed: a NIR fluorescence imaging system (an open system or integrated minimal invasive system) and a fluorescent agent (targeted or non-targeted). The fluorescent agent needs to be administered to the patient prior to imaging. Depending on the clearance pattern and pharmacokinetic profile of the agent, the interval between administration and imaging can range from minutes to days. During surgery, an open NIR light source can be positioned above the patient with a working distance of approximately 15-20 cm, or the NIR light can be encased within the laparoscope for minimal invasive procedures. The emitted fluorescence can then simultaneously be displayed in images (color, overlay and NIR) on the camera system screens in real-time for the surgeons to interpret. Various commercially available NIR imaging systems have already been developed, which can be used during open and minimal invasive

laparoscopic or robotic procedures. This unique technology provides visual enhancement of vital structures or cancerous tissue to equip surgeons with illustrative information for complete removal of tumor tissue, lymph nodes or metastases and better distinction of vital structures to avoid inadvertent injury.<sup>7</sup>

In recent years, the number of new studies involving novel fluorescent agents in oncologic patient populations has steadily been increasing. One of the most challenging aspects of this research is the clinical translation and adoption of fluorescence into standard of care, as it requires strict regulatory assessments to ensure patient safety. To fulfill these regulatory requirements, studies with novel agents are often centralized in specialized centers where the safety and efficacy are primarily studied. For this research and thesis, a unique collaboration has been set up between the academic hospital Leiden University Medical Center (LUMC) and the Centre for Human Drug Research (CHDR) in Leiden, to ensure an optimal roadmap for the clinical translation of fluorescent agents. CHDR is a dedicated research center with the means and knowledge to perform early phase (including first-in-human) pharmacological studies in a safe and controlled environment. LUMC, on the other hand, has the most experience in conducting oncologic trials with fluorescence imaging agents and has a certified GMP facility for the development of novel agents.

This thesis describes the intraoperative fluorescent imaging during abdominal surgery with non-targeted and tumor-targeted fluorescent agents for the enhancement and detection of the ureters and gastrointestinal tumors, colorectal cancer in particular, with the use of dedicated open and minimal invasive NIR camera systems.

## THESIS OUTLINE

This thesis is divided into three parts:

**Part I** of the thesis describes the clinical translation of novel zwitterionic fluorescent agents. Chapter 2 provides an illustrative overview of the roadmap towards clinically implementing novel agents into the clinic. Chapter 3 presents a study where the clinical translation of the novel non-targeted zwitterionic dye, ZW800-1, is described with its ability to visualize the ureters during laparoscopic abdominopelvic surgery. Chapter 4 describes the clinical translation and validation of the zwitterionic tumor-targeted fluorescent agent, CRGD-ZW800-1, for the intraoperative fluorescence imaging of colon cancer.

**Part II** of the thesis focuses on colorectal cancer imaging with a dedicated carcinoembryonic antigen (CEA) specific fluorescent agent, SGM-101. Chapter

5 describes the intraoperative fluorescence imaging of primary and recurrent colorectal cancer with SGM-101, whereas Chapter 6 explores the use of SGM-101 in patients with peritoneal metastasized colorectal cancer during cytoreductive surgery and hyperthermic intraperitoneal chemotherapy (HIPEC). Chapter 7 sightsees the pharmacokinetics of SGM-101, which have not been described before.

**Part III** concludes the thesis with a summary, general discussion and appendices.

## REFERENCES

- 1 Arnold M, Sierra MS, Laversanne M, Soerjomataram I, Jemal A, Bray F. Global patterns and trends in colorectal cancer incidence and mortality. *Gut*. 2017;66(4):683-691.
- 2 Navarro M, Nicolas A, Ferrandez A, Lanas A. Colorectal cancer population screening programs worldwide in 2016: An update. *World J Gastroenterol*. 2017;23(20):3632-3642.
- 3 Torre LA, Bray F, Siegel RL, Ferlay J, Lortet-Tieulent J, Jemal A. Global cancer statistics, 2012. *CA Cancer J Clin*. 2015;65(2):87-108.
- 4 Olson MT, Ly QP, Mohs AM. Fluorescence Guidance in Surgical Oncology: Challenges, Opportunities, and Translation. *Mol Imaging Biol*. 2019;21(2):200-218.
- 5 Andersen P, Andersen LM, Iversen LH. Iatrogenic ureteral injury in colorectal cancer surgery: a nationwide study comparing laparoscopic and open approaches. *Surg Endosc*. 2015;29(6):1406-1412.
- 6 Wibe A, Rendedal PR, Svensson E, et al. Prognostic significance of the circumferential resection margin following total mesorectal excision for rectal cancer. *Br J Surg*. 2002;89(3):327-334.
- 7 Vahrmeijer AL, Hutteman M, van der Vorst JR, van de Velde CJ, Frangioni JV. Image-guided cancer surgery using near-infrared fluorescence. *Nat Rev Clin Oncol*. 2013;10(9):507-518.

PART 1

**CLINICAL  
TRANSLATION  
OF NOVEL  
ZWITTERIONIC  
AGENTS**

Chapter II

**THE CLINICAL TRANSLATION  
OF NOVEL NEAR-INFRARED  
FLUOROPHORES FOR  
FLUORESCENCE GUIDED SURGERY**

*Adapted from Proc. SPIE 10862,  
Molecular-Guided Surgery: Molecules, Devices,  
and Applications V, 10862oW. 2019 Mar  
doi: 10.1117/12.2516413*

KS de Valk<sup>1,2</sup>, AL Vahrmeijer<sup>1,2</sup>

1. Leiden University Medical Center, Leiden, NL
2. Centre for Human Drug Research, Leiden, NL

## ABSTRACT

Near-infrared fluorescence imaging is a promising intraoperative technique for real-time visualization of vital structures and tumor tissue during surgery. This manuscript describes the applications and limitations of NIR fluorescence imaging, and provides a general overview of two novel fluorescent agents and the process of clinical translation. The process of clinical translation of novel fluorescent agents is an essential part in the evolution of NIR fluorescence guided surgery. Treatments and surgeries are constantly advancing, which can occasionally cause challenges or difficulties for the surgeons. Poor visualization of tumors during surgery is one of the major challenges surgeons often face in oncologic patients, mainly due to the improved neo-adjuvant treatment patients receive. In these cases, NIR fluorescence imaging with the use of tumor-targeted fluorescent agents can play an essential role and help provide better results or outcomes. However, before this technique can be implemented in standard of care, optimal tumor-targeted fluorescent agents need to be developed and novel fluorescent agents need to undergo a successful process of clinical translation.

## INTRODUCTION

Intraoperative near-infrared (NIR) fluorescence imaging is a novel technique that combines the use of a fluorescent agent with a dedicated NIR camera system, to allow real-time visualization of lymph nodes, tumor tissue and/or vital anatomic structures for surgical guidance.<sup>1</sup> NIR light ranges in the wavelength of 700-900 nanometers, is invisible to the naked eye and can only be detected with the use of a dedicated NIR imaging system, which are currently available from various commercial companies. Fluorescent agents are mainly administered intravenously at a given time prior or during surgery, in order to enable real-time imaging during surgery. The time of injection is dependent on the distribution factors of the specific agent. After injection the fluorescent agent is cleared by either the liver and/or kidneys and accumulates in the target (i.e. lymph node, tumor or vital structure) by either physiological processes (enhanced permeability and retention effect), specific targeting or through their clearance route.

Enhancing tumors or vital structures using NIR (tumor-targeted) fluorescent agents is an innovative technique that is currently under extensive development. Visual inspection and palpation have always been the principle methods in surgery to differentiate between different types of tissue or uncover vital structures. However, due to the technical advancements, such as the introduction of laparoscopes and robots, the palpation aspect in surgery has disap-

peared in most cases and surgeons are limited to visual inspection. With the use of NIR fluorescence imaging, tumor tissue and vital structures can be enhanced in real-time during surgery, to assist surgeons and conceivably improve surgical (i.e. improved radical resections and less iatrogenic damage of vital structures) and patient outcomes.

A known challenge in the field of fluorescence-guided surgery is the development of ideal NIR fluorophores. Currently, the only clinically available NIR fluorophores are methylene blue (MB) and indocyanine green (ICG), which have shown successful imaging results in different clinical studies.<sup>2-4</sup> However, both MB and ICG are non-targeted fluorophores and cannot easily be conjugated to other molecules, which is conversely an essential part for the development of tumor-targeted fluorescent agents. For advancement in the field of NIR fluorescence guided surgery, the following steps need to embrace the development and clinical translation of novel conjugatable fluorophores.

## NOVEL FLUORESCENT AGENTS

In the past years, several translational studies have been conducted with different kind of tumor-targeted fluorescent agents.<sup>5-10</sup> However the most optimal agent still needs to be found. Recently, a promising novel fluorophore has been introduced that could potentially cause a paradigm shift in fluorescent guided surgery.

### **zw800-1**

zw800-1 is a novel fluorophore, geometrically neutral, with unique and improved optical and biodistribution properties. This fluorophore emits light at a wavelength of approximately 788 nm, produces a high fluorescent signal with low non-specific binding and uptake in normal tissue and most importantly, it has a renal-exclusive clearance.<sup>11,12</sup> This extraordinary clearance route is a major step forward for reliable intraoperative imaging of gastrointestinal tumors. ICG, for example, is a well-known fluorophore and has been used in several different imaging indications, but has an exclusive hepatic clearance, which is often disadvantageous. This clearance route results in high uptake in the liver, often resulting in compromised imaging of the gastrointestinal tract (i.e. gastrointestinal tumors).<sup>3</sup>

zw800-1, however, was extensively investigated in small and large animal studies and showed that the renal-exclusive clearance route is particularly suitable for NIR fluorescence imaging of the ureters.<sup>12,13</sup> As iatrogenic ureteral injury is a feared complication of lower abdominal surgery, the clinical need

for improved visualization of these vital structures is sought.<sup>14-17</sup> Most of the ureteral injuries occur in patients during oncologic surgeries, as these patients frequently have increased risk factors, such as previous multiple surgeries and/or radiotherapy in the pelvic area. An urethral injury can often be restored when detected during the surgical procedure, however most injuries remain undetected and come to light a few days later resulting in long-term complications and morbidity. As avoiding damage to vital structures is of clinical importance during surgery, NIR fluorescence imaging with ZW800-1 may be a novelty for adequate and safe ureter mapping during surgery.

Regardless of the fact that ZW800-1 can be used to create a major step forward in the clinic with ureter imaging, the true promise of this novel fluorophore lies in the conjugation to targeting moieties. ZW800-1 can easily be conjugated to other molecules, creating endless possibilities for developing novel targeted ligands. These targets can either be tumor-specific molecules, known to be upregulated on malignant cells or tumor-associated tissue, or mechanisms involved in tumor survival such as neoangiogenic vessel formation or stroma. This concurrent advantage of ZW800-1 can potentially solve the longstanding problem of optimal targeted-fluorophore development.

#### **CRGD-ZW800-1**

Tumor visualization with NIR fluorescence imaging is an innovative and powerful surgical tool that can aid surgeons during oncologic surgery. Discriminating between malignant and benign tissue during surgery can occasionally be challenging as oncologic patients frequently receive neo-adjuvant chemo-radiotherapy, which often results in diminished tumor visibility during surgery. Different strategies, such as the use of tumor-targeting agents, are being explored to overcome the problem of poor tumor visibility.

The different hallmarks of cancer describe the underlying principles for the existence of cancer cells and can be used as a guideline for the development and identification of tumor-specific targets for fluorescence surgery. An effective target for NIR tumor imaging is integrins associated with neoangiogenesis, such as  $\alpha v \beta 3$ . The integrin  $\alpha v \beta 3$  is a receptor for RGD-containing proteins, and has shown to be upregulated in the process of angiogenesis.<sup>18,19</sup> Tumors larger than 1-2 cm depend on neoangiogenesis to acquire sufficient oxygen and nutrients to grow.<sup>20</sup> Therefore, integrin  $\alpha v \beta 3$  is highly and widely expressed on angiogenic endothelium, in both tumor stroma and tumor cells, and not on normal human tissue.<sup>21,22</sup>

CRGD is a peptide that recognizes and binds to the integrins associated with neoangiogenesis, therefore being a functional target to enable NIR imaging of

tumors. This resulted in a development of a novel tumor-targeted agent, CRGD-ZW800-1, which subsequently has already preclinically been validated *in vitro* on glioblastoma and colorectal cell-lines, and also in orthotopic mouse models with colorectal, breast, pancreatic and head-and-neck tumors.<sup>23</sup> According to the preclinical data this novel tumor-targeted fluorescent agent has the potential to become a useful agent for real-time intraoperative imaging of different cancer types.

## **CLINICAL TRANSLATION**

The pathway from invention to proof of efficacy, i.e. clinical adaption, of novel fluorescent agents is a costly and time-consuming path. For successful implementation in the clinic, several important steps need to be completed.

### **Development of a novel fluorescent agent**

The number one step is the development of a promising fluorescent agent. A clinical need to improve the intraoperative detection of either a vital structure or specific kind of malignancy during surgery is needed to initiate the development of a novel agent. Once this has been determined, the following vital step is identifying the specific target that will enable the NIR imaging. As previously mentioned the different hallmarks of cancer are often used as a guideline for the identification of tumor-specific targets. Subsequently, this target will need to be conjugated to a fluorescent dye to form a fluorescent agent suitable for NIR imaging. This novel agent will then undergo pilot testing in animal models to determine whether further translation is useful.

### **Preclinical studies**

Preclinical studies are of great importance, as it acts as a pilot study to determine whether further studies are consequential, and most importantly they are crucial in the step towards the clinic (i.e. humans) as the preclinical data is needed to validate and determine the toxicity of a novel agent before it gets exposed to humans. The studies provide useful information regarding the toxicology as well as the initial diagnostic value of a new agent. Once the novel agent has passed the validation process of whether it is useful for further employment, it will undergo the Good Manufacturing Practice (GMP) production so that it can be used in humans. The GMP batch will yet again undergo, more extensive, toxicity testing in animals.

For any first-in-human study, the toxicological profile is needed to determine a safe starting dose for humans. The guideline of the Food and Drug



Administration (FDA) is usually recommended, where the approach is based on the no-observed adverse event level (NOAEL) in animals, specifically in the most sensitive species in the preclinical toxicology study.<sup>24</sup> This dose is then calculated to the human equivalent dose using an algorithm and safety factors.

In most preclinical studies, especially for new therapeutic drugs for example, the maximum tolerated dose is also recognized. However, a major difference between therapeutic study drugs and fluorescent agents is that for fluorescent agents the maximal tolerated dose is not necessarily required to obtain the best result. The effect of a fluorescent agent is based on the ratio of fluorescence seen in the target (i.e. tumor) and the surrounding normal tissue, which is usually achieved with well below therapeutic dosage. The ratio between the target and the surrounding tissue is also known as the tumor/target-to-background ratio (TBR) and the higher the ratio, the more distinct the fluorescence of the target will be. Experience has shown that low doses of a fluorescent agent is often enough to achieve an optimal effect, as high doses frequently lead to unwanted excessive background fluorescence, resulting in low TBRs. Therefore, in studies with fluorescent agents a more informative concept can be applied; the concept of the 'pharmacological active dose' where lower conservative doses can be employed to obtain the effective result.<sup>25</sup> With this concept possible irrelevant and unsafe high dosages can also be avoided.

### **Phase I: First-in-human studies**

After completion of the preclinical studies and approval by the medical ethics committee, the first major step in the clinic can be performed, which is the exposure of the novel agent in humans. First-in-human studies with novel fluorescent agents can be performed in either healthy volunteers or on a selected group of the target patients. However, a first-in-human study in healthy volunteers is superior to patients. The safety, tolerability, pharmacokinetics and pharmacodynamics of the fluorescent agent can adequately be studied in a controlled setting with a homogenous healthy subject population, based on medical screening, minimalizing contamination of safety data. Additionally, it prevents that vulnerable (oncologic) patient groups are being exposed to potentially harmful adverse events. Furthermore, easy escalation and de-escalation procedures can take place where different doses can be evaluated in a short period of time. Pharmacokinetics can also be assessed in more detail without having to interrupt standard of care procedures. Blood and urine samples can be obtained and fluorescence imaging of the skin, for example, can be performed at specified time points which provides valuable information regarding the time window of infusion to imaging (in the surgical setting) in a time and cost effective manner.

### **Phase II: Patient studies**

Once the novel agent has proven to be tolerable and safe in healthy volunteers, it can be implemented in patients to study the feasibility, optimal dose and timing of injection for suitable and optimum fluorescence imaging. The pharmacokinetic data obtained in healthy volunteers can be effective in designing an efficient patient study, as the pharmacokinetics in healthy volunteers can fairly predict the dose range and injection time range of the fluorescent agent for further assessment. This is crucial as the guiding principle in these studies is to avoid exposing too many (vulnerable) patients to suboptimal doses. Due to the frequently adequate dose and timing predications, patient studies can be completed in a timely manner while preserving safety of the patients. Blood and urine samples are often also collected in patients, which can substantiate the pharmacokinetic results in healthy volunteers. Furthermore, determining the efficacy of the fluorescent agent is also accomplished in patients, where the assessment and concordance of the fluorescence with the pathology results (histological evidence of tumor for example) is performed.

### **Phase III/IV trials**

Once the feasibility, efficacy, optimal dose and injection time has been established in the phase I/II studies, the translation of the agent is proceeded in a phase III trial. In this phase the goal is to acquire more proof for the benefit of the imaging technique using the novel fluorescent agent in a large patient population group and compare it to the standard of care procedures. These studies are therefore often blinded and randomized for adequate validation. Phase IV studies are often also known as post-marketing studies and are usually done after clinical approval for optimization of the product.

## **CONCLUSION**

The use of NIR imaging and novel fluorescent agents are currently under wide development and exploration. NIR imaging itself is an emerging field with great potential to improve and change the surgical practice. However, major steps still need to be taken before this technique can be used in standard of care for oncologic procedures. The clinical translation of ZW800-1 and CRGD-ZW800-1 are rapidly on its way, where phase I/II studies have been performed. The package of preclinical, healthy volunteer (phase I) and patient (phase II) data have proven to be important and indispensable in the design of the ensuing phase III/IV studies, for cost-effective and timely adaptation in standard-of-care. The unique collaboration within the Image Guided Surgery group in Leiden, the Netherlands,

between the Centre for Human Drug Research (CHDR) and Leiden University Medical Center (LUMC), has helped develop an optimal roadmap for the clinical translation of promising fluorescent agents.

This collaboration has also permitted the clinical translation of other tumor-targeted agents such as OTL38 (a folate receptor alpha (FR $\alpha$ ) targeting moiety), SGM-101 (a carcinoembryonic antigenic (CEA) targeting agent), and VB5-845D-800CW (an Epithelial Adhesion Molecule (EPCAM) specific agent). NIR fluorescence imaging has emerged rapidly with significant potential for clinical efficacy, especially in the field of surgical oncology. Despite its progress, there are still many opportunities for growth in the field, such as advancements in NIR clinical imaging systems and further refinement of imaging agents to provide better precision and clarity necessary for clinical translation.

## REFERENCES

- Vahrmeijer AL, Hutteman M, van der Vorst JR et al. Image-guided cancer surgery using near-infrared fluorescence. *Nat Rev Clin Oncol* **9**, 507-518 (2013).
- Boogerd LS, Handgraaf HJ, Lam HD, et al. Laparoscopic detection and resection of occult liver tumors of multiple cancer types using real-time near-infrared fluorescence guidance. *Surgical endoscopy* **31**, 952-961 (2016).
- Schaafsma BE, Mieog JS, Hutteman M, et al. The clinical use of indocyanine green as a near-infrared fluorescent contrast agent for image-guided oncologic surgery. *J Surg Oncol* **104**, 323-332 (2011).
- Verbeek FP, van der Vorst JR., Schaafsma BE, et al. Intraoperative near infrared fluorescence guided identification of the ureters using low dose methylene blue: a first in human experience. *J Urol* **2**, 574-579 (2013).
- Hoogstins CES, Boogerd LSF, Sibinga Mulder BG, et al. Image-Guided Surgery in Patients with Pancreatic Cancer: First Results of a Clinical Trial Using SGM-101, a Novel Carcinoembryonic Antigen-Targeting, Near Infrared Fluorescent Agent. *Ann Surg Oncol* **11**, 3350-3357 (2018).
- Boogerd LSF, Hoogstins CES, Schaap DP, et al. Safety and effectiveness of SGM-101, a fluorescent antibody targeting carcinoembryonic antigen, for intraoperative detection of colorectal cancer: a dose-escalation pilot study. *Lancet Gastroenterol Hepatol* **3**, 181-191 (2018).
- Hoogstins CE, Tummers QR, Gaarenstroom KN, et al. A Novel Tumor-Specific Agent for Intraoperative Near Infrared Fluorescence Imaging: A Translational Study in Healthy Volunteers and Patients with Ovarian Cancer. *Clin Cancer Res* **12**, 2929-38 (2016).
- Boogerd LSF, Hoogstins CES, Gaarenstroom KN, et al. Folate receptor- $\alpha$  targeted near-infrared fluorescence imaging in high-risk endometrial cancer patients: a tissue microarray and clinical feasibility study. *Oncotarget* **1**, 791-801 (2017).
- Tummers QR, Hoogstins CE, Gaarenstroom KN, et al. Intraoperative imaging of folate receptor alpha positive ovarian and breast cancer using the tumor specific agent EC17. *Oncotarget* **22**, 32144-55 (2016).
- Handgraaf HJM, Sibinga Mulder BG, Shahbazi Feshtali S, et al. Staging laparoscopy with ultrasound and near infrared fluorescence imaging to detect occult metastases of pancreatic and periampullary cancer. *PLoS One* **11** (2018).
- Choi HS, Gibbs SL, Lee JH, et al. Targeted zwitterionic near-infrared fluorophores for improved optical imaging. *Nat Biotechnol* **2**, 148-153 (2013).
- Choi HS, Nasr K, Alyabyev S, et al. Synthesis and *in vivo* fate of zwitterionic near-infrared fluorophores. *Angew Chem Int Ed Engl* **28**, 6258-6263 (2011).
- Hyun H, Bordo MW, Nasr K, et al. cGMP-Compatible preparative scale synthesis of near-infrared fluorophores. *Contrast Media Mol Imaging* **6**, 516-524 (2012).
- Delacroix Jr SE, Winters JC. Urinary tract injuries: recognition and management. *Clin Colon Rectal Surg* **2**, 104-112 (2010)
- Andersen P, Andersen LM, Iversen LH. Iatrogenic ureteral injury in colorectal cancer surgery: a nationwide study comparing laparoscopic and open approaches. *Surg Endosc* **6**, 1406-1412 (2015).
- Engel O, Rink M, Fisch M. Management of iatrogenic uretral injury and techniques for ureteral reconstruction. *Curr Opin Urol* **4**, 331-335 (2015)
- Minas V, Gul N, Aust W, et al. Urinary tract injuries in laparoscopic gynaecological surgery; prevention, recognition and management. *TOG* **1**, 19-28 (2014).
- Cheresh DA. Human endothelial cells synthesize and express an Arg-Gly-Asp-directed adhesion receptor involved in attachment to fibrinogen and von Willebrand factor. *Proc. Natl. Acad. Sci* **18**, 6471-6475 (1987).
- Brooks PC, Clark RA, Cheresh DA. Requirement of vascular integrin  $\alpha$ v $\beta$ 3 for angiogenesis. *Science* **515**, 569-571 (1994).
- Naumov GN, Akslen LA, Folkman J. Role of angiogenesis in human tumor dormancy: animal models of the angiogenic switch. *Cell Cycle* **16**, 1779-87 (2006).
- Beer AJ, Niemeyer M, Carlsen J, et al. Patterns of  $\alpha$ v $\beta$ 3 expression in primary and metastatic human breast cancer as shown by 18F-Galacto-RGD PET. *J Nucl Med* **2**, 255-9 (2008).
- Avraamides CJ, Garmy-Susini B, and Varner VA. Integrins in angiogenesis and lymphangiogenesis. *Nat Rev Cancer* **8**, 604-617 (2008).
- Handgraaf JMH, Boonstra MC, Prevoo HAJM et al. Real-time near-infrared fluorescence imaging using cRGD-zw800-1 for intraoperative visualization of multiple cancer types. *Oncotarget* **13**, 21054-12066 (2017).
- FDA. Estimating the safe starting dose in clinical trials for therapeutics in adult healthy volunteers. 2340-2341
- Cohen A. Should we tolerate tolerability as an objective in early drug development? *Br J Clin Pharmacol* **64**, 249-252 (2007).

Chapter III

**A ZWITTERIONIC NEAR-INFRARED  
FLUOROPHORE FOR REAL-TIME  
URETER IDENTIFICATION DURING  
LAPAROSCOPIC ABDOMINOPELVIC  
SURGERY**

*Nat commun.* 2019 Jul 16;10(1):3118,  
*doi:* 10.1038/s41467-019-11014-1  
*Supplementary data available online*

KS de Valk<sup>1,2\*</sup>, HJM Handgraaf<sup>2\*</sup>, MM Deken<sup>2</sup>,  
BG Sibinga Mulder<sup>2</sup>, ARPM Valentijn<sup>2</sup>,  
AGT Terwisscha van Scheltinga<sup>2</sup>, J Kuil<sup>2</sup>,  
MJ van Esdonk<sup>1</sup>, J Vuijk<sup>2</sup>, RF Bevers<sup>2</sup>, KCMJ Peeters<sup>2</sup>,  
FA Holman<sup>2</sup>, JV Frangioni<sup>3</sup>, J Burggraaf<sup>1</sup>, AL Vahrmeijer<sup>2</sup>

\*SHARED FIRST AUTHORSHIP

1. Centre For Human Drug Research, Leiden, NL
2. Leiden University Medical Center, Leiden, NL
3. Curadel, LLC, Marlborough, MA, USA

## ABSTRACT

Iatrogenic injury of the ureters is a feared complication of abdominal surgery. Zwitterionic near-infrared fluorophores are molecules with geometrically-balanced, electrically-neutral surface charge, which leads to renal-exclusive clearance and ultralow non-specific background binding. Such molecules could solve the ureter mapping problem by providing real-time anatomic and functional imaging, even through intact peritoneum. Here we present the first-in-human experience of this chemical class, as well as the efficacy study in patients undergoing laparoscopic abdominopelvic surgery. The zwitterionic near-infrared fluorophore ZW800-1 is safe, has pharmacokinetic properties consistent with an ideal blood pool agent, and rapid elimination into urine after a single low-dose intravenous injection. Visualization of structure and function of the ureters starts within minutes after ZW800-1 injection and lasts several hours. Zwitterionic near-infrared fluorophores add value during laparoscopic abdominopelvic surgeries and could potentially decrease iatrogenic urethral injury. Moreover, ZW800-1 is engineered for one-step covalent conjugatability, creating possibilities for developing novel targeted ligands.

## INTRODUCTION

Intraoperative near-infrared (NIR) fluorescence imaging has evolved rapidly over the past decade. The technology permits detection of specific targets, such as malignant cells, nerves, blood vessels, and lymph nodes, in real-time during surgery.<sup>1</sup> Because NIR wavelengths exhibit reduced scattering, absorption, and autofluorescence compared to visible wavelengths, NIR fluorophores permit detection of targets through millimeters of blood and tissue with high sensitivity.

However, a fundamental problem with NIR fluorescence imaging is that conventional NIR fluorophores are polysulfonated, and highly anionic, in order to shield the central hydrophobic resonance structure and improve solubility, and thus exhibit non-specific uptake in tissues and organs after intravenous (IV) injection. This results in high background fluorescence and consequently a lower signal-to-background ratio (SBR). Another problem is that amphiphiles, like indocyanine green (ICG), are rapidly (blood half-life  $\approx$  3 min) and exclusively cleared by the liver after IV injection, thus contaminating the bile and compromising imaging of the gastrointestinal tract. The same applies for other anionic fluorophores, such as IRDYE800CW.<sup>2</sup>

To solve these problems, a chemical class of geometrically balanced, electrically neutral, polyionic polymethine indocyanines (zwitterionic for short) NIR fluorophores were developed.<sup>3,4</sup> Having strong charge (sulfonates and quaternary amines) that is balanced electrically and geometrically over the surface of the molecule, zwitterionic NIR fluorophores are self-shielding and exhibit extremely low non-specific binding and tissue uptake *in vivo* after IV injection.

In small and large animal validation studies the prototype zwitterionic NIR fluorophore ZW800-1 exhibited renal-exclusive clearance and elimination of the entire injected dose into urine over a period of 4-6 h.<sup>3,5</sup> While passing from the kidneys to the bladder, ZW800-1 provided exquisite visualization of the ureters, including structure (i.e., anatomical traverse) and function (i.e., flow and patency).

Iatrogenic ureteral injury is amongst the most feared complications of lower abdominal surgery, with the incidence varying from 0.5-1% in cancer surgery, to as high as 10% in gynecologic oncologic surgery.<sup>6-9</sup> Ureters are thin-walled and at risk for injury as they are poorly distinguished from surrounding retroperitoneal tissue and are usually in a collapsed state. Unrecognized ureteral damage during surgery can lead to long-term morbidity, including kidney failure. Ureteral stent placement is often used to decrease iatrogenic damage, but is associated with complications and can itself result in iatrogenic ureteral damage.<sup>10</sup> NIR fluorescence imaging could potentially add value during abdominopelvic surgeries by providing non-invasive, real-time visualization of the ureters even before surgical exploration.<sup>11,12</sup> In this study, we present the complete clinical translation of ZW800-1, the first zwitterionic NIR fluorophore, and demonstrate its utility in visualizing and assessing ureter structure and function during laparoscopic lower abdominal surgery within 10 min after IV administration, without altering the look of the surgical field.

## METHODS

### Preclinical studies

Preclinical toxicity studies included:

- off-target receptor binding assay (Eurofins Cerep S.A., France);
- bacterial mutation assay;
- single infusion range-finding toxicity studies in rats and dogs to support definitive single IV infusion toxicity study in rats (with a genotoxicity and functional observation assessment);

- single dose toxicity study in dogs;
- a single IV infusion study to evaluate cardiovascular and respiratory function in conscious telemetered dogs.

The toxicology studies were approved by the National Institutes of Health and conducted by the National Cancer Institute's NExT Program and complied with all relevant ethical regulations.

### **GMP production zW800-1**

The GMP Facility LUMC at Leiden University Medical Center, The Netherlands, manufactured zW800-1 as a sterile, lyophilized powder. zW800-1 was prepared in a procedure consisting of seven reaction steps, in which after each reaction the product was purified by precipitation. Each precipitated intermediate was, as an in-process control, checked for identity and purity by ultra-performance liquid chromatography-ultraviolet-mass spectrometry (UPLC-UV-MS). The intermediate drug substance, zW800-1 before purification, was analyzed with UPLC-UV-MS, nuclear magnetic resonance, thin layer chromatography, and ultraviolet-visible spectroscopy and appearance. Purification of zW800-1 was performed using preparative gradient reversed-phase highperformance liquid chromatography (RP-HPLC). Purity of fractions after preparative RP-HPLC purification was controlled using analytical UPLC with UV and MS detection, before pooling the fractions. Absorption spectroscopy analysis on the drug substance pool was performed in order to calculate the volume of zW800-1 solution to be filled and lyophilized in the final medicinal drug product vials. Identity, purity, content, and general quality control parameters, including appearance, pH, sterility, endotoxins, particles, fluorescence, osmolality, and water, were performed. Stability studies were also performed. Aseptic pre-administration preparation was done at the hospital pharmacy of Leiden University Medical Center. The vial containing 5.1 mg zW800-1 was completely dissolved in 5.1 ml glucose 5% infusion fluid by gently swirling the vial by hand, resulting in a clear dark green solution of 1.0 mg/ml zW800-1 drug product. The reconstituted drug product was stored at 2 to 8 °C until administration. The time between reconstitution and administration varied between 1 and 18 h, as the study drug was prepared by the pharmacy either late in the afternoon the day before dosing or the morning of dosing.

### **Phase I: First-in-human study with healthy volunteers**

A total of sixteen healthy volunteers (eight men and eight women) with a median age of 23.5 years (range 18-57 years) participated in this study. The volunteers were considered healthy based on medical screening. A first-in-

human, randomized, placebo-controlled study was performed to determine the safety, tolerability, and PKs (in serum, urine, and skin) of zW800-1. Three dose levels of zW800-1 (0.5, 2.5, and 5.0 mg) were investigated in three non-overlapping cohorts. Placebo consisted of 0.9% NaCl. The first cohort used a sentinel approach. Subjects were randomized to a 4:2 ratio of zW800-1 and placebo. In the following two cohorts, the subjects were randomized to a 4:1 ratio of zW800-1 and placebo. Thus, of the 16 healthy volunteers, 12 received zW800-1 and 4 received placebo. The study was double-blinded where the investigator, staff, and healthy volunteers were blinded with respect to the treatment until the end of the study. Placebo and zW800-1 were formulated identically and the syringes were wrapped in aluminum foil. The IV cannulas were covered during dosing and flushed directly after injection with saline. The same independent physician administered zW800-1 or placebo during the study. Safety and tolerability were assessed by the occurrence of AES, changes in clinical laboratory parameters, vital signs, electrocardiogram parameters, physical examination, and injection site. At defined time points, blood and urine samples were collected for PK assessment. Moreover, NIR fluorescence imaging of the foot was performed frequently with the Lab-FLARE® Model R1 Open Space Imaging System (Curadel ResVet Imaging, LLC, Marlborough, MA, USA) to assess the perfusion and uptake of zW800-1 in the skin.

### **Phase II: First-in-patient feasibility study**

An open-label exploratory study was performed in 12 patients (nine men and three women) with a median age of 61 years (range 30-73 years), scheduled for laparoscopic abdominal or pelvic surgery to assess the feasibility and performance of intraoperative NIR fluorescence imaging of the ureters with zW800-1. All patients received zW800-1, which was administered via an IV bolus injection during surgery while the patients were under anesthesia. Three doses of zW800-1 (1.0, 2.5, and 5.0 mg) were evaluated to determine the optimal dose for surgery. Assignment to the dosage groups was based on the order of enrollment in the study (four patients per dose level). The optimal dose was determined by the calculated SBR obtained from the NIR images during surgery; for each hour of surgery, a mean SBR was calculated. Fluorescence imaging was performed with CE-marked NIR fluorescence medical imaging systems such as those made by Olympus® (CLV-S200-IR, The Netherlands) and Intuitive Surgical (da Vinci® Firefly Imaging System, USA), as well as the model FLARE® MIS prototype (Curadel, USA). During surgery the patients were closely monitored for any abnormalities in vital signs or electrocardiogram. At four different time points (0-15, 15-90, 90-300, and 300-720 min), blood samples were obtained and one urine

sample at the end of surgery for PK analysis. Both the healthy volunteer and patient studies were approved by a certified medical ethics review board and conducted in concordance with the Declaration of Helsinki of 1975 (as amended in Tokyo, Venice, Hong Kong, Somerset West, Edinburgh, Washington, and Seoul), ICH-GCP guidelines, and the laws and regulations of the Netherlands. The medical ethics review board Stichting BEBO in Assen, The Netherlands, approved the healthy volunteer study and the medical ethics review board METC LUMC in Leiden, The Netherlands, approved the patient study. All subjects provided written informed consent prior to the start of any study-related procedure. The healthy volunteer and patient studies are registered in the European Clinical Trials Database under numbers 2016-003919-35 and 2017-001954-32, respectively, as well as in the Netherlands Trial Register under ID NL7209.

### PKs and statistical analysis

The phase I study was designed using commonly accepted subjects per group. For the phase II study, the sample size was not based on statistical power considerations due to the exploratory nature of the study. All PK samples acquired in both the healthy volunteer and patient study were measured within 2 h after withdrawal with the Pearl Impulse (LI-COR Biosciences, Lincoln, NE, USA), with an excitation wavelength of 785 nm and emission wavelengths of 805-850 nm. ZW800-1 concentrations in blood and urine were estimated using calibration curves in fresh human blood and phosphate-buffered saline, respectively, and analyzed with PK variable programming dedicated for PK analysis (R 2.12.0 for Windows). The individual ZW800-1 concentration profiles were analyzed using noncompartmental methods. The fluorescence signal in the skin (healthy volunteers) and the ureters (patients) were quantified using the software ImageJ 1.51j8 (National Institute of Health, MD, USA). The SBR was calculated by drawing a region of interest (ROI) around the background area (as baseline) and the fluorescent signal. The ROI around the fluorescent signal was then subtracted from the background. The quantified value of the fluorescence and background were then divided from each other to obtain a SBR. Data are summarized in graphs and bar charts generated by the GraphPad Prism (version 7.0).

## RESULTS

### ZW800-1

ZW800-1 (molecular formula  $C_{51}H_{66}N_4O_9S_2$ ; molecular weight 943 Da) is a small zwitterionic molecule with peak absorption of 770 nm, an extinction coefficient at peak absorption 253,900  $M^{-1} cm^{-1}$ , peak emission of 788 nm, and a quantum

yield in serum of 15.0%. It was manufactured as a sterile, lyophilized powder under Good Manufacturing Practices (GMPs) in the GMP Facility of Leiden University Medical Center, The Netherlands.

### Preclinical studies

In off-target assays, ZW800-1 showed no significant inhibition of 44 selected targets recommended by four major pharmaceutical companies.<sup>13</sup> No evidence of genotoxicity was observed in the *in vitro* bacterial mutation assay, *in vivo* micronucleus assay using hematopoietic cells, or Comet assays for the assessment of DNA strand breakage in liver cells. The no observable adverse event level (NOAEL) in rats was 24.5 mg/kg, with the human equivalent dose (HED) set at 3.95 mg/kg.<sup>14</sup> The maximum-tolerated dose in rats was 1000 mg/kg. The cardiovascular and respiratory study in dogs indicated that administration of a single IV 30 min infusion of ZW800-1 at doses of 0.7 and 7.0 mg/kg does not elicit any effects on the cardiovascular, pulmonary, or body temperature parameters. The preclinical data in rats and pigs suggested that ZW800-1 is pharmacologically inert, and the human dose for adequate ureter visualization would be in the range between 0.5 and 5.0 mg.<sup>3,5</sup> To be conservative, we opted to start with the lowest dose in this range, instead of a higher dose permitted by the toxicology. We then increased the dose to 2.5 mg and then 5.0 mg during the phase I study. These doses were supported by the toxicology findings, which suggested that even a starting dose of 27.65 mg for a 70 kg adult could be justified (10% of the HED derived from the rat NOAEL, which was 3.95 mg/kg).<sup>15</sup>

### Clinical studies: safety and tolerability

A total of 28 subjects (16 healthy volunteers and 12 patients) were enrolled in the study (*Supplementary Table 1*). There were no serious adverse events (AES) attributed to ZW800-1. Those AES reported during the trial were mild or moderate, none required interruption of the trials, and all resolved without sequelae. Within the healthy volunteer group, seven volunteers (one received placebo) reported a total of ten AES. In the patient group, three patients experienced a total of four AES, all unrelated to ZW800-1. The reported AES were associated with the post-operative course of the undertaken surgery. A detailed listing of reported AES is provided in *Supplementary Table 2*. No trends or changes of clinical importance were observed in the vital signs, clinical laboratory tests, or electrocardiograms after dosing in both groups. Overall, all the administered doses (0.5, 1.0, 2.5, and 5.0 mg) were tolerated well. Doses up to 5.0 mg did not elicit any acute toxicity, nor any hypersensitivity reactions.

### Clinical studies: pharmacokinetics

The pharmacokinetic (PK) results in blood acquired in both studies were consistent (*Supplementary Figure 1*). PK analysis showed that ZW800-1 fluorescence was measurable in serum up to 24-48 h post dose. No differences were observed between males and females. Of the 16 included healthy volunteers, two volunteers (one in the 2.5 mg dose level and one in the 5.0 mg dose level) were completely excluded from the PK analysis due to subcutaneous infusion of the study drug. Even though the IV line appeared to be inserted correctly, fluorescence imaging demonstrated a fluorescent spot at the infusion site. Subcutaneous infusion did not lead to local side effects. Blood PK data from one volunteer (2.5 mg dose level) was excluded because blood was erroneously drawn from the ZW800-1 infusion cannula, tampering with the accuracy of the data. All of the PK blood results of the patients were included in the analysis. NIR fluorescence imaging of the skin in healthy volunteers was concordant with the pharmacodynamic measurements (i.e., dose-response relationship) and showed increasing SBR with higher doses (*Supplementary Figure 2*). After an initial vascular flush that highlighted arteries, capillaries, and veins approximately 8-10 s after intravenous bolus injection (*Supplementary Movie 1*), which is similar to that seen using ICG, the maximum SBR in skin was observed approximately 2 h post injection in all three dosing cohorts, and declined to baseline at 24 h post injection (*Supplementary Figure 2*), suggesting extravasation and reabsorption. In the healthy volunteers, the cumulative urine excretion of ZW800-1, expressed as the percentage of the injected dose, decreased as the dose increased (*Supplementary Figure 3*). The lowest dose group (0.5 mg) had an average cumulative excretion of 93% ZW800-1 at 12 h post dosing. In the higher dose groups (2.5 and 5.0 mg), the average cumulative excretion of ZW800-1 at 12 h post dosing were 70% and 63%, respectively. The decrease in excretion in the higher doses might be explained by the breakdown of ZW800-1 over time, which is known to occur by serum proteins in blood.<sup>16</sup> Other clearance routes are unlikely, as the calculated clearance rates correlate with the human glomerular filtration rate. The majority of ZW800-1 was cleared within the first 2 h after administration. Based on the excretion of approximately 40% of the injected dose of ZW800-1 within the first hour after intravenous injection into human volunteers, we hypothesized that optimal visualization of the ureters intraoperatively would occur at a dose of 2.5 mg administered approximately 5-10 min before ureter visualization is desired. In the patients, the amount of urine collected was noticeably variable and considerably more concentrated than the healthy volunteers, making the two groups (healthy volunteers and patients) incomparable to each other. There

were major differences in fluid intake and urine excretion between the healthy volunteers and patients undergoing laparoscopic surgery, explaining the inter-subject variability of the PK urine results within the groups. The variability in urine production can be explained by the physiological effects during surgery. It is known that during laparoscopic surgery, the urinary output decreases due to the created pneumoperitoneum. Due to the significantly decreased and inconsistent urine production during surgery, the cumulative urine excretion for the patients could not be measured accurately.

### Assessment of ureter structure and function

During laparoscopic surgery, ZW800-1 was administered once the surgeon had identified the location of the ureters under white light, either fully exposed or still covered by peritoneum. During and after administration, the ureters were observed with the NIR channel on the imaging system. ZW800-1 produced high-quality images on all surgical imaging systems tested, including the Olympus®, the Da Vinci® robot, and the FLARE® MIS system (*Figure 1*). Importantly, the ureters could be identified while residing under peritoneum (*Figure 2*) or even under eschar produced by cauterization during cancer resection.

Tissue perfusion was visible directly after administration and the ureters became fluorescent within 10 min (ranging from 2-10 min) after ZW800-1 injection in all patients (1.0, 2.5, and 5.0 mg). With 1.0 mg ZW800-1, the ureters were clearly visible in the first hour after administration, with a mean SBR of 2.3. With 2.5 mg ZW800-1, the visibility of the ureters was comparable to 1.0 mg ZW800-1, with a slightly stronger signal (SBR of 2.7) in the first hour. However, in the second hour the signal of 2.5 mg was considerably higher when compared to 1.0 mg (2.1 vs. 1.4; unequal variance t test:  $p=0.06$ ). The signal decreased slightly as time passed; however, with 2.5 mg the ureters were still clearly visible after at least 3.6 h, which was the longest surgical procedure included in the study. In both the 1.0 and 2.5 mg dose, background fluorescence was negligible enabling the surgeons to perform parts of the procedure in the NIR channel, in conjunction with the highlighted ureters. In patients who received 5.0 mg ZW800-1, background fluorescence was perceptibly more evident in the surrounding tissue, organs (i.e., colon), and major blood vessels. This hindered the visibility of the surgical field in the NIR channel and resulted in a significant lower mean SBR within the first hour post dosing compared to 2.5 mg (1.6 vs. 2.7; unequal variance t test:  $p=0.003$ ; *Figure 3*) and 1.0 mg (1.6 vs. 2.3; unequal variance t test:  $p=0.01$ ; *Figure 3*).

Distinguishing ureters can occasionally be challenging where surgeons initially mistakenly identify other structures as the ureter (*see Supplementary*



*Movie 2*). In this movie, a case is shown where the performing surgeon thought he had identified the ureter. However, during inspection, once ZW800-1 was administered, fluorescence revealed that the ureter was located directly under the initial structure. Mistaking the ureter does not necessarily result in iatrogenic injury, as dissection and isolation is typically done, but unnecessary time can be lost in dissecting the wrong structure. ZW800-1 guidance can aid surgeons in locating the correct structure faster and potentially revise an initial approach.

Not only does ZW800-1 provide visualization of the structure but simultaneously allows real-time assessment of ureter function, and if needed, image-guided repair as it also visualizes its motility. Due to ureteral pulsations, the emitted fluorescence permits clear visualization of the motility and patency of the ureter (*Figure 4*; see also *Supplementary Movie 3*). This time-lapse video shows pulsations of urine down the ureter over a 2 s interval.

## DISCUSSION

Technical advances in the field of surgery, such as laparoscopy and surgical robots, have led to shorter hospitalization and faster recovery.<sup>17</sup> Despite successful implementation, it has not reduced the incidence of visceral injuries. With the use of laparoscopic techniques, surgeons have lost the ability to physically palpate tissue or vital structures during surgery. This study demonstrates that zwitterionic NIR fluorophores like ZW800-1 and NIR fluorescence imaging devices can provide more precise and safer surgery by visualizing ureter structure and function in real time, even when not yet fully exposed.

Methylene blue (MB) and ICG are currently the only NIR fluorescent agents approved (typically for non-NIR indications) by the Food and Drug Administration (FDA) and the European Medicines Agency. Ureter visualization with NIR fluorescence has previously been studied with MB;<sup>18</sup> however, it is a less favorable fluorophore due to the suboptimal clearance and fluorescent properties. MB is a blue dye that is simultaneously cleared by the liver and kidneys with a peak emission of 700 nm, resulting in higher tissue autofluorescence and reduced penetration capacity.<sup>18</sup> ICG was approved in 1958 as a dark green dye (i.e., a photon absorber) for liver function tests. Yet, it was only in the late 1990s that the fluorescent properties of this heptamethine indocyanine were exploited for imaging. Imaging with ICG is currently being implemented in different surgical indications, such as demarcation of liver metastasis, bile duct imaging, and perfusion assessment.<sup>19,20</sup> As mentioned previously, ICG is not applicable to ureter

imaging because of its hepatic-exclusive clearance. However, for other applications, such as biliary tract imaging, it is ideal.<sup>21</sup> Importantly, the safety profile of heptamethine indocyanines, such as ICG, is remarkable.<sup>22</sup> The new chemical class of zwitterionic NIR fluorophores were built upon the foundation of ICG, but have added valuable features such as low non-specific binding and uptake in tissue, single-step conjugation to any targeting ligand, and most important for this study, renal-exclusive clearance and elimination from the body into urine.

ZW800-1 appears to solve several problems in laparoscopic surgery using only a single low dose (1.0-2.5 mg). First, it permits non-invasive, precise structural delineation of the ureters in a patient-specific manner, that is, personalized surgery. Second, ureter identification does not require surgical dissection as it can be visualized with overlying tissue. If ZW800-1 is injected 10 min before identification is needed, the ureters are instantly and constantly identified throughout dissection. Third, ZW800-1 provides a large safety window because an extremely low dose is required. A dose of 1 mg is adequate for up to an hour of imaging and may be repeated if needed. A dose of 2.5 mg provides over 3 h of imaging. Both doses require 10 min, at most, to obtain optimal signal strength. Fourth, ZW800-1 works on most available commercial imaging systems, even those optimized for ICG, which means widespread availability for patients. Fifth, ZW800-1 permits ureter function as well as structure to be quantified. The ability to assess ureter function (i.e., patency and flow) is of huge importance after repair of iatrogenic or traumatic injury and may even broaden its applicability to demonstrate urethral dysfunction during laparoscopy. Along this same line, we know from animal validation studies that micro-nicks of the ureter are quickly identified using NIR fluorescence imaging, which provides intraoperative identification and repair.<sup>11,12</sup> If an injury occurs during surgery, the surgeon should be able to use ZW800-1 to find the site, repair it, and assess ureter function after the repair. Based on the unexpected cases of subcutaneous infusion in healthy volunteers, it appears that tissue damage related to high local concentrations of ZW800-1 is unlikely. Finally, ZW800-1 was engineered for one-step conjugatability using NHS or TFP esters, creating endless possibilities in terms of developing novel targeting ligands.

ZW800-1 can identify ureters on multiple surgical fluorescence imaging systems, which is a key feature of the compound to accelerate clinical adoption. The excitation wavelengths for the Olympus®, Da Vinci® Firefly, and FLARE® imaging systems used in this study were 710-790, 806, and 760 nm, respectively, while the collected emission wavelengths were 810-920, 826-850, and 780-900 nm, respectively. Being engineered for heptamethine indocyanines such as ZW800-1, FLARE® had the highest overlap with peak fluorophore excitation

and emission, but qualitatively all three systems performed well. Additionally, the possibility of visualizing ureters under overlying peritoneum or eschar on these systems is of paramount importance during surgery. During oncologic surgery the formation of eschar is inevitable when resecting vascularized tumors, and limiting unnecessary dissection, if possible, is advantageous. This is also why the high penetration depth of NIR light (due to low absorption and scattering) and ZW800-1's excellent optical properties are important features for image-guided surgery. The studies presented herein demonstrate the complete clinical translation of a new chemical class from invention, to proof of safety and efficacy, in 8 years. Its package of *in vitro*, *in vivo*, healthy volunteer (phase I) and patient (phase II) data can support the design of an appropriately powered phase III pivotal trial. The healthy volunteer study also provided valuable information on safety, PKs, and pharmacodynamics, without exposing vulnerable patients to potentially harmful AEs, and avoiding time-consuming lengthy dose-finding studies in the target population. Interestingly, in the case of nontoxic pharmacologically inert imaging agents such as ZW800-1, the imaging-enabling dose will often be much lower than what NOAEL would suggest.<sup>23</sup> The data obtained in our phase I human volunteer study, for example, resulted in a precise dose estimation for design of an effective phase II study using doses far below NOAEL. Furthermore, because of the conjugatability of ZW800-1 and other zwitterionic NIR fluorophores, the development of zwitterionic NIR fluorescence targeted agents should be much more time- and cost-efficient. Currently, the first cancer-targeted molecule using ZW800-1 is being studied in a phase II patient study (European Clinical Trials Database 2017-002772-60). This translational study suggests that the first-in-class zwitterionic NIR fluorophore ZW800-1 has optimal *in vivo* and clearance properties, without any observable toxicity. After a single low-dose injection, ZW800-1 provides visualization of the ureters for at least 3 h without altering the look of the surgical field or requiring dissection, and can be used on most commercially available surgical imaging systems. ZW800-1 can also be conjugated to any molecule, including antibodies and other proteins, peptides, and nanoparticles, to create novel targeted NIR fluorescent contrast agents. Taken together, ZW800-1 heralds a paradigm shift in the safety profile of laparoscopic and robotic abdominopelvic surgery.

## REFERENCES

- Vahrmeijer AL, Hutteman M, van der Vorst JR, van de Velde CJ, Frangioni JV. Image-guided cancer surgery using near-infrared fluorescence. *Nat Rev Clin Oncol*. 2013;10(9):507-518.
- Choi HS, Gibbs SL, Lee JH, et al. Targeted zwitterionic near-infrared fluorophores for improved optical imaging. *Nat Biotechnol*. 2013;31(2):148-153.
- Choi HS, Nasr K, Alyabyev S, et al. Synthesis and *in vivo* fate of zwitterionic near-infrared fluorophores. *Angew Chem Int Ed Engl*. 2011;50(28):6258-6263.
- Hyun H, Henary M, Gao T, et al. 700-nm Zwitterionic Near-Infrared Fluorophores for Dual-Channel Image-Guided Surgery. *Mol Imaging Biol*. 2016;18(1):52-61.
- Hyun H, Bordo MW, Nasr K, et al. cGMP-Compatible preparative scale synthesis of near-infrared fluorophores. *Contrast Media Mol Imaging*. 2012;7(6):516-524.
- Delacroix SE, Jr., Winters JC. Urinary tract injuries: recognition and management. *Clin Colon Rectal Surg*. 2010;23(2):104-112.
- Andersen P, Andersen LM, Iversen LH. Iatrogenic ureteral injury in colorectal cancer surgery: a nationwide study comparing laparoscopic and open approaches. *Surg Endosc*. 2015;29(6):1406-1412.
- Engel O, Rink M, Fisch M. Management of iatrogenic ureteral injury and techniques for ureteral reconstruction. *Curr Opin Urol*. 2015;25(4):331-335.
- Minas V, Gul NAT, Doyle M, Rowlands D. Urinary tract injuries in laparoscopic gynaecological surgery; prevention, recognition and management. *The Obstetrician & Gynaecologist*. 2014;16:19-28.
- Dyer RB, Chen MY, Zagoria RJ, Regan JD, Hood CG, Kavanagh PV. Complications of ureteral stent placement. *Radiographics*. 2002;22(5):1005-1022.
- Tanaka E, Ohnishi S, Laurence RG, Choi HS, Humblet V, Frangioni JV. Real-time intraoperative ureteral guidance using invisible near-infrared fluorescence. *J Urol*. 2007;178(5):2197-2202.
- Matsui A, Tanaka E, Choi HS, et al. Real-time, near-infrared, fluorescence-guided identification of the ureters using methylene blue. *Surgery*. 2010;148(1):78-86.
- Bowes J, Brown AJ, Hamon J, et al. Reducing safety-related drug attrition: the use of *in vitro* pharmacological profiling. *Nat Rev Drug Discov*. 2012;11(12):909-922.
- Reagan-Shaw S, Nihal M, Ahmad N. Dose translation from animal to human studies revisited. *FASEB J*. 2008;22(3):659-661.
- FDA. Estimating the Maximum Safe Starting Dose in Initial Clinical Trials for Therapeutics in Adult Healthy Volunteers. 2005.
- Hyun H, Owens EA, Narayana L, et al. Central C-C Bonding Increases Optical and Chemical Stability of NIR Fluorophores. *RSC Adv*. 2014;4(102):58762-58768.
- Buia A, Stockhausen F, Hanisch E. Laparoscopic surgery: A qualified systematic review. *World J Methodol*. 2015;5(4):238-254.
- Verbeek FP, van der Vorst JR, Schaafsma BE, et al. Intraoperative near infrared fluorescence guided identification of the ureters using low dose methylene blue: a first in human experience. *J Urol*. 2013;190(2):574-579.
- Boogerd LS, Handgraaf HJ, Lam HD, et al. Laparoscopic detection and resection of occult liver tumors of multiple cancer types using real-time near-infrared fluorescence guidance. *Surg Endosc*. 2017;31(2):952-961.
- Schaafsma BE, Mieog JS, Hutteman M, et al. The clinical use of indocyanine green as a near-infrared fluorescent contrast agent for image-guided oncologic surgery. *J Surg Oncol*. 2011;104(3):323-332.
- Ishizawa T, Bandai Y, Iijichi M, Kaneko J, Hasegawa K, Kokudo N. Fluorescent cholangiography illuminating the biliary tree during laparoscopic cholecystectomy. *Br J Surg*. 2010;97(9):1369-1377.
- Benya R, Quintana J, Brundage B. Adverse reactions to indocyanine green: a case report and a review of the literature. *Cathet Cardiovasc Diagn*. 1989;17(4):231-233.
- Cohen A. Should we tolerate tolerability as an objective in early drug development? *Br J Clin Pharmacol*. 2007;64(3):249-252.

**FIGURE 1** High sensitivity detection of ZW800-1 NIR fluorescence in patients using three different commercial imaging systems. Invisible NIR fluorescence of ZW800-1 is pseudo colored in green and overlaid in real-time onto the anatomical images.



**FIGURE 2** Ureter residing under peritoneum. The ureter (dashed circle) is captured during a pulse of urine flow during surgery. The darker green areas in the NIR fluorescence image (small arrows) is background fluorescence caused by the vessels in the surrounding tissue. The images were acquired using the Olympus® imaging system during laparoscopic surgery.

WHITE LIGHT (COLOR)



COLOR-NIR MERGE

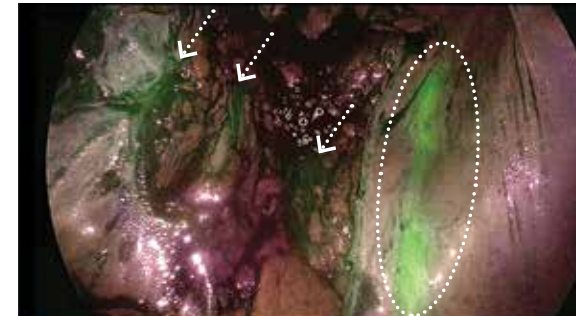


**FIGURE 3 Signal-to-background ratio (SBR) of the ureter.** Note: the SBR of 5.0 mg is significantly lower than the SBR of 2.5 mg (unequal variance t-test:  $p=0.003$ ) and 1.0 mg (unequal variance t-test:  $p=0.01$ ) in the first hour post-dose. The values represent the mean  $\pm$  SD (n=4 patients each group). Source data are provided as a Source Data file.

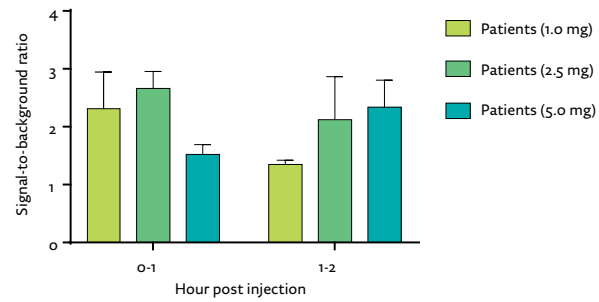
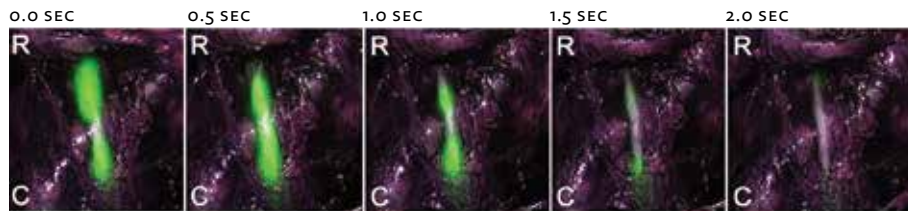


**FIGURE 4 Functional assessment of ureter flow and patency with zw800-1.** (acquired using the Olympus® imaging system)



#### Chapter IV

### FIRST-IN-HUMAN ASSESSMENT OF CRGD-ZW800-1, A ZWITTERIONIC, INTEGRIN-TARGETED NEAR-INFRARED FLUORESCENT PEPTIDE IN COLON CARCINOMA

*Clin Canc Res.* 2020 Aug 1;26(15):3990-3998.

doi: 10.1158/1078-0432.CCR-19-4156

Supplementary data available online

KS de Valk<sup>1,2</sup>, MM Deken<sup>2</sup>, HJM Handgraaf<sup>2</sup>,  
 SS Bhairosingh<sup>2</sup>, OD Bijlstra<sup>2</sup>, MJ van Esdonk<sup>1</sup>,  
 AGT Terwisscha Van Scheltinga<sup>2</sup>, ARPM Valentijn<sup>2</sup>,  
 TL March<sup>2</sup>, J Vuijk<sup>2</sup>, KCMJ Peeters<sup>2</sup>, FAHolman<sup>2</sup>,  
 DE Hilling<sup>2</sup>, JSD Mieog<sup>2</sup>, JV Frangioni<sup>3</sup>, J Burggraaf<sup>1</sup>,  
 AL Vahrmeijer<sup>2</sup>

1. Centre For Human Drug Research, Leiden, NL

2. Leiden University Medical Center, Leiden, NL

3. Curadel, LLC, Marlborough, MA, USA

## ABSTRACT

Incomplete oncologic resections and damage to vital structures during colorectal cancer surgery increases morbidity and mortality. Moreover, neoadjuvant chemoradiotherapy has become the standard treatment modality for locally advanced rectal cancer, where subsequent downstaging can make identification of the primary tumor more challenging during surgery. Near-infrared (NIR) fluorescence imaging can aid surgeons by providing real-time visualization of tumors and vital structures during surgery. We present the first-in-human clinical experience of a novel NIR fluorescent peptide, CRGD-ZW800-1, for the detection of colon cancer. CRGD-ZW800-1 was engineered to have an overall zwitterionic chemical structure and neutral charge in order to lower non-specific uptake and thus background fluorescent signal. We performed a Phase I study in 11 healthy volunteer as well as a Phase II feasibility study in 12 patients undergoing an elective colon resection, assessing 0.005 mg/kg, 0.015 mg/kg and 0.05 mg/kg CRGD-ZW800-1 for the intraoperative visualization of colon cancer. CRGD-ZW800-1 appears safe, and exhibited rapid elimination into urine after a single low intravenous dose. Minimal invasive intraoperative visualization of colon cancer through full-thickness bowel wall was possible after an intravenous bolus injection of 0.05 mg/kg at least 2 h prior to surgery. Longer intervals between injection and imaging improved the tumor-to-background ratio. CRGD-ZW800-1 enabled fluorescence imaging of colon cancer in both open and minimal invasive surgeries. Further development of CRGD-ZW800-1 for widespread use in cancer surgery may be warranted given the ubiquitous overexpression of various integrins on different types of tumors and their vasculature.

## INTRODUCTION

Colorectal cancer is the third most common cancer and one of the leading causes of death in developed countries in both males and females.<sup>1,2</sup> However, mortality rates have drastically improved in the last decade due to implemented screening programs and advancements in neoadjuvant therapies and surgical techniques.<sup>2,3</sup> These developments have not only improved patient survival and oncological outcomes, but have also resulted in faster and better surgical recovery.<sup>4,5</sup> Nevertheless, neoadjuvant therapies and enhanced surgical techniques have also created new challenges. Neoadjuvant chemoradiotherapy has become the standard treatment modality for locally advanced rectal cancer, where approximately 15-20% of patients achieve a pathologic complete response, resulting in improved oncologic outcomes.<sup>6-8</sup> Subsequent downstaging, however, can make identification of the primary tumor more challenging during surgery.<sup>9</sup>

Nowadays, minimally invasive laparoscopic surgery (MIS) is promoted as the standard procedure for elective colorectal resections as studies have shown better short-term outcomes and lower mortality and morbidity rates when compared to open surgery.<sup>4,5,10</sup> However, MIS deprives the surgeons of tactile feedback and provides less visual information compared to open surgery and thus creates surgical challenges, especially after neoadjuvant therapy. Strategies such as endoscopic tattooing with ink are commonly used to intraoperatively recognize tumor locations. Yet, 2-15% of endoscopic tattoos are invisible during surgery, caused by variability in technique and accuracy, or by overlying tissue that masks the ink.<sup>11,12</sup> Failing to identify the lesion for resection due to invisible tattoos spots can result in open conversion or, in rare cases, removal of the wrong segment of bowel.<sup>11,12</sup>

Achieving safe and accurate radical resections is of paramount importance during oncologic surgery. Incomplete resections and damage to critical structures are often associated with poor patient survival, and increased risk of complications. Near-infrared (NIR) fluorescence imaging is an evolving technique that enhances normal and tumor anatomy by creating visual contrast where none otherwise exists. Multiple clinical studies with NIR agents have already been reported for malignancies (i.e. colorectal, pancreatic and ovarian cancer), metastases (i.e. liver and peritoneal), and vital structures, such as the biliary tract and ureters.<sup>13-18</sup>

CRGD-ZW800-1 is a novel NIR targeted peptide, which consists of a cyclic pentapeptide (CRGD) conjugated to the 800 nm zwitterionic NIR fluorophore ZW800-1.<sup>18</sup> CRGD is a clinically well-known peptide that binds to integrins, such as  $\alpha v \beta 6$ , which are expressed on tumor cells and tumor-associated vascular endothelium associated with neoangiogenesis.<sup>19</sup> Studies have shown  $\alpha v \beta 6$  integrin is a suitable target for tumor imaging, as it has a limited expression in normal tissue and a high prevalence in invasive epithelial tumors, such as colorectal cancer.<sup>20-22</sup> Moreover, CRGD also has the ability to bind to integrins such as  $\alpha v \beta 3$  and  $\alpha v \beta 5$ , which are overexpressed on various malignant tumors.<sup>17,23,24</sup> Previous phase I and II clinical trials with RGD-based PET tracers confirmed uptake in multiple tumor types, including melanomas, glioblastomas, breast, colorectal, head and neck, and pancreatic cancer.<sup>25-28</sup> Preclinical animal work with CRGD-ZW800-1 supported this finding as clear tumor demarcation was possible *in vivo* in multiple cancer types after a low dose of CRGD-ZW800-1.<sup>17,29</sup> *In vivo* dose-ranging studies have been performed to determine the optimal imaging dose for the first-in-human trial.<sup>17</sup> A subsequent preclinical toxicology study in rats is performed in this study to recommend a safe starting dose for the phase I/II clinical trial.

The aim of this study was to describe the first clinical experience with CRGD-ZW800-1, by assessing the safety and pharmacokinetics in healthy volunteers and evaluating its feasibility and optimal dosing in detecting colon cancer during surgery in patients undergoing an elective colon resection.

## MATERIALS AND METHODS

### Investigational product

The Hospital Pharmacy department of Leiden University Medical Center manufactured CRGD-ZW800-1 (molecular formula  $C_{78}H_{106}N_{13}O_{16}S_2$ ; molecular weight 1729 Da) by developing and conjugating the fluorophore ZW800-1 to cyclic pentapeptide cyclo(Arg-Gly-Asp-D-Tyr-Lys), also known as CRGD. The product was aseptically lyophilized in sterile single dose vials each containing 0.725 mg without additional excipients. CRGD-ZW800-1 was ready for intravenous (IV) administration after aseptic reconstitution into 0.9% sodium chloride (saline) solution. Placebo consisted of saline solution.

### Toxicology

Preclinical studies demonstrated that tumor visualization in mice was possible after IV administration of 10 nmol CRGD-ZW800-1 per mouse, which corresponds to a human equivalent dose (HED) of 0.06 mg/kg.<sup>17</sup> Based on these results, a generic extended non-clinical toxicity study in rats was designed, including control groups and two treatment groups with single doses of 15.0 mg/kg and 5.0 mg/kg CRGD-ZW800-1 according to ICH M3 (R2), FDA, EMEA and GLP regulations. Both dose groups consisted of 10 males and 10 females, which were subjected to a full post mortem examination on day 2 post dosing. In addition, 5 recovery animals per sex were added in the control and 5.0 mg/kg dose group and were followed for 14 days post dosing.

### Clinical study design

The study consisted of a phase I study in healthy volunteers and a phase II study in patients with colon cancer. The phase I, first-in-human, randomized, placebo-controlled study was performed in 11 healthy volunteers to assess the safety, tolerability, and pharmacokinetics (in blood, urine and skin) of a single IV dose of CRGD-ZW800-1. The volunteers were considered healthy based on medical screening. Two dose levels of CRGD-ZW800-1 (0.001 mg/kg and 0.005 mg/kg) were evaluated in two non-overlapping cohorts. Microdosing was performed since a single-dose toxicity study was performed in only one animal species. In the first patient cohort a sentinel approach was used and subjects were ran-

domized to a 4:2 ratio of CRGD-ZW800-1 and placebo (sterile saline). In the second cohort, subjects were randomized to a 4:1 ratio of CRGD-ZW800-1 and placebo. Thus, of the 11 healthy volunteers, eight subjects received a bolus injection of CRGD-ZW800-1 and three subjects received placebo. The study was double-blinded where the investigator, staff, and study subjects were blinded with respect to the treatment until the end of the study. The syringes were wrapped in aluminum foil and the IV cannulas were covered during dosing and flushed directly afterwards with saline. Safety and tolerability were assessed by the occurrence of AES, changes in clinical laboratory values, vital signs, electrocardiogram, and physical examination including injection site assessment. At defined time points blood and urine samples were collected for pharmacokinetic assessment. NIR fluorescence imaging of the hand was performed with the LabFLARE Model R1 Open Space Imaging system (Curadel LLC, Natick, MA, USA) at specified time points to assess perfusion and uptake of CRGD-ZW800-1 in the skin. Skin fluorescence was measured by calculating the SBR, where the fluorescence values post-dose were divided by the pre-dose (baseline) value. This was done using the software ImageJ 1.51j8 (National Institute of Health, MD, USA).

After concluding the phase I study, a phase II study was executed to evaluate the feasibility and determine the optimal dose and injection time window of CRGD-ZW800-1 for the intraoperative imaging of colon cancer. An open-label ascending dose study was performed in 12 colon cancer patients who were scheduled for an elective MIS or open colon resection. Patients received an IV bolus injection of CRGD-ZW800-1 at least 2 h prior to surgery at the preoperative holding area. Patients who received CRGD-ZW800-1 18 h prior to surgery were admitted the day before surgery for administration, which was also done under supervision at the preoperative holding area. Three doses of CRGD-ZW800-1 (0.005 mg/kg, 0.015 mg/kg and 0.05 mg/kg) were explored in three non-overlapping cohorts. Assignment to the dose level was based on the order of enrollment in the study (four patients per dose level). Patients were closely monitored after infusion for any abnormalities in vital signs or electrocardiogram. At different time points (0-30 min, 30-120 min, 120-300 min and 300-720 min) after CRGD-ZW800-1 administration, blood samples were obtained for additional pharmacokinetic analysis.

### Intraoperative NIR imaging of colon tumors

Intraoperative fluorescence imaging of the surgical field was performed using CE-marked MIS laparoscopic or open fluorescence imaging systems optimized for measurements in the 800 nm NIR-spectrum. The CE-marked systems used were Olympus Visera Elite II (CLV-S200-IR, Hamburg, Germany); a minimal

invasive laparoscopic system, and Quest Spectrum Platform (Quest Medical Imaging, Middenmeer, The Netherlands); an imaging system that can be used for both minimal invasive or open procedures. Fluorescence imaging was performed during initial inspection of the abdomen, after dissection (before tumor resection), and after tumor resection. Intraoperative fluorescence was measured by calculating the tumor-to-background ratio (TBR) using ImageJ 1.51j8. A region of interest (ROI) was drawn around tumor fluorescence and one directly around the surrounding background area. The quotient of the tumor and background signal constituted the intraoperative TBR.

### **Ex vivo NIR imaging and immunohistochemistry**

All resected colon tumor specimens and lymph nodes were assessed by a gastrointestinal pathologist, according to hospital protocol. *Ex vivo* imaging on gross macroscopy of the colon tumors and lymph nodes was performed. Bread loafs of the colon tumors were imaged with the Pearl Trilogy Small Animal Imaging System (LI-COR Biosciences, Lincoln, NE, USA) and the lymph nodes were imaged with the Lab-FLARE Model R1 (Curadel) for the TBR analysis. The resected specimen and lymph nodes were processed and inserted into histology cassettes for tumor assessment, using standardized hematoxylin and eosin (H&E) staining. Additional immunohistochemistry staining of the  $\alpha v \beta 6$  integrin was performed on 4  $\mu$ m sectioned formalin-fixed paraffin-embedded tumor tissue and lymph nodes to demonstrate and confirm  $\alpha v \beta 6$  expression. The  $\alpha v \beta 6$  staining was scored with an immunohistochemistry score (*Supplementary Figure S1*). Imaging of the pathology slides was performed using the Odyssey CLx scanner (LI-COR Biosciences, NE, USA) to correlate CRGD-ZW800-1 fluorescence with H&E (i.e. tumor status) and  $\alpha v \beta 6$  expression on a microscopic level. Since  $\alpha v \beta 6$  is present on normal and tumor tissue, concordance assessment was solely based on tumor status and fluorescence. Four different conclusions could be made; 1) a malignant tumor or lymph node with fluorescence was regarded as a true positive (TP); 2) a benign tumor or lymph node without fluorescence was regarded as a true negative (TN); 3) a benign tumor with fluorescence was regarded as a false positive (FP); 4) a malignant tumor or lymph node without fluorescence was regarded as a false negative (FN). Fluorescence was quantified by measuring the mean fluorescence intensity (MFI) in tumor (colon tumors and metastasized lymph nodes) and normal tissue (normal mucosa and normal lymph nodes) using ImageJ 1.51j8 and ImageStudio (LI-COR Biosciences, Lincoln, NE, USA) for the FLARE and Pearl images, respectively. The measured MFI was then used to calculate the *ex vivo* TBR using the following formula:  $TBR = MFI_{tumor\ tissue} / MFI_{normal\ tissue}$ .

### **Pharmacokinetics and statistical analysis**

The phase I study in healthy volunteers was designed using commonly accepted subjects per group. For the phase II patient study, the sample size was not based on statistical power considerations due to the exploratory nature of the study. All pharmacokinetic samples acquired were measured with the Pearl Imaging System. CRGD-ZW800-1 concentrations in blood and urine were estimated using calibration curves created in human whole blood and phosphate-buffered saline (PBS), respectively. The calibration curve was created by measuring each diluted concentration using the Pearl. Data was plotted in fluorescence intensity over concentration. Results were analyzed with software dedicated for PK analysis (R 2.12.0 for Windows) using non-compartmental methods. Differences in MFI between tumor and normal tissue were tested between different dose groups using descriptive statistics, multiple t-tests and one-way ANOVA. Data are summarized in graphs and bar charts generated by GraphPad Prism (version 8.0).

### **Ethical committee approval**

The preclinical toxicity study in rats was reviewed and approved by the Animal Welfare Officer and the Ethical Committee (DEC 14-59) as required by the Dutch Act on Animal Experimentation (February 1997). Both the clinical Phase I and Phase II studies were approved by a certified medical ethics review board (Stichting BEBO in Assen, the Netherlands, and METC LUMC in Leiden, the Netherlands, respectively) and conducted in concordance with the principles of the Helsinki Declaration of 1975 (as amended in Tokyo, Venice, Hong Kong, Somerset West, Edinburgh, Washington, and Seoul), and the laws and regulations of the Netherlands. All subjects provided written informed consent prior to the start of any study-related procedure. Both studies are registered in the European Trials Database under numbers 2016-000397-38 and 2017-002772-60, as well as in the Netherlands Trial Register under ID NL7724.

## **RESULTS**

### **Toxicology**

In rats, no treatment-related mortality occurred and no significant clinical signs or changes in pathology (including macroscopic and microscopic) were seen. Discolored (green) urine was observed in both the 5.0 mg/kg and 15.0 mg/kg dose groups on the day of administration. No effects on body weight, food consumption, hematology, biochemistry or macroscopic and



microscopic alterations were observed when compared to the control group. One accidental death (control male on day 2) occurred due to blood sampling. No clinical signs, findings on pathology, or microscopic findings were found indicating cause of death. Routine hematology parameters and biochemistry remained within normal range and were considered not toxicologically relevant. Histopathological examination did not raise a safety signal. Microscopic findings at the injection site (tail vein) included perivascular inflammation, perivascular hemorrhage and vascular necrosis, and were present at similar incidence and severity in both the control and treated rats. These were considered procedure-related rather than treatment-related. Based on these results, it was concluded that a single dose of 5.0 mg/kg and 15.0 mg/kg (with a no observed adverse effect level (NOAEL) of at least 5.0 mg/kg) were well tolerated in rats, which corresponds to HED of 0.8 mg/kg.

### Clinical study results

A total of 23 subjects (11 healthy volunteers and 12 patients) participated in the study. The 11 healthy volunteers consisted of three men and eight women with a median age of 28.9 years (range 19-65 years). The 12 colon cancer patients were divided in seven men and five women with a median age of 66.8 years (range 49-80 years). Patient demographics and details on the surgical procedure, histology and tumor imaging are summarized in *Supplementary Table S1*.

### Safety and tolerability

None of the healthy volunteers or patients showed signs of acute or chronic toxicity, and in particular no hypersensitivity reactions were encountered. Within the healthy volunteers, a total of eight adverse events (AEs) were reported in four subjects (one placebo). The reported AEs were mild, did not require interruption of the trial, and resolved without sequelae. In the patient group, eight patients experienced a total of 10 AEs and four serious adverse events (SAEs). None of the reported AEs or SAEs were related to CRGD-ZW800-1, but were associated with the post-operative course of the particular surgery. No adverse events occurred in the hours between CRGD-ZW800-1 administration and surgery, during which blood levels of the contrast agent peaked. A detailed listing of reported AE and SAEs is provided in *Supplementary Table S2*. No significant clinical changes or trends were observed in the vital signs, laboratory parameters or electrocardiograms after dosing. Overall, all the administered doses (0.001 mg/kg, 0.005 mg/kg, 0.015 mg/kg, 0.05 mg/kg) were well tolerated.

### Pharmacokinetics

In healthy volunteers, the concentrations of CRGD-ZW800-1 in blood were measurable (> lower limit of quantification (LLOQ) of 1.56 ng/mL) up to 1 h after injection in the 0.001 mg/kg cohort and up to 8 h after injection in the 0.005 mg/kg group. In patients, CRGD-ZW800-1 concentrations were measurable at least 8-10 h after injection in all three dose levels. Due to the opportunistic sampling approach in patients, a non-compartmental analysis (NCA) was only performed on the dense pharmacokinetic (PK) data acquired from the healthy volunteer study. There were too few PK blood samples obtained in surgical patients for a NCA of the 0.05 mg/kg dose. Based on the NCA of the highest dose administered to healthy volunteers (0.005 mg/kg), CRGD-ZW800-1 showed a mean apparent terminal half-life of 3.31 h, with a mean clearance rate of 10.14 L/h and a mean distribution volume of 47.25 L. The PK of CRGD-ZW800-1 was similar between healthy volunteers and patients, which can most clearly be seen by the overlap in concentrations from both healthy volunteers and patients in the 0.005 mg/kg dose level (*Supplementary Figure S2*).

The urine samples obtained in the healthy volunteers showed that the cumulative excretion of CRGD-ZW800-1, expressed as the percentage of the injected dose, decreased with increasing dose (*Supplementary Figure S2*). In the lowest dose (0.001 mg/kg), an average cumulative excretion of 83% CRGD-ZW800-1 was observed 8 h post dosing, while this was 68% for the 0.005 mg/kg dose.

### CRGD-ZW800-1 uptake in skin

NIR fluorescence of the skin in healthy volunteers was concordant with the pharmacokinetic measurements (i.e. dose-response relationship) and showed increasing signal-to-baseline ratio (SBR) with higher doses. The maximum SBR in skin was observed approximately 1-2 h post dose and returned to baseline at 24 h. Interestingly, one healthy volunteer in the 0.005 mg/kg cohort had a recent wound on the hand with a scab present at the time of CRGD-ZW800-1 administration. At the site of this lesion, distinct measurable fluorescence was present which became visible within 15 minutes after administration and remained above background for at least 24 h (*Supplementary Figure S3*).

### Intraoperative fluorescence imaging of colon carcinoma

A total of 12 patients underwent an elective MIS (n=11) or open (n=1) colon resection. MIS laparoscopic tumor visualization through bowel wall was possible with the highest dose of 0.05 mg/kg CRGD-ZW800-1 (*Figure 1*). The intraoperative

TBR ranged from 1.1 in the patients who received 0.05 mg/kg 2-4 h prior to surgery to 1.6 in the patients who received 0.05 mg/kg 18 h prior to surgery. No fluorescence through bowel wall was visible during the MIS procedures in the lower doses of 0.005 mg/kg and 0.015 mg/kg. However, one patient in the lowest dose level (0.005 mg/kg) underwent an open colon resection where tumor fluorescence was visible through bowel wall with the open imaging system, with an intraoperative TBR of 1.5. Furthermore, ureter visualization was possible in all three dose levels when CRGD-ZW800-1 was administered 2-4 h prior to surgery. Ureter fluorescence became brighter as the dose increased. *Supplementary Figure S4* illustrates laparoscopic ureter visualization in a patient who received 0.05 mg/kg CRGD-ZW800-1 2-4 h prior to surgery.

### CRGD-ZW800-1 injection time window

Ten of the 12 patients received an IV bolus of CRGD-ZW800-1 approximately 2-4 h prior to surgery. Since tumor fluorescence during MIS was realized with the highest dose (0.05 mg/kg), it was decided to also evaluate a longer injection time window in this dose level to assess whether this could improve the TBR. The cohort of 0.05 mg/kg with four patients was therefore used to evaluate an early dosing scheme and a late dosing scheme, where two patients received the dose 2-4 h prior to surgery and two patients approximately 18 h prior to surgery. *Figure 2* demonstrates the MFI measured in the colon tumors and normal mucosa, including the calculated *ex vivo* TBR, in the different dose levels and injection time windows. The results display a significant increase in tumor MFI as the dose increases ( $p < 0.001$ ). Furthermore, the difference in MFI between tumor and normal mucosa is clearly visible within the dose levels. This difference is significant in the 0.015 mg/kg and both 0.05 mg/kg groups ( $p = 0.037$ ,  $p = 0.023$  and  $p = 0.037$ , respectively). The dose 0.005 mg/kg, 0.015 mg/kg and 0.05 mg/kg 2-4 h prior to surgery showed a mean *ex vivo* TBR of 1.4, 4.0 and 4.1, respectively. The dose 0.05 mg/kg 18 h prior to surgery displays the highest *ex vivo* TBR of 6.2. The TBR increase was significant among dose 0.005 mg/kg and 0.015 mg/kg ( $p = 0.031$ ), and dose 0.005 mg/kg and 0.05 mg/kg 18 h ( $p = 0.004$ ). The *ex vivo* results coincides with the intraoperative TBR, which was also the highest in the patients with a longer injection time window of 18 h (1.1 in 2-4 h vs. 1.6 in 18 h).

### Histopathology assessment and $\alpha v \beta 6$ expression of colon tumors

All patients had true-positive colon tumors ( $n = 12$ ). All the resected colon tumor specimens contained malignancy, showed a strongly positive  $\alpha v \beta 6$  expression (score 9-12) and displayed intense fluorescence on a microscopic level. Normal mucosa expressed milder  $\alpha v \beta 6$  expression (score 2-4) and accordingly exhibited

less, to minimal, fluorescence when compared to the tumor (*Figure 3*). This was also clearly perceived on *ex vivo* intraluminal images of the colon tumor after the resected specimen was cut open (*Figure 4*).

### Lymph nodes assessment

In the 12 Phase II patients, a total of 209 colon lymph nodes were removed and in 35 of these lymph node metastases were found. In these metastatic lymph nodes, immunohistochemistry showed negative ( $n = 1$ ), mild ( $n = 6$ ), moderate ( $n = 5$ ) or strongly positive ( $n = 23$ )  $\alpha v \beta 6$  expression. All the lymph nodes without metastasis showed negative  $\alpha v \beta 6$  expression. The average MFI of tumor positive and tumor negative lymph nodes were measured and a MFI threshold of fluorescence was established per cohort to determine the concordance. The MFI threshold was grounded on the 95% confidence interval (CI) of tumor negative MFI per cohort, where the upper limit of the CI was used as the threshold. In the dose 0.005 mg/kg 2-4 h, the MFI for tumor positive lymph nodes was 109 (SD + 51.7) compared to 43 (SD + 17.4) for tumor negative lymph nodes (MFI threshold = 48). In the dose 0.015 mg/kg 2-4 h, the MFI for tumor positive lymph nodes was 128 (SD + 41.7) compared to 65 (SD + 40.4) for tumor negative lymph nodes (MFI threshold = 74). In the dose 0.05 mg/kg 2-4 h, the MFI for tumor positive lymph nodes was 235 (SD + 8.4) compared to 124 (SD + 63.0) for tumor negative lymph nodes (MFI threshold = 187), whereas in the dose 0.05 mg/kg 18 h, the MFI for tumor positive lymph nodes was 62 (SD + 0.0) compared to 44 (SD + 12.7) for tumor negative lymph nodes (MFI threshold = 52) (*Figure 5*). The dose 0.05 mg/kg 18 h prior to surgery, showed the most ideal test characteristics for lymph node detection of tumor metastasis, with a sensitivity of 100%, a specificity of 87% and a false positive rate of 13%. However, the small number of positive lymph nodes in some cohorts requires a larger study to confirm these results.

## DISCUSSION

In this study, we demonstrated the safety and feasibility of colon tumor imaging with the novel zwitterionic NIR fluorescent peptide CRGD-ZW800-1. CRGD-ZW800-1 enables intraoperative imaging of colon cancer, in both MIS and open settings. (Over)expression of  $\alpha v \beta 6$  was visible in the resected colon tumors and metastasized lymph nodes. All colon tumors displayed vivid *ex vivo* fluorescence and showed binding of CRGD-ZW800-1 at the microscopic level, thus confirming preclinical studies (17, 29). This result also suggests value in margin discrimination after surgical resection. Real-time imaging of colon cancer, even through the full-thickness of the bowel wall, was possible during

laparoscopic surgery in all patients who received the highest dose (0.05 kg/mg) of CRGD-ZW800-1, with an injection time window ranging from 2-18 h prior to surgery.

CRGD-ZW800-1 was engineered with rather unique chemical structure and physicochemical properties. When coupled to the zwitterionic NIR fluorophore ZW800-1, CRGD-ZW800-1 itself becomes a “zwitterion” with polyionicity balanced both geometrically and electronically over the surface of the molecule, and with a net charge of 0 at pH 7.4 (Figure 6). Our hypothesis is that zwitterionic chemical structures exhibit unusually low non-specific background uptake and binding *in vivo*. To date, this hypothesis appears to hold true in chemical structures as diverse as quantum dots and small molecules, and in species ranging from rodent, pig, and human.<sup>18,30,31,32,33</sup> In fact, a previously published comparison of CRGD-ZW800-1 to both CRGD-IRDYE800-CW and CRGD-CY5.5 suggested that although signal strengths were similar for all three contrast agents, background was reduced for CRGD-ZW800-1 leading to a much higher TBR.<sup>31</sup> CRGD-ZW800-1 appears to be yet another example where in human, too, non-specific background can be reduced significantly by combining zwitterionicity with sufficient washout time, thus improving the TBR. Finally, many zwitterionic molecules, such as CRGD-ZW800-1, exhibit renal-predominant clearance, thus providing rather rapid elimination from the body, and importantly, low non-specific fluorescence in bowel.

CRGD is a clinically well-known peptide that binds to a wide range of integrins, including  $\alpha\nu\beta 1$ ,  $\alpha\nu\beta 3$ ,  $\alpha\nu\beta 5$ ,  $\alpha\nu\beta 6$ , and  $\alpha\nu\beta 8$ .<sup>23,24</sup> The specificity of CRGD for these integrins was previously demonstrated and also showed that  $\alpha\nu\beta 6$  negative tumors internalized CRGD-ZW800-1 due to overexpression of  $\alpha\nu\beta 3$  and/or  $\alpha\nu\beta 5$ .<sup>17</sup> For this study, integrin  $\alpha\nu\beta 6$  was chosen for immunohistochemistry as different studies have shown that it has a higher overexpression on malignant epithelial tumors, including colorectal cancer, compared to the other integrins.<sup>17,23,24,34</sup> Furthermore, it is known that normal epithelial cells have low basal  $\alpha\nu\beta 6$  expression and that an overexpression is often considered an indicator for tumor localization as it is habitually detected in epithelial cancers.<sup>20-22</sup> Interestingly, integrin  $\alpha\nu\beta 6$  is also upregulated in neovasculature and wound keratinocytes of skin epidermis during wound healing.<sup>23,35-39</sup> The coincidental finding in a healthy volunteer with a wound on the hand at the time of CRGD-ZW800-1 administration confirmed this, and provided indirect evidence that CRGD-ZW800-1 was hitting its target. However, this finding also serves as a reminder that CRGD-binding integrins are upregulated in benign conditions such as wounds, thrombotic lesions, vascular diseases, and autoimmune diseases, and requires the surgeon to use their clinical judgement when interpret-

ing NIR fluorescence images.<sup>40</sup> In the Phase II study, all resected colon tumors showed a strong positive overexpression of integrin  $\alpha\nu\beta 6$ , whereas normal mucosa showed only mild expression, and NIR fluorescence intensity correlated with this pattern. As suggested, multiple integrins could be contributing to the high TBR found in this study.

After IV administration, some fraction of CRGD-ZW800-1 binds its target and likely becomes internalized, helping explain why less than 100% of the dose is retrieved in urine. Confirming preclinical studies and previous clinical studies with ZW800-1, a large fraction of the dose enhances the ureters during colon resections in patients who received CRGD-ZW800-1 2-4 h prior to surgery.<sup>18</sup> The longer injection time window of 18 h did not enable ureter fluorescence, as the fluorophore was already eliminated from the body. However, in case ureter visualization is desired, a separate IV bolus of ZW800-1 could be given perioperatively for ureter enhancement to help prevent iatrogenic injury.<sup>18</sup> It cannot be emphasized enough that clearance patterns are of great importance for fluorescent imaging agents, especially in the gastrointestinal tract. Imaging agents with renal clearance are superior as contamination of the liver and intestines by bile are bypassed, resulting in cleaner intraoperative images without high background fluorescence in the viscera.

In lymph nodes, a noteworthy finding was  $\alpha\nu\beta 6$  expression in the metastasis-containing lymph nodes, while normal lymph nodes showed negative expression. This finding suggests  $\alpha\nu\beta 6$  integrin is not only involved in the pathogenesis of colon cancer, but might also be involved in the lymphatic metastasis of colon cancer. As expected, the MFI in tumor positive lymph nodes increased as the dose increased. Yet, when a longer injection time window was implemented, the MFI of tumor positive lymph nodes decreased. This can possibly be explained by the fact that more time permits residual contrast agent in lymph nodes to be washed out. Additionally, this is most likely also the source for the decrease in false-positives from 27% to 13% (0.05 mg/kg 2-4 h vs 0.05 mg/kg 18 h). The shorter injection time window of 2-4 h results in a higher fluorophore accumulation at the primary tumor site, which consequently diffuses away through the lymphatic system resulting in non-specific staining of lymph nodes (i.e. false positives). This confirms that dose and clearance (i.e. timing) are major contributors to the accuracy of lymph node detection.

The future use of contrast agents like CRGD-ZW800-1 is for real-time margin detection in colorectal tumors, and especially lower rectal tumors, as well as detection of metastases in lymph nodes. Circumferential resection margin involvement in rectal tumors is an important prognostic factor for survival, development of local recurrence, or distant metastasis.<sup>41</sup> In this first-in-human

feasibility study, we purposely included only colon cancers to evaluate tumor detection feasibility, as the majority of rectal cancers are treated with neoadjuvant chemoradiation, which can result in impaired tumor detection. In addition, experience has shown that mesorectal fat around rectal tumors is often too thick for adequate intraoperative imaging. We were surprised, therefore, to see tumors through the full thickness of bowel at relatively low dose levels. Overall, the *ex vivo* results on colon tumors and lymph nodes are much more important for future margin and metastasis detection, and suggest that CRGD has a reasonably high sensitivity and specificity for both applications. In addition, we envision two possible roles for CRGD-ZW800-1 in the setting of neoadjuvant therapy. First, because of NIR fluorescence's high inherent contrast, it could help find small nests of viable tumor intermixed within a fibrotic response after neoadjuvant therapy. Second, using NIR fluorescence colonoscopy, it could help assess the duration of clinical complete responses in "watch and watch" protocols. Of course, the present feasibility study did not include patients treated with neoadjuvant therapy, so these issues will have to be explored in future clinical trials.

The main goals of these Phase I and II studies were to demonstrate safety of CRGD-ZW800-1 and its feasibility in tumor detection in cancer patients. The efficacy of CRGD-ZW800-1 for real-time margin assessment in difficult cases, such as after lower rectal tumor resections, will need to be assessed in a larger follow-up study. With respect to dose and timing of imaging, both require further optimization. Background in normal tissues was low even at the highest injected dose, suggesting that further dose increases should be studied for the intraoperative use in laparoscopic procedures. Similarly, there appears to be a significant advantage of long systemic clearance times as more unbound fluorophore can be eliminated from the body and flushed out of non-involved lymph nodes. The longer injection time window of 18 hours should be validated in a subsequent study, as it has shown to provide superior TBRS and therefore better recognition of malignant tissue for resection and margin assessment. In addition to optimization of dose and timing in colon cancer, multiple other tumor types, including pancreas, breast, brain, and head and neck tumors overexpress various integrins, and almost all tumors overexpress integrins  $\alpha v \beta 6$  or  $\alpha v \beta 5$  on their neovasculature.<sup>17,19,34</sup> Preclinically, CRGD-ZW800-1 allowed fluorescence imaging of these tumors. It will therefore be interesting to study the effectiveness of CRGD-ZW800-1 in a variety of other cancer surgeries.

## REFERENCES

- Torre LA, Bray F, Siegel RL, Ferlay J, Lortet-Tieulent J, Jemal A. Global cancer statistics, 2012. *CA Cancer J Clin*. 2015;65(2):87-108.
- Navarro M, Nicolas A, Ferrandez A, Lanas A. Colorectal cancer population screening programs worldwide in 2016: An update. *World J Gastroenterol*. 2017;23(20):3632-3642.
- Giorgi Rossi P, Vicentini M, Sacchetti C, et al. Impact of Screening Program on Incidence of Colorectal Cancer: A Cohort Study in Italy. *Am J Gastroenterol*. 2015;110(9):1359-1366.
- Arezzo A, Passera R, Scozzari G, Verra M, Morino M. Laparoscopy for rectal cancer reduces short-term mortality and morbidity: results of a systematic review and meta-analysis. *Surg Endosc*. 2013;27(5):1485-1502.
- Biondi A, Grosso G, Mistretta A, et al. Laparoscopic vs. open approach for colorectal cancer: evolution over time of minimal invasive surgery. *BMC Surg*. 2013;13 Suppl 2:S12.
- Kalady MF, de Campos-Lobato LF, Stocchi L, et al. Predictive factors of pathologic complete response after neoadjuvant chemoradiation for rectal cancer. *Ann Surg*. 2009;250(4):582-589.
- Maas M, Nelemans PJ, Valentini V, et al. Long-term outcome in patients with a pathological complete response after chemoradiation for rectal cancer: a pooled analysis of individual patient data. *Lancet Oncol*. 2010;11(9):835-844.
- van der Valk MJM, Hilling DE, Bastiaannet E, et al. Long-term outcomes of clinical complete responders after neoadjuvant treatment for rectal cancer in the International Watch & Wait Database (IWWD): an international multicentre registry study. *Lancet*. 2018;391(10139):2537-2545.
- Torres ML, McCafferty MH, Jorden J. The difficulty with localization of rectal cancer after neoadjuvant chemoradiation therapy. *Am Surg*. 2010;76(9):974-976.
- Ghadban T, Reeh M, Bockhorn M, et al. Minimally invasive surgery for colorectal cancer remains underutilized in Germany despite its nationwide application over the last decade. *Sci Rep*. 2018;8(1):15146.
- Trakarnsanga A, Akaraviputh T. Endoscopic tattooing of colorectal lesions: Is it a risk-free procedure? *World J Gastrointest Endosc*. 2011;3(12):256-260.
- Conaghan PJ, Maxwell-Armstrong CA, Garrioch MV, Hong L, Acheson AG. Leaving a mark: the frequency and accuracy of tattooing prior to laparoscopic colorectal surgery. *Colorectal Dis*. 2011;13(10):1184-1187.
- Boogerd LSF, Hoogstins CES, Schaap DP, et al. Safety and effectiveness of SGM-101, a fluorescent antibody targeting carcinoembryonic antigen, for intraoperative detection of colorectal cancer: a dose-escalation pilot study. *Lancet Gastroenterol Hepatol*. 2018;3(3):181-191.
- Hoogstins CES, Boogerd LSF, Sibinga Mulder BG, et al. Image-Guided Surgery in Patients with Pancreatic Cancer: First Results of a Clinical Trial Using SGM-101, a Novel Carcinoembryonic Antigen-Targeting, Near-Infrared Fluorescent Agent. *Ann Surg Oncol*. 2018;25(11):3350-3357.
- Hoogstins CE, Tummers QR, Gaarenstroom KN, et al. A Novel Tumor-Specific Agent for Intraoperative Near-Infrared Fluorescence Imaging: A Translational Study in Healthy Volunteers and Patients with Ovarian Cancer. *Clin Cancer Res*. 2016;22(12):2929-2938.
- Ishizawa T, Bandai Y, Ijichi M, Kaneko J, Hasegawa K, Kokudo N. Fluorescent cholangiography illuminating the biliary tree during laparoscopic cholecystectomy. *Br J Surg*. 2010;97(9):1369-1377.
- Handgraaf HJM, Boonstra MC, Prevoo H, et al. Real-time near-infrared fluorescence imaging using CRGD-ZW800-1 for intraoperative visualization of multiple cancer types. *Oncotarget*. 2017;8(13):21054-21066.
- de Valk KS, Handgraaf HJ, Deken MM, et al. A zwitterionic near-infrared fluorophore for real-time ureter identification during laparoscopic abdominopelvic surgery. *Nat Commun*. 2019;10(1):3118.
- Desgrosellier JS, Cheresh DA. Integrins in cancer: biological implications and therapeutic opportunities. *Nat Rev Cancer*. 2010;10(1):9-22.
- Bandyopadhyay A, Raghavan S. Defining the role of integrin alphavbeta6 in cancer. *Curr Drug Targets*. 2009;10(7):645-652.
- Koivisto L, Bi J, Hakkinen L, Larjava H. Integrin alphavbeta6: Structure, function and role in health and disease. *Int J Biochem Cell Biol*. 2018;99:186-196.
- Niu J, Li Z. The roles of integrin alphavbeta6 in cancer. *Cancer Lett*. 2017;403:128-137.
- Humphries JD, Byron A, Humphries MJ. Integrin ligands at a glance. *J Cell Sci*. 2006;119(Pt 19):3901-3903.
- Ruoslahti E. RGD and other recognition sequences for integrins. *Annu Rev Cell Dev Biol*. 1996;12:697-715.
- Sharma R, Kallur KG, Ryu JS, et al. Multicenter Reproducibility of 18F-Fluciclatide PET Imaging in Subjects with Solid Tumors. *J Nucl Med*. 2015;56(12):1855-1861.
- Beer AJ, Lorenzen S, Metz S, et al. Comparison of integrin alphaVbeta3 expression and glucose

- metabolism in primary and metastatic lesions in cancer patients: a PET study using 18F-galacto-RGD and 18F-FDG. *J Nucl Med.* 2008;49(1):22-29.
- 27 Beer AJ, Niemeier M, Carlsen J, et al. Patterns of alphavbeta3 expression in primary and metastatic human breast cancer as shown by 18F-galacto-RGD PET. *J Nucl Med.* 2008;49(2):255-259.
- 28 Sibinga Mulder BG, Handgraaf HJ, Vugts DJ, et al. A dual-labeled CRGD-based PET/optical tracer for pre-operative staging and intraoperative treatment of colorectal cancer. *Am J Nucl Med Mol Imaging.* 2018;8(5):282-291.
- 29 Verbeek FP, van der Vorst JR, Tummers QR, et al. Near-infrared fluorescence imaging of both colorectal cancer and ureters using a low-dose integrin targeted probe. *Ann Surg Oncol.* 2014;21 Suppl 4:S28-537.
- 30 Choi HS, Liu W, Misra P, et al. Renal clearance of quantum dots. *Nat Biotechnol.* 2007;25(10):1165-1170.
- 31 Choi HS, Gibbs SL, Lee JH, et al. Targeted zwitterionic near-infrared fluorophores for improved optical imaging. *Nat Biotechnol.* 2013;31(2):148-153.
- 32 Choi HS, Nasr K, Alyabyev S, et al. Synthesis and *in vivo* fate of zwitterionic near-infrared fluorophores. *Angew Chem Int Ed Engl.* 2011;50(28):6258-6263.
- 33 Hyun H, Bordo MW, Nasr K, et al. cGMP-Compatible preparative scale synthesis of near-infrared fluorophores. *Contrast Media Mol Imaging.* 2012;7(6):516-524.
- 34 Schittenhelm J, Klein A, Tatagiba MS, et al. Comparing the expression of integrins alphavbeta3, alphavbeta5, alphavbeta6, alphavbeta8, fibronectin and fibrinogen in human brain metastases and their corresponding primary tumors. *Int J Clin Exp Pathol.* 2013;6(12):2719-2732.
- 35 AlDahlawi S, Eslami A, Hakkinen L, Larjava HS. The alphavbeta6 integrin plays a role in compromised epidermal wound healing. *Wound Repair Regen.* 2006;14(3):289-297.
- 36 Breuss JM, Gallo J, DeLisser HM, et al. Expression of the beta 6 integrin subunit in development, neoplasia and tissue repair suggests a role in epithelial remodeling. *J Cell Sci.* 1995;108 ( Pt 6):2241-2251.
- 37 Clark RA, Ashcroft GS, Spencer MJ, Larjava H, Ferguson MW. Re-epithelialization of normal human excisional wounds is associated with a switch from alpha v beta 5 to alpha v beta 6 integrins. *Br J Dermatol.* 1996;135(1):46-51.
- 38 Eslami A, Gallant-Behm CL, Hart DA, et al. Expression of integrin alphavbeta6 and TGF-beta in scarless vs scar-forming wound healing. *J Histochem Cytochem.* 2009;57(6):543-557.
- 39 Haapasalmi K, Zhang K, Tonnesen M, et al. Keratinocytes in human wounds express alpha v beta 6 integrin. *J Invest Dermatol.* 1996;106(1):42-48.
- 40 Adorno-Cruz V, Liu H. Regulation and functions of integrin alphaz in cell adhesion and disease. *Genes Dis.* 2019;6(1):16-24.
- 41 Wibe A, Rendedal PR, Svensson E, et al. Prognostic significance of the circumferential resection margin following total mesorectal excision for rectal cancer. *Br J Surg.* 2002;89(3):327-334.

**FIGURE 1 Intraoperative colon tumor imaging.** (A) Intraoperative imaging of the colon tumor was performed using the Quest Spectrum MIS imaging system in a patient who received 0.05 mg/kg CRGD-zw800-1 18 h prior to surgery. (B) After resection of the specimen from (A), back table imaging was performed with the Quest Spectrum open system for additional fluorescence assessment.

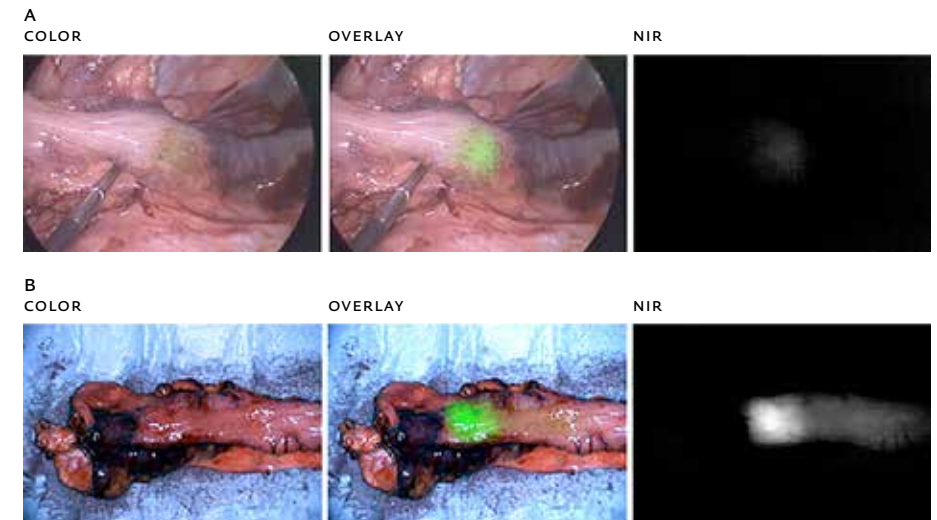


**FIGURE 2** Mean fluorescence intensity (MFI) of tumor and normal mucosa and *ex vivo* tumor-to-background ratio (TBR) per dose level using the Pearl Trilogy Imaging System. The stars symbolize a significant MFI difference between tumor and normal mucosa in (A) and a significant increase in *ex vivo* TBR in (B). Figure (c) displays an example illustrating the fluorescence in tumor and normal mucosa.

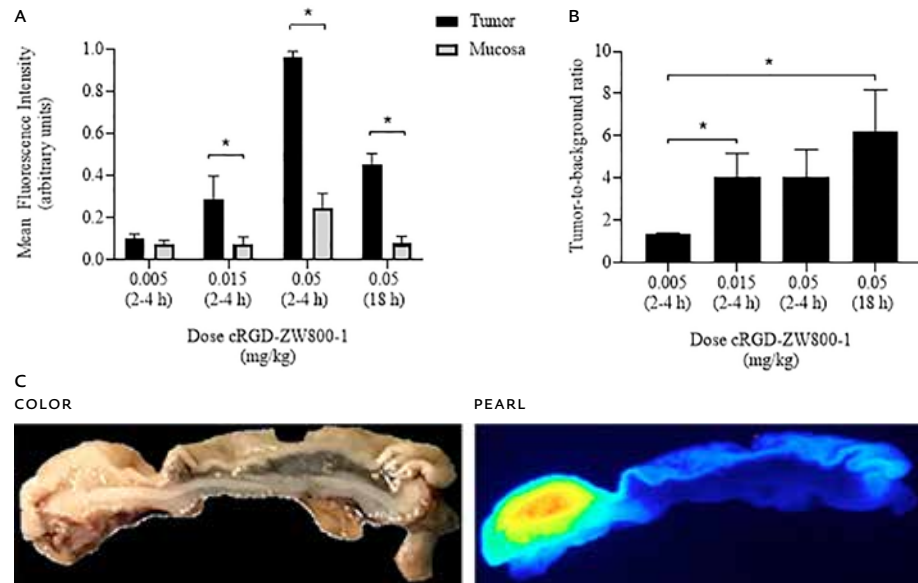


**FIGURE 3** Immunohistochemistry staining of  $\alpha v \beta 6$  on formalin-fixed paraffin-embedded colon tumor tissue and normal mucosa. Images were obtained with the Odyssey CLx Imaging system. The colon tumor shows a positive strong  $\alpha v \beta 6$  expression and fluorescence, whereas normal mucosa shows a milder  $\alpha v \beta 6$  expression with intensely less fluorescence (same fluorescence settings).

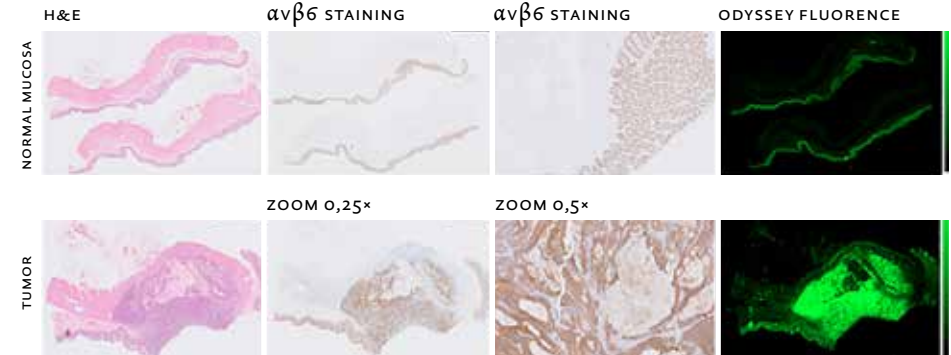
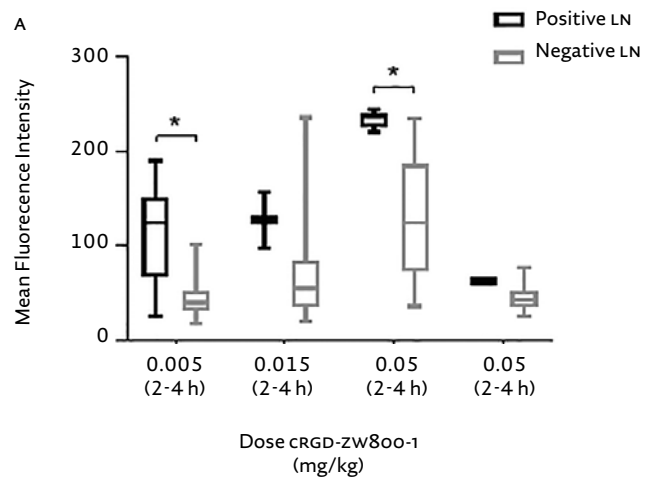


**FIGURE 4** Gross macroscopy of a colon tumor (intraluminal aspect) in a patient who received 0.05 mg/kg CRGD-ZW800-1 2-4 h prior to surgery. This image illustrates the visible difference in fluorescence in tumor and normal mucosa, conform the microscopic images. Images were obtained with the Quest open imaging system.



**FIGURE 5** *Ex vivo* lymph node detection with the Lab-FLARE Model R1 on fresh lymph node tissue. (A) MFI of tumor positive and tumor negative lymph nodes per dose level with test characteristics per dose. The star symbolizes a significant MFI difference. (B) Gross macroscopic bread-loaf containing tumor (red dashed circle) and a tumor-positive lymph node (black dashed circle), imaged with the Lab-FLARE Model R1



	0.005 mg/kg (2-4 h)	0.015 mg/kg (2-4 h)	0.05 mg/kg (2-4 h)	0.05 mg/kg (18 h)
Sensitivity	74%	100%	100%	100%
Specificity	79%	69%	73%	87%
Positive predictive value	71%	6%	70%	33%
Negative predictive value	82%	100%	100%	100%
False positive rate	21%	33%	27%	13%
Accuracy	77%	68%	83%	88%

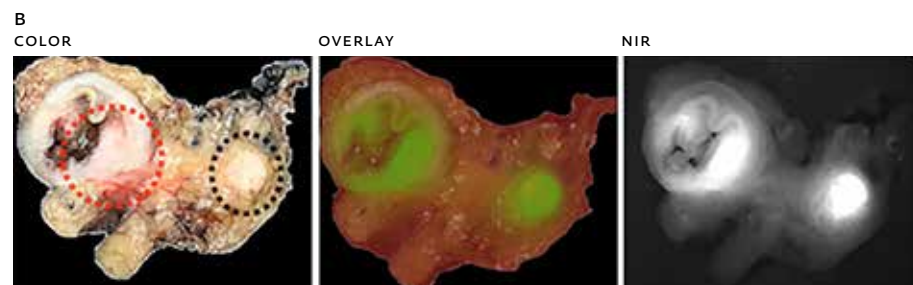
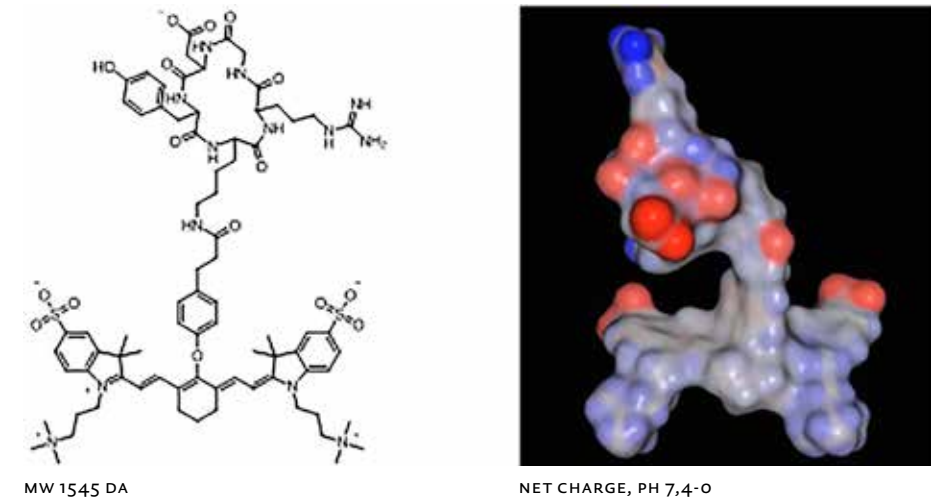


**FIGURE 6** Chemical structure CRGD-ZW800-1.





PART 2

**FLUORESCENCE  
IMAGING  
WITH SGM-101**

Chapter v

**DOSE-FINDING STUDY OF A  
CEA-TARGETING AGENT, SGM-101, FOR  
INTRAOPERATIVE FLUORESCENCE  
IMAGING OF COLORECTAL CANCER**

*Ann Surg Oncol.* 2021 Mar;28(3):1832-1844.,

doi: 10.1245/s10434-020-09069-2

*Supplementary data available online*

KS de Valk<sup>1,2</sup>, MM Deken<sup>2</sup>, DP Schaap<sup>3</sup>, RPJ Meijer<sup>1,2</sup>,  
LS Boogerd<sup>2</sup>, CE Hoogstins<sup>1,2</sup>, MJM van der Valk<sup>2</sup>,  
IM Kamerling<sup>1</sup>, SS Bhairosingh<sup>2</sup>, B Framery<sup>4</sup>,  
DE Hilling<sup>2</sup>, KCMJ Peeters<sup>2</sup>, FA Holman<sup>2</sup>, M Kusters<sup>5</sup>,  
HJ Rutten<sup>3</sup>, F Cailler<sup>4</sup>, J Burggraaf<sup>1</sup>, AL Vahrmeijer<sup>2</sup>

1. Centre For Human Drug Research, Leiden, NL

2. Department of Surgery, Leiden University Medical Center, Leiden, NL

3. Department of Surgery, Catharina Hospital Eindhoven, Eindhoven, NL

4. SurgiMab, Montpellier, FR

5. Department of Surgery, Amsterdam University  
Medical Center, Amsterdam, NL

## ABSTRACT

Carcinoembryonic antigen (CEA) is overexpressed in colorectal cancer (CRC), making it an optimal target for fluorescence imaging. A phase I/II study was designed to determine the optimal imaging dose of SGM-101 for intraoperative fluorescence imaging of primary and recurrent CRC. Patients were included and received a single dose of SGM-101 at least 24 hours prior to surgery. Patients who received routine anticancer therapy (i.e. radiotherapy or chemotherapy) also were eligible. A dedicated near-infrared imaging system was used for real-time fluorescence imaging during surgery. Safety assessments were performed and SGM-101 efficacy was evaluated per dose level to determine the most optimal imaging dose. Thirty-seven patients with CRC were included in the analysis. Fluorescence was visible in all primary and recurrent tumors. In seven patients no fluorescence was seen; all were confirmed as pathological complete responses after neoadjuvant therapy. Two tumors showed false positive fluorescence. In the 37 patients, a total of 97 lesions were excised. The highest mean intraoperative tumor-to-background ratio (TBR) of 1.9 ( $p=0.019$ ) was seen in the 10 mg dose. This dose showed a sensitivity of 96%, specificity of 63%, and negative predictive value of 94%. Nine patients (24%) had a surgical plan alteration based on fluorescence, with additional malignant lesions detected in six patients. The optimal dose was established at 10 mg four days before surgery. The results accentuate the potential of SGM-101 and designated a promising base for the multinational phase III study which enrolled the first patients in June 2019.

## INTRODUCTION

Colorectal cancer (CRC) is one of the most commonly diagnosed cancers and fourth leading cause of cancer death worldwide.<sup>1</sup> Yet, mortality rates have been stabilizing because of improved screening programs, which have led to earlier detection and prevention through polypectomy.<sup>2</sup> Additionally, improvements in neoadjuvant therapies have contributed to the subsiding trend in mortality.<sup>3</sup> Neoadjuvant (chemo-)radiation followed by curative surgery is currently the definitive treatment method for advanced rectal cancer. Neoadjuvant chemoradiation has proven to effectively downstage primary tumors in about 20% of patients, where a pathologic complete response (pCR) is realized, with advantageous long-term outcomes.<sup>3-5</sup> Nevertheless, surgery remains the cornerstone treatment of CRC. During surgery, surgeons rely on visual inspection and palpation assessments to differentiate between malignant and benign tissue for resection. Yet, discriminating between these

tissues can be challenging after neoadjuvant therapy, due to tumor reduction with subsequent diminished tumor visibility intraoperatively. Also, formation of fibrotic tissue may impair proper assessment of the surgical field. Reduced tumor visibility during surgery can result in unnecessary resections (i.e. benign tissue) or residual malignant tissue (i.e. millimeter lesions or positive resection margins). Therefore, enhancing intraoperative tumor visibility can be a helpful tool for surgeons to aid in achieving R0 resections for better survival.

Near-infrared (NIR) fluorescence imaging is a rapidly evolving technique that allows real-time detection of malignant tissue during surgery.<sup>6</sup> This technique enhances tumor visibility as it enables the visualization of resection margins and millimeter malignant lesions that are undetectable with the naked eye or preoperative imaging techniques.<sup>7-10</sup> SGM-101 is a tumor-targeting agent consisting of the fluorophore BM-104 covalently bound to the monoclonal antibody that targets carcinoembryonic antigen (CEA), a well-known tumor marker for CRC. CEA is overexpressed in >90% of CRC cells, with limited expression in normal tissue making it an optimal imaging target for CRC.<sup>11,12</sup> Preclinical studies with SGM-101 have shown favorable toxicity profiles in animals, clear delineation of tumors in different colon cancer models, capacity to penetrate and target millimeter sized tumor nodules and importantly, make them detectable with fluorescence.<sup>13,14</sup> Boogerd et al. published the first efficacy results of SGM-101 in CRC patients.<sup>8</sup> Results showed SGM-101 up to 10 mg was safe, offered successful detection of primary, recurrent and metastasized CRC during surgery, and led to an altered treatment plan in one third of the patients.<sup>8</sup> Driven by these results, the study was continued to evaluate the safety of higher doses, efficacy of SGM-101 in a larger and more homogenous cohort and determine the optimal imaging dose of SGM-101 for the detection of colorectal neoplastic lesions in primary and recurrent CRC patients.

## METHODS

### Study design

An ascending dose, exploratory study was performed in 37 patients with primary or recurrent CRC (*Figure 1*). Besides safety and efficacy assessments, the study aimed at determining the most optimal dose of SGM-101 for intraoperative fluorescence imaging of colorectal neoplastic lesions. 21 of the 37 patients (nine primary and 12 recurrent CRC) have previously been described in the pilot analysis by Boogerd et al.<sup>8</sup> The study was a collaborative project performed in the Netherlands between the Centre for Human Drug Research (CHDR) in Leiden and the departments of surgery of Leiden University Medical

Center (LUMC) in Leiden and Catharina Hospital Eindhoven (CZE) in Eindhoven. The study was approved by a certified medical ethics review board (Stichting BEBO, Assen, the Netherlands) and performed in accordance with the laws and regulations on drug research in humans of the Netherlands. The study is registered in ClinicalTrials.gov under identifier NCT02973672.

The study was conducted in 5 dosing cohorts, where a single dose of SGM-101 (dose range: 5 mg, 7.5 mg, 10 mg, 12.5 mg or 15 mg per patient) was administered intravenously over 30 min at least 24 h before surgery. Four patients were included in the 5 mg and 7.5 mg dose levels respectively, 19 patients (additional patients included at optimal dose) were included in the 10 mg dose, and five patients were included in the 12.5 mg and 15 mg dose levels, respectively. Patients were admitted to CHDR for SGM-101 administration and were clinically observed for at least 6 h for safety assessments. The dosing-surgery interval of at least 24 h was based on observations in preclinical animal studies and the first-in-human trial (NCT02784028), which showed a sufficient fluorescent signal between 24 and 72 h.<sup>13</sup> The first five patients in this study were dosed two days before surgery. However, the fluorescence results obtained in these patients were not optimal due to strong background fluorescence. This was most likely due to the high concentration of SGM-101 that was still present in the systemic circulation after two days.<sup>8</sup> Consequently, a longer dosing-surgery interval of four days was chosen in the subsequent patients. It was also explored if fluorescence imaging was possible six days after SGM-101 administration. Doses were administered in an escalating manner, following review of safety and fluorescence data. In the cohort with the most optimal dose, additional patients were included for further appraisal. Due to the exploratory nature of the study, population size was not based on statistical considerations. Eligible CRC patients were selected during multidisciplinary team meetings and approached at the outpatient clinic by the treating surgeon. All subjects provided written informed consent prior to the start of any study-related procedure.

### **Surgery**

Fluorescence imaging during surgery was performed with the Quest Spectrum Platform (Quest Medical Imaging BV, Middenmeer, The Netherlands), a CE-marked dedicated imaging system optimized for measurements in two NIR channels (700 to 830 nm and 830 to 1100 nm).<sup>15</sup> Before fluorescence imaging was initiated, visual and/or palpation assessments were done under white light by the surgeon to identify the lesion(s) of interest. Fluorescence imaging was performed prior to surgical resection, after resection to identify any remaining fluorescence in the surgical field and on the back table. In case fluorescence im-

aging was warranted throughout other moments, such as during additional resections or inspection, this could be employed. Each lesion was recorded as clinically suspect for malignancy or not and as fluorescent or non-fluorescent. The efficacy of SGM-101 was determined by calculating the tumor-to-background ratio (TBR) of each lesion (intraoperative and back table measurements) and assessing its concordance with tumor histopathology, to determine the optimal dose. Intraoperative TBR was defined as the fluorescent signal of the lesion inside the patient prior to surgical resection. Back table TBR was defined as the fluorescent signal of the lesion after resection on the back table. Back table imaging was implemented to evaluate the resection margins and to determine fluorescence that was possibly not visible intraoperatively. Removal of additional tissue (re-resections and tissue resections elsewhere) or changes in surgical plans due to fluorescence were considered an alteration of initial surgical plan. If removal of a clinically non-suspect but fluorescent lesion would lead to a larger or complex resection, a frozen section was performed to confirm whether the resection was required. In cases where removal of additional tissue was minor without consequences for the patient, it was the decision of the surgeon.

### **Concordance**

The resected lesion(s) were sent to the pathology department for assessment according to hospital protocol using standardized Hematoxylin and Eosin (H&E) staining. Of each lesion, tumor status was assessed and correlated with the intraoperative or back table fluorescence to determine concordance. Four different conclusions could be made: a malignant fluorescent lesion was regarded as a true positive (TP); a benign fluorescent lesion was regarded as a false positive (FP); a malignant non-fluorescent lesion was regarded as a false negative (FN); and a benign non-fluorescent lesion was regarded as a true negative (TN). In addition, immunohistochemistry for CEA expression was performed on 4 µm formalin-fixed, paraffin-embedded sections. To correlate SGM-101 fluorescence with tumor status and CEA expression on a microscopic level, sections were scanned using the Odyssey imager (LI-COR Biosciences, NE, USA).

### **Fluorescence and statistical assessment**

Fluorescence assessments were done by study personnel who were also present during surgery. After surgery, images were viewed and processed using the software Architector Vision Suite version 1.8.3 (Quest innovations, Middenmeer, the Netherlands) and analyzed with ImageJ 1.51j8 (National Institute of Health, MD, USA) to quantify the TBR. The TBR was calculated by drawing a region of interest (ROI) around tumor fluorescence and the directly surrounding background

area. The ROI of the tumor was then subtracted from the background. The quotient of the tumor and background signal strength constituted the TBR. This was done for every fluorescent lesion identified. The efficacy analysis was done with SAS software version 9.4 (SAS Institute, NC, USA).

## RESULTS

From January 2016 to January 2019, a total of 37 patients (23 males and 14 females) with primary (n = 16) or recurrent (n = 21) CRC were analysed. The majority of patients (30/37 = 81%) received neoadjuvant therapy, consisting of either chemoradiation (n=27), radiation alone (n=1) or chemotherapy alone (n=2). The rest of the patients (7/37 = 19%) had surgery first. All patients received SGM-101 and underwent surgery according to standard of care. The performed procedures included low anterior resections (n=13), abdominoperineal resections (n=10), sigmoid resections (n=2), recurrence resections (n=8), total exenterations (n=2), hemicolectomy (n=1) and a pancreaticoduodenectomy with colon resection (n=1). *Table 1* provides a patient overview, including demographics, dosing-surgery intervals, diagnosis, type of neoadjuvant therapy, type of surgery and concordance of the primary and recurrent tumors per dose level.

### Safety and tolerability

All doses up to 15 mg SGM-101 were well tolerated. None of the patients experienced an allergic reaction or event that was considered of clinical importance or led to discontinuation. None of the reported adverse events (AEs) or serious adverse events (SAEs) had a direct causal relationship to SGM-101. A total of 36 post-dose AEs and five SAEs were recorded in 37 patients (*Supplementary Table 1*). The majority of the AEs were unrelated (n=30) to SGM-101 and considered general postoperative complications. Six AEs were judged as possible (n=5) or unlikely (n=1) related and included symptoms such as headache (n=3), abdominal pain (n=1), rash (n=1) and redness of a finger (n=1). The five SAEs (renal injury and paralytic ileus in the 5 mg dose, pyelonephritis in a patient receiving 10 mg, hepatic necrosis most likely due to an infection in the 12.5 mg dose and cerebral hemorrhage in a patient receiving 15 mg) were all interpreted as unrelated to SGM-101 and related to the surgical procedure or disease. Patients dosed with a higher dose of SGM-101 did not experience more AEs or SAEs.

### Primary and recurrent colorectal tumors

In all primary and residual tumors (n=27), fluorescence was visible during surgery. There were seven patients, all treated with neoadjuvant therapy, where no fluorescence could be detected in the primary (n=4) or recurrent (n=3) tumor.

These patients had a PCR, conforming the absence of fluorescence. *Figure 2* shows an example of intraoperative fluorescence in a true positive tumor and absence of fluorescence in a true negative case (PCR after neoadjuvant therapy). One tumor was excluded as no fluorescence was measured due to logistic reasons. In two recurrent CRC tumors, fluorescence was detected, however, histopathology showed no malignancy (*Table 1*). One of these false positives was a suspected recurrent tumor mass near the left iliopsoas muscle, which emitted fluorescence. Histopathology showed extensive necrosis and fibrosis with mucin producing cells positive for CEA, possibly clarifying the binding of SGM-101.<sup>8</sup> The second false positive was a suspected recurrent tumor against the retroperitoneum with evident intraoperative and back table fluorescence. Histopathology showed fat tissue with fibrosis and inflammation without malignancy. Additional immunohistochemistry showed weak CEA expression in epithelial tissue, conceivably explaining SGM-101 binding and fluorescence (*Supplementary Fig. 1*).

### Total excised lesions

In 37 patients, a total of 97 lesions were excised, including the primary and recurrent tumors (*Supplementary Table 2*). Of the 97 excised lesions, 49 lesions were malignant and 48 lesions benign. Of the 49 malignant lesions, 47 lesions were true positive (96%). Unfortunately, not all true positive lesions could be identified intraoperatively due to anatomic positioning, but were fluorescent on the back table after excision. Merely 20 of the 47 true positive lesions (43%) were visible intraoperatively. Two malignant lesions were false negative (no intraoperative or back table fluorescence). One false negative contained a conglomerate of three metastasized lymph nodes with adenocarcinoma (10 mg dose) and CEA expression in immunohistochemistry. The second false negative was a frozen section biopsy of a resected tumor with mucinous adenocarcinoma (12.5 mg dose). This biopsy was performed to evaluate the resection margin, as the surgeon had doubts on the radicality, despite the absence of fluorescence. Conversely, immunohistochemistry of the biopsy showed no CEA expression which complements the absence of fluorescence. Of the 48 benign lesions, 26 lesions were true negatives (54%). There were 22 false positive lesions, which included lymph nodes, reproductive organs (i.e. ovaries and vesicula seminalis) and frozen section biopsies of resection planes and tissue around the sacrum and pelvic floor. These biopsies were taken to determine whether an additional resection was needed.

### Additional lesions and alteration in surgical plan

Initial surgical plan alterations due to SGM-101 fluorescence occurred in 12 of the 37 patients (*Table 3*). In nine patients the alteration was warranted (24%). In seven

of these patients additional tissue was removed after initial tumor resection. A total of eight additional malignant lesions were identified in six patients, which were otherwise left behind. These lesions were not visible with white light and clinically unsuspect for malignancy. They were only visible with fluorescence with a mean intraoperative TBR of 1.8 (SD 0.06). Lesions were generally detected after initial tumor resection when imaging of the surgical field was performed to assess remaining fluorescence. Two patients had downstaging of the surgical plan due to absence of fluorescence, confirmed benign with frozen sections. Hence, the resections in these two patients were assessed as radical which resulted in tissue salvaging around the lateral piriformis in one patient and omitting intraoperative radiotherapy (IORT) on the sciatic nerve in the second patient. In the remaining three patients, the additional tissue removed were false positive. The false positive tissue removed was minor and did not have consequences for the patient. Details on the surgical plan alterations are provided in *Table 3*.

### Performance and optimal dose

The mean intraoperative TBR of the true positive lesions for the 5 mg, 7.5 mg, 10 mg, 12.5 mg and 15 mg dose levels are 1.5 (SD 0.07), 1.6 (SD 0.30), 1.9 (SD 0.15), 1.6 (SD 0.38) and 1.1 (SD 0.00), respectively (*Figure 3*;  $p=0.019$  one-way ANOVA). Fluorescence did not improve at higher doses. Surgical observations and TBR measurements showed 10 mg SGM-101 with a dosing-surgery interval of four days was the most optimal, resulting in additional patient inclusions in this dosing regime. It should be taken into consideration that not all patients in the study had the same dosing-surgery interval. Due to relatively small patient numbers in each dose, the TBR was calculated per dose and not split per dosing-surgery interval. Nonetheless, the majority of patients (27 of 37 patients) had a dosing-surgery interval of four days. The dose 10 mg revealed a sensitivity of 96%, a specificity of 63% and a negative predictive value of 94% (*Table 2*). *Supplementary Figure 2* provides an overview of the back table TBRs.

## DISCUSSION

This dose finding study in primary and recurrent CRC patients showed that doses up to 15 mg SGM-101 are safe, but that 10 mg SGM-101 was the most optimal in exposing CRC and, more importantly, in detecting neoplastic lesions that were invisible with white light. A strong benefit of SGM-101 in the study was the identification of additional malignant lesions that were clinically unsuspect for malignancy or invisible with the naked eye, but only detectable under

fluorescence. In six patients, SGM-101 was of additional value as it led to the removal of additional malignant tissue which was otherwise left behind. This bares great potential as current preoperative imaging modalities are known to have a detection threshold of approximately 1 cm.<sup>16</sup> Due to this limited resolution, lesions less than 1 cm can be left undetected, causing undesirable uncertainty in oncologic staging and treatment.<sup>8,16</sup>

A noteworthy result is that SGM-101 has a high NPV (94%) and sensitivity (96%) with the dose of 10 mg, making it a promising tool for the management of CRC. This opens the possibility for clinical decision making based on fluorescence, with the prospect of salvaging tissue. It also accentuates SGM-101 can play an important role in watch-and-wait (w&w) strategies after neoadjuvant therapy, when combined with NIR endoscopy.<sup>17</sup> w&w was implemented to avoid morbidity by preventing unnecessary surgery in patients with a clinical complete response (CCR) after neoadjuvant therapy.<sup>18,19</sup> In recent years, w&w has been gaining popularity as different studies have shown it is a good alternative to major surgery with little oncological risk.<sup>17,20,21</sup> The identification of CCR is best accomplished with a combination of rectal exam, endoscopy, and high resolution imaging (i.e magnetic resonance imaging (MRI)).<sup>3,22,23</sup> Since local regrowths occur in 25% of all patients and is almost exclusively (97%) situated within the bowel wall<sup>3</sup>, endoscopy is the preferred screening technique. The use of NIR endoscopy can offer a safe and effective method to monitor tumor regrowth in real-time. Malignant tissue, especially small regrowths which are negligible on current imaging modalities, can be probed efficiently using NIR light and perhaps improve the early detection in w&w.<sup>16</sup> In this current report, all patients with a PCR after neoadjuvant therapy (n=7) had no fluorescence on the remaining scar tissue, substantiating the value of SGM-101 in complete response cases.

Intraoperative and back table TBR measurements were obtained to evaluate the performance of SGM-101 and concordance to histopathology at each dose level. Intraoperative TBR is considered leading, as the decision to resect tissue is done during surgery. On the other hand, decision making on intraoperative fluorescence has its drawbacks for deep-seated tumors, precluding proper imaging due to the anatomic position. The use of NIR light allows detection of structures or tissues up to 1 cm in depth. Yet, this penetration depth has shown to be insufficient for mesorectal fat around deeply seated rectal tumors, as this is too thick.<sup>8</sup> Therefore, back table imaging should also be taken into account, especially for the recognition of resection margins in possible R1 resections. Another profit of back table imaging can be to improve the guidance of IORT in cases of tight resection margins. The majority of patients underwent surgery in CZE, which is a tertiary referral center for IORT. Indications for IORT have

been described before, and is applied in patients with close involved margins, such as in locally advanced and recurrent rectal cancer.<sup>24</sup> This has also been incorporated in Dutch Oncology Guidelines, suggesting that in aforementioned cases IORT may have added value for local control.

Since not all malignant lesions could be identified intraoperatively, mainly due to anatomic positioning and depth, it was decided concordance assessment should be based on both intraoperative and back table fluorescence. However, several considerations must be kept in mind with this approach. Combining intraoperative and back table fluorescence diminishes the chance that a lesion is labelled false negative, as it is not detected during the surgical procedure itself. Yet, back table imaging is necessary to provide essential information on resection margins and supplementary fluorescence assessment in cases of deep-seated tumors which restrict optimal intraoperative imaging, substantiating the combined approach.

A shortcoming of the study is the unequal amount of patients in each dose level, resulting in a sub-optimal comparison. Likewise, the dosing-surgery time interval varies between patients, possibly hampering a fair comparison of intraoperative TBRs per dose. Yet, all patients with an intraoperative TBR in the 10 mg dose had a dosing-surgery interval of 4 days. Furthermore, it is clear that a higher dose of 12.5 mg and 15 mg did not result in higher TBRs, which can conceivably be explained by the higher intensity of background fluorescence.

In the study, false positive lesions were found in 22 of the 97 excised lesions. False positive lesions could be explained by CEA positivity found in histiocytes within lymph nodes, in fibrotic and chronic inflamed tissue, as well as the presence of mucin producing cells, which express CEA, explaining SGM-101 uptake.<sup>8</sup> Hypotheses for the lesions without CEA expression may be the use of NIR light around the 700 nm wavelength. It is known that this wavelength has higher tissue auto-fluorescence when compared to 800 nm. Collagen-rich structures, calcifications or the sacral bone could have likely triggered fluorescence during surgery, due to its auto-fluorescence properties. Perhaps, conjugation of the anti-CEA monoclonal antibody to a NIR 800 nm dye could limit this problem. Studies have indicated that longer-wavelength dyes have increased penetration depth, enhanced sensitivity for small tumor deposits detection, and generally a lower background signal.<sup>25</sup> Several preclinical studies have been performed with anti-CEA conjugated to a NIR 800 nm dye, such as IRDYE-800CW, which revealed successful tumor specificity and distribution of the tracer.<sup>26,27</sup> Besides wavelength limitations, the enhanced permeability and retention (EPR) effect could also play a part in the high false positive rate, as hyper vascularization and compromised lymphatic drainage can result in non-specific accumu-

lation of SGM-101 in tissue.<sup>28,29</sup> It is however conspicuous that a majority of the false positives were found in the reproductive organs (i.e. ovaries and vesicula seminalis). Yet, why these organs emit fluorescence without containing tumor cells cannot clearly be explained and should be inspected in ensuing studies.

This study confirms that SGM-101 is a safe tumor-targeted fluorescence imaging agent for CRC. The dose 10 mg with a dosing-surgery interval of four days is the most favorable regimen for implementation and further exploration in CRC patients. The results emphasize the potential of SGM-101 and have led to a follow-up multinational phase III study to provide supportive data for changing the standard of care in CRC patients. A multicenter, randomized, controlled phase III study (NCT03659448) is currently ongoing evaluating SGM-101 in a larger homogenous population to assess the efficacy in terms of clinical benefits in additional lesion detection and its influence in radical resection (RO) rates, which should ultimately result in improved local control and overall survival in CRC patients.

## REFERENCES

- Arnold M, Sierra MS, Laversanne M, Soerjomataram I, Jemal A, Bray F. Global patterns and trends in colorectal cancer incidence and mortality. *Gut*. 2017;66(4):683-691.
- Center MM, Jemal A, Smith RA, Ward E. Worldwide variations in colorectal cancer. *CA Cancer J Clin*. 2009;59(6):366-378.
- van der Valk MJM, Hilling DE, Bastiaannet E, et al. Long-term outcomes of clinical complete responders after neoadjuvant treatment for rectal cancer in the International Watch & Wait Database (IWWDB): an international multicentre registry study. *Lancet*. 2018;391(10139):2537-2545.
- Maas M, Nelemans PJ, Valentini V, et al. Long-term outcome in patients with a pathological complete response after chemoradiation for rectal cancer: a pooled analysis of individual patient data. *Lancet Oncol*. 2010;11(9):835-844.
- Al-Sukhni E, Attwood K, Mattson DM, Gabriel E, Nurkin SJ. Predictors of Pathologic Complete Response Following Neoadjuvant Chemoradiotherapy for Rectal Cancer. *Ann Surg Oncol*. 2016;23(4):1177-1186.
- Vahrmeijer AL, Hutteman M, van der Vorst JR, van de Velde CJ, Frangioni JV. Image-guided cancer surgery using near-infrared fluorescence. *Nat Rev Clin Oncol*. 2013;10(9):507-518.
- Harlaar NJ, Koller M, de Jongh SJ, et al. Molecular fluorescence-guided surgery of peritoneal carcinomatosis of colorectal origin: a single-centre feasibility study. *Lancet Gastroenterol Hepatol*. 2016;1(4):283-290.
- Boogerd LSF, Hoogstins CES, Schaap DP, et al. Safety and effectiveness of SGM-101, a fluorescent antibody targeting carcinoembryonic antigen, for intraoperative detection of colorectal cancer: a dose-escalation pilot study. *Lancet Gastroenterol Hepatol*. 2018;3(3):181-191.
- Boonstra MC, Prakash J, Van De Velde CJ, et al. Stromal Targets for Fluorescent-Guided Oncologic Surgery. *Front Oncol*. 2015;5:254.
- Boogerd LS, Handgraaf HJ, Lam HD, et al. Laparoscopic detection and resection of occult liver tumors of multiple cancer types using real-time near-infrared fluorescence guidance. *Surg Endosc*. 2017;31(2):952-961.
- Hammarstrom S. The carcinoembryonic antigen (CEA) family: structures, suggested functions and expression in normal and malignant tissues. *Semin Cancer Biol*. 1999;9(2):67-81.
- Tiernan JP, Perry SL, Verghese ET, et al. Carcinoembryonic antigen is the preferred biomarker for *in vivo* colorectal cancer targeting. *Br J Cancer*. 2013;108(3):662-667.
- Gutowski M, Framery B, Boonstra MC, et al. SGM-101: An innovative near-infrared dye-antibody conjugate that targets CEA for fluorescence-guided surgery. *Surg Oncol*. 2017;26(2):153-162.
- Framery B, Gutowski M, Dumas K, et al. Toxicity and pharmacokinetic profile of SGM-101, a fluorescent anti-CEA chimeric antibody for fluorescence imaging of tumors in patients. *Toxicol Rep*. 2019;6:409-415.
- AV DS, Lin H, Henderson ER, Samkoe KS, Pogue BW. Review of fluorescence guided surgery systems: identification of key performance capabilities beyond indocyanine green imaging. *J Biomed Opt*. 2016;21(8):080901.
- Frangioni JV. New technologies for human cancer imaging. *J Clin Oncol*. 2008;26(24):4012-4021.
- Renehan AG, Malcomson L, Emsley R, et al. Watch-and-wait approach versus surgical resection after chemoradiotherapy for patients with rectal cancer (the OnCoRe project): a propensity-score matched cohort analysis. *Lancet Oncol*. 2016;17(2):174-183.
- Breugom AJ, van de Velde CJ. Is it time for watchful waiting for rectal cancer? *Lancet Oncol*. 2015;16(8):875-876.
- van der Valk MJM, Hilling DE, van de Velde CJH. What is there to learn for watch-and-wait in rectal cancer? *Lancet Gastroenterol Hepatol*. 2017;2(7):467-468.
- Dossa F, Chesney TR, Acuna SA, Baxter NN. A watch-and-wait approach for locally advanced rectal cancer after a clinical complete response following neoadjuvant chemoradiation: a systematic review and meta-analysis. *Lancet Gastroenterol Hepatol*. 2017;2(7):501-513.
- Martens MH, Maas M, Heijnen LA, et al. Long-term Outcome of an Organ Preservation Program After Neoadjuvant Treatment for Rectal Cancer. *J Natl Cancer Inst*. 2016;108(12).
- Bhoday J, Smith F, Siddiqui MR, et al. Magnetic Resonance Tumor Regression Grade and Residual Mucosal Abnormality as Predictors for Pathological Complete Response in Rectal Cancer Postneoadjuvant Chemoradiotherapy. *Dis Colon Rectum*. 2016;59(10):925-933.
- Lambrechts DM, Lahaye MJ, Heijnen LA, et al. MRI and diffusion-weighted MRI to diagnose a local tumour regrowth during long-term follow-up of rectal cancer patients treated with organ preservation after chemoradiotherapy. *Eur Radiol*. 2016;26(7):2118-2125.
- Dresen RC, Gosens MJ, Martijn H, et al. Radical resection after IORT-containing multimodality treatment is the most important determinant for outcome in patients treated for locally recurrent rectal cancer. *Ann Surg Oncol*. 2008;15(7):1937-1947.
- DeLong JC, Hoffman RM, Bouvet M. Current status and future perspectives of fluorescence-guided surgery for cancer. *Expert Rev Anticancer Ther*. 2016;16(1):71-81.
- DeLong JC, Murakami T, Yazaki PJ, Hoffman RM, Bouvet M. Near-infrared-conjugated humanized anti-carcinoembryonic antigen antibody targets colon cancer in an orthotopic nude-mouse model. *J Surg Res*. 2017;218:139-143.
- Boonstra MC, Tolner B, Schaafsma BE, et al. Preclinical evaluation of a novel CEA-targeting near-infrared fluorescent tracer delineating colorectal and pancreatic tumors. *Int J Cancer*. 2015;137(8):1910-1920.
- Maeda H, Wu J, Sawa T, Matsumura Y, Hori K. Tumor vascular permeability and the EPR effect in macromolecular therapeutics: a review. *J Control Release*. 2000;65(1-2):271-284.
- Matsumura Y, Maeda H. A new concept for macromolecular therapeutics in cancer chemotherapy: mechanism of tumorotropic accumulation of proteins and the antitumor agent smancs. *Cancer Res*. 1986;46(12 Pt 1):6387-6392.



**TABLE 1 Patient overview**

Demographics		SGM-101 dosing		Diagnosis and treatment		Imaging and concordance to histopathology				
PID	Age	Sex	Dose	Interval	Diagnosis	Surgical procedure	NAT	Fluores- TBR	Histopathology	Concordance
1	67	M	5 mg	2 days	Primary CRC (rectal)	APR	Chemoradiation	yes	1,8* Adeno- carcinoma	True positive
2	68	F	5 mg	2 days	Primary CRC (rectal)	APR	Chemoradiation	yes	1,5 Adeno- carcinoma	True positive
3	66	M	5 mg	2 days	Primary CRC (rectal)	LAR	Chemoradiation	no	Complete response	True negative
4	65	M	5 mg	2 days	Recurrent CRC (sigmoid)	Lymph node resection	none	yes	1,4 Mucinous adenocarcinoma	True positive
5	60	M	7,5 mg	2 days	Recurrent CRC (transv.colon)	Pancreatic-oduodenectomy	Chemotherapy	yes	1,4 Intestinal adenocarcinoma	True positive
6	64	M	7,5 mg	4 days	Primary CRC (sigmoid)	Sigmoid resection	none	yes	2,1 Adeno- carcinoma	True positive
7	63	M	7,5 mg	4 days	Primary CRC (rectal)	LAR	Chemoradiation	no	Complete response	True negative
8	79	F	7,5 mg	4 days	Primary CRC (rectal)	LAR	Chemoradiation	yes	5,0* Adeno- carcinoma	True positive
9	75	F	10 mg	4 days	Primary CRC (asc. colon)	Hemicolectomy	none	yes	1,9 Adeno- carcinoma	True positive
10	69	M	10 mg	4 days	Primary CRC (rectal)	LAR	Radiotherapy	NOT MEASURED	EXCLUDED FROM ANALYSIS	
11	69	F	10 mg	4 days	Primary CRC (sigmoid)	Sigmoid resection	none	yes	1,8 Adeno- carcinoma	True positive
12	63	M	10 mg	4 days	Recurrent CRC (sigmoid)	LAR	Chemoradiation	yes	1,7 Adeno- carcinoma	True positive
13	53	M	10 mg	4 days	Recurrent CRC (rectal)	Resection recurrence	Chemoradiation	yes	1,9* Adeno- carcinoma	True positive
14	56	M	10 mg	4 days	Recurrent CRC (rectal)	Resection recurrence	Chemoradiation	yes	1,9 Adeno- carcinoma	True positive
15	47	F	10 mg	4 days	Recurrent CRC (sigmoid)	LAR	Chemoradiation	yes	1,6* Adeno- carcinoma	True positive
16	49	M	10 mg	4 days	Recurrent CRC (rectal)	Resection recurrence	Chemoradiation	yes	2,0 Low grade intestinal adenocarcinoma	True positive
17	69	F	10 mg	4 days	Recurrent CRC (rectal)	APR	Chemoradiation	yes	2,2* Adeno- carcinoma	True positive
18	58	F	10 mg	4 days	Recurrent CRC (rectal)	APR	Chemoradiation	no	Complete response	True negative

19	62	F	10 mg	4 days	Recurrent CRC (sigmoid)	Resection recurrence	Chemoradiation	yes	1,5 Fibrosis; no tumor cells	False positive
20	67	M	10 mg	4 days	Recurrent CRC (rectal)	Total exenteration	Chemoradiation	yes	1,7* Sarcomatous differentiated carcinoma	True positive
21	63	M	10 mg	4 days	Recurrent CRC (rectal)	Resection recurrence	Chemoradiation	yes	2,4* Adeno- carcinoma	True positive
22	71	M	10 mg	4 days	Recurrent CRC (sigmoid)	APR	none	yes	1,5* Adeno- carcinoma	True positive
23	51	M	10 mg	4 days	Recurrent CRC (rectal)	Resection recurrence	Chemoradiation	yes	1,5* Adeno- carcinoma	True positive
24	75	M	10 mg	4 days	Recurrent CRC (asc. colon)	Resection recurrence	none	yes	1,5 Fibrosis; no tumor cells	False positive
25	43	M	10 mg	4 days	Recurrent CRC (sigmoid)	LAR	Chemoradiation	no	Complete response	True negative
26	59	M	10 mg	6 days	Recurrent CRC (sigmoid)	LAR	Chemoradiation	no	Complete response	True negative
27	55	F	10 mg	6 days	Primary CRC (rectal)	LAR	Chemoradiation	yes	1,4* Adeno- carcinoma	True positive
28	56	F	12,5 mg	3 days	Recurrent CRC (rectal)	APR	Chemoradiation	yes	1,8* Adeno- carcinoma	True positive
29	44	M	12,5 mg	4 days	Primary CRC (sigmoid)	LAR	none	yes	2,0 Adeno- carcinoma	True positive
30	63	M	12,5 mg	4 days	Primary CRC (rectal)	LAR	Chemoradiation	yes	1,4* Adeno- carcinoma	True positive
31	61	F	12,5 mg	4 days	Primary CRC (rectal)	LAR	Chemoradiation	no	Complete response	True negative
32	58	M	12,5 mg	4 days	Recurrent CRC (rectal)	APR	Chemoradiation	yes	1,8* Mucinous adenocarcinoma	True positive
33	75	M	15.0 mg	4 days	Primary CRC (rectal)	APR	Chemoradiation	yes	1,1* Adeno- carcinoma	True positive
34	58	M	15.0 mg	4 days	Primary CRC (rectal)	LAR	Chemoradiation	yes	1,1 Adeno- carcinoma	True positive
35	61	F	15.0 mg	4 days	Recurrent CRC (rectal)	APR	Chemoradiation	yes	1,9 Adeno- carcinoma	True positive
36	57	F	15.0 mg	6 days	Primary CRC (rectal)	APR	Chemotherapy	no	Complete response	True negative
37	72	F	15.0 mg	6 days	Recurrent CRC (rectal)	Total exenteration	Chemoradiation	yes	1,6* Vital tumor cells	True positive

PID: patient ID; NAT: neoadjuvant therapy; TBR: tumor-to-background ratio; CRC: colorectal cancer; APR: abdominal perineal resection; LAR: low anterior resection. \* indicates ex vivo TBR, as no in vivo TBR measurement was done or possible. In the diagnosis column, the data in parenthesis indicate the location of the primary tumor

**TABLE 2 Efficacy of SGM-101 per dose level.** The sensitivity, specificity, positive predictive value, negative predictive value and accuracy of SGM-101 was calculated per dose level. The concordance of all 97 resected lesions are included in the analysis.

Dose (mg)	TP	FP	FN	TN	Sensitivity	Specificity	PPV	NPV	Accuracy	False positive rate
5	3	1	0	1	3/3 (100%)	1/2 (50%)	3/4 (75%)	1/1 (100%)	4/5 (80%)	1/2 (50%)
7.5	7	3	0	2	7/7 (100%)	2/5 (40%)	7/10 (70%)	2/2 (100%)	9/12 (75%)	3/5 (60%)
10	23	10	1	17	23/24 (96%)	17/27 (63%)	23/33 (70%)	17/18 (94%)	40/51 (78%)	10/27 (37%)
12.5	7	3	1	3	7/8 (88%)	3/6 (50%)	7/10 (70%)	3/4 (75%)	10/14 (71%)	3/6 (50%)
15	7	5	0	3	7/7 (100%)	3/8 (38%)	7/12 (58%)	3/3 (100%)	10/15 (67%)	5/8 (63%)

TP: true positive; FP: false positive; FN: false negative; TN: true negative; PPV: positive predictive value; NPV: negative predictive value

**TABLE 3 Initial surgical plan alterations due to SGM-101 fluorescence.**

Treatment	PID	Diagnosis	Procedure	Alteration	Description lesion	Conclusion
5 mg SGM-101	3	Primary rectal cancer	LAR	Additional resection	Clinically non suspect fluorescent lesion on the bladder wall; resected per decision of the surgeon	Histopathology = benign; bladder dysplasia. <b>False positive</b>
10 mg SGM-101	1.2	Recurrent sigmoid cancer	LAR	Additional resection	Clinically non suspect fluorescent lesion near the left ureter; resected per decision of the surgeon.	<b>True positive: additional lesion</b>
	1.4	Recurrent rectal cancer	APR	Additional resection	Clinically non suspect fluorescent lesion proximal of recurrence; resected per decision of the surgeon.	<b>True positive: additional lesion</b>
	1.5	Recurrent sigmoid cancer	LAR	Additional resection	Clinically non suspect fluorescent lesion on lateral pelvic wall; resected per decision of the surgeon.	<b>True positive: additional lesion</b>
	1.7	Recurrent rectal cancer	APR	Additional resection	Remaining fluorescence in surgical field (clinically non suspect); two re-resections performed.	<b>True positive (2): additional lesions</b>
	2.1	Recurrent rectal cancer	Resection recurrence	Additional resection	1. Remaining fluorescence visible in surgical field (clinically non suspect); re-resection performed. 2. Clinically non suspect fluorescent lesion on lateral pelvic wall; resected per decision of the surgeon.	<b>True positive (2): additional lesions</b>
	2.2	Recurrent sigmoid cancer	APR	Additional resection	Remaining fluorescence visible in surgical field (clinically non suspect); re-resection performed.	<b>False positive</b>
	2.3	Recurrent rectal cancer	Resection recurrence	Additional resection	Remaining fluorescence visible in surgical field (clinically non suspect); re-resection performed.	<b>False positive</b>
12.5 mg SGM-101	3.2	Recurrent rectal cancer	APR	Additional resection	Clinically non suspect fluorescent lesion on lateral pelvic wall; resected per decision of the surgeon.	<b>True positive: additional lesion</b>
15 mg SGM-101	3.4	Primary rectal cancer	LAR	Downstaging treatment	No remaining fluorescence visible in surgical field after resection. Initial surgical plan included a more extensive resection, however due to negative fluorescence (confirmed benign with FS), the surgeon decided to salvage tissue around the lateral piriformis.	<b>True positive: additional lesion</b> <b>True negative</b>
	3.5	Recurrent rectal cancer	APR	Additional resection	Remaining fluorescence visible in surgical field (clinically suspect); re-resection performed.	<b>True positive *</b>
	3.6	Primary rectal cancer	APR	Downstaging treatment	No remaining fluorescence visible in surgical field or specimen after resection. The surgeon assessed the resection as radical, which was confirmed with FS (surgical field and specimen). The surgeon decided to spare the patient the planned IO RT, as this would have been on the sciatic nerve, giving morbidity.	<b>True positive</b> <b>True negative</b>

CRC: colorectal carcinoma; LAR: low anterior resection; APR: abdominal perineal resection; FS: frozen section; IO RT: intraoperative radiotherapy

\* Lesion was clinically suspect for malignancy, therefore not judged as an additional lesion

**FIGURE 1** FLOW diagram showing the patient inclusion for this study.

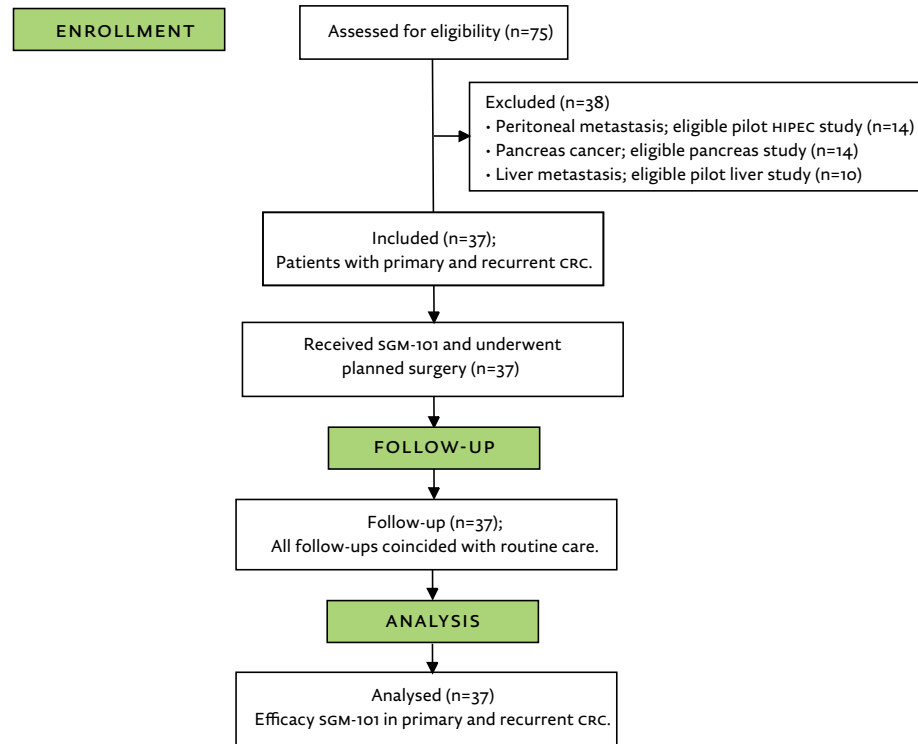
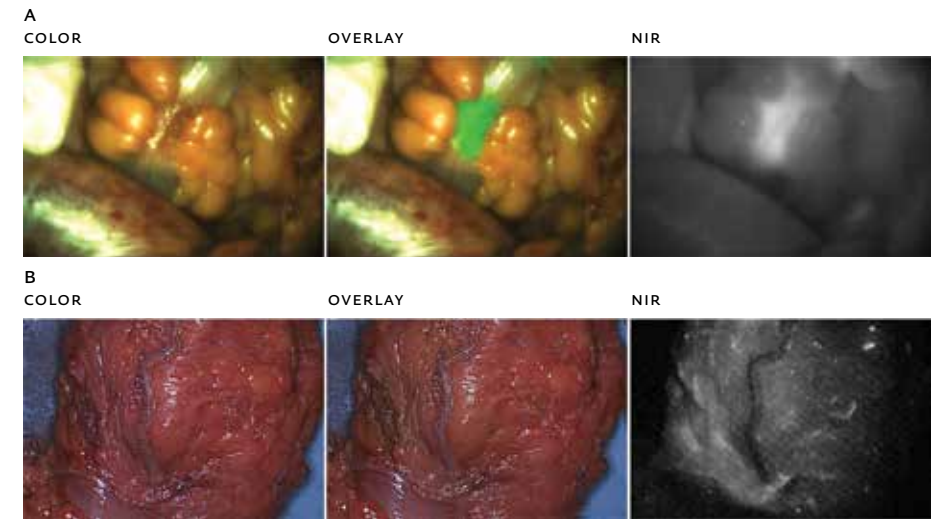
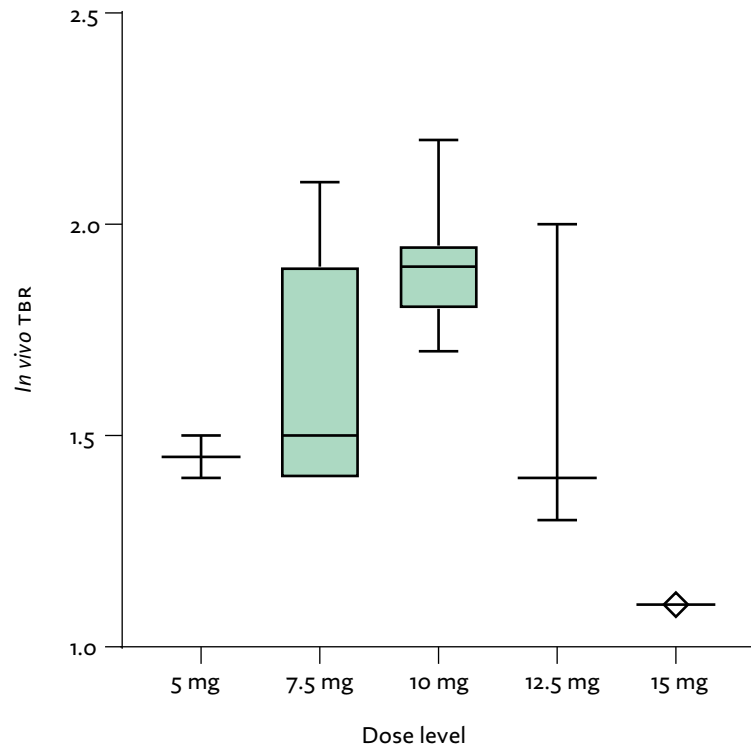


**FIGURE 2** Example of a true positive and a true negative colorectal carcinoma. Figure A shows intraoperative fluorescence of a palpable colorectal tumor during surgery, with a TBR of 2.0 (true positive). Figure B shows absence of fluorescence in a tumor, which was confirmed as a pathological complete response by histopathology (true negative).



TBR: tumor-to-background ratio; NIR: near-infrared

**FIGURE 3** Intraoperative tumor-to-background ratio (TBR) per dose level. The figure displays the median and range of the intraoperative TBRs. Note: the dosing-surgery interval time varies within the different dose levels.



Chapter vi

**CARCINOEMBRYONIC  
ANTIGEN-SPECIFIC, FLUORESCENT  
IMAGE-GUIDED CYTOREDUCTIVE  
SURGERY WITH HYPERTHERMIC  
INTRAPERITONEAL CHEMOTHERAPY  
FOR METASTASTIC COLORECTAL  
CANCER**

*Br J Surg.* 2020 Mar;107(4):334-337,

*doi: 10.1002/bjs.11523*

*Supplementary data available online*

KS de Valk<sup>2,3\*</sup>, DP Schaap<sup>1\*</sup>, MM Deken<sup>2,3</sup>,  
RPJ Meijer<sup>2,3</sup>, J Burggraaf<sup>2</sup>, AL Vahrmeijer<sup>3</sup>,  
M Kusters<sup>4</sup>, *on behalf of the SGM-101 study group*

\*SHARED FIRST AUTHORSHIP

1. Department of Surgery, Catharina Hospital Eindhoven, Eindhoven, NL

2. Centre for Human Drug Research, Leiden, NL

3. Department of Surgery, Leiden University Medical Center, Leiden, NL

4. Department of Surgery, Amsterdam University Medical  
Center, Amsterdam, NL

## ABSTRACT

This multicentre pilot study investigated the role of peroperative carcinoembryonic antigen (CEA)-specific fluorescence imaging during cytoreductive surgery-hyperthermic intraperitoneal chemotherapy surgery in peritoneal metastasized colorectal cancer. A correct change in peritoneal carcinomatosis index (PCI) owing to fluorescence imaging was seen in four of the 14 included patients. The use of SGM-101 in patients with peritoneally metastasized colorectal carcinoma is feasible, and allows intraoperative detection of tumor deposits and alteration of the PCI.

## INTRODUCTION

The peritoneal cavity is the second most common location for the development of isolated metastases of colorectal origin.<sup>1,2</sup> Peritoneal metastatic disease was once considered an end-stage disease with a poor median survival of several months after palliative treatment.<sup>3-5</sup> However, survival rates have improved since the introduction of cytoreductive surgery (CRS) with hyperthermic intraperitoneal chemotherapy (HIPEC). Numerous studies have identified the peritoneal carcinomatosis index (PCI), a measure of the extent of peritoneal disease, and completeness of CRS as important prognostic factors for oncological outcome.<sup>6-10</sup> However, identification of peritoneal lesions, especially in diffuse miliary disease, and discriminating between benign fibrosis (common after surgery and neoadjuvant therapy) and malignant lesions can be challenging. Therefore, a reliable method for identifying (small) peritoneal tumor deposits could be of great importance to achieving complete CRS.

Near-infrared (NIR) fluorescence imaging techniques using tumor-targeting tracers may aid in this respect. In recent years, fluorescence-guided surgery has gained interest, and has been able to provide surgeons with real-time feedback and visualization of malignant tissues.<sup>11-14</sup> SGM-101, a carcinoembryonic antigen (CEA)-specific tumor-targeted fluorescent agent, can be used for fluorescence imaging to identify malignant tissue of colorectal origin. The fact that CEA is overexpressed in more than 90 per cent of all colorectal cancer cells, with limited expression in benign tissue, makes it an ideal target for fluorescence imaging of colorectal neoplastic lesions.<sup>15-17</sup> The aims of this study were to evaluate the effectiveness of fluorescence imaging with SGM-101 for the detection of peritoneal metastases of colorectal origin and the potential influence on intraoperative decision-making. The main objective was to distinguish whether the PCI, and thus the completeness of cytoreduction, can be changed with SGM-101 and fluorescence imaging.

## METHODS

An exploratory, multicentre pilot study was performed in patients with peritoneal metastatic colorectal cancer. Patients were scheduled for CRS-HIPEC, and SGM-101 was administered intravenously 4-6 days before surgery. During surgery, a clinical PCI was determined using standard tactile and visual feedback. Subsequently, a fluorescence-based peritoneal carcinomatosis index (FPCI) was determined using the Quest Spectrum® fluorescence camera system (Quest Medical Imaging, Middenmeer, the Netherlands), an imaging system dedicated to fluorescence imaging in the 700-nm NIR spectrum. Both clinically suspected malignant and fluorescent lesions were resected and assessed by the pathologist. Changes in the PCI and surgical plan, and the concordance between clinical detection and fluorescence imaging were correlated with the histopathological analysis. Details of the methods can be found in *Appendix S1* (supporting information).

## RESULTS

Between January 2017 and January 2019, 14 patients diagnosed with peritoneal metastases of colorectal origin were included in this study. The clinical characteristics and PCI outcomes are summarized in *Tables S1* and *S2* respectively (supporting information). Of the 14 patients, six were diagnosed with a locally advanced or recurrent rectal tumor with peritoneal metastases, and received neoadjuvant treatment consisting of either induction chemotherapy followed by chemoradiotherapy (CRT) or CRT alone. Nine patients presented with synchronous and five with metachronous peritoneal metastases. SGM-101 was well tolerated in all patients; no allergic or anaphylactic reactions were reported during or after SGM-101 administration. CRS-HIPEC was executed successfully in 12 of the 14 patients. Only an exploratory laparotomy was performed in two patients, as the disease was too extensive and unresectable. However, for clinical purposes, clinical and fluorescence-based PCI inspections were performed, and biopsies were taken that were also investigated for fluorescence signal. Median clinical PCI was 7 (2-39) and median FPCI was 6.5 (2-39). The PCI changed owing to fluorescence imaging in seven patients. In six of these patients, the FPCI was higher than the clinical PCI, which was accurate in four patients, as confirmed by histopathological analysis. One patient had a PCI increase from 10 to 11 owing to a fluorescent lesion on the mesentery of the proximal ileum, which was not considered malignant on traditional inspection or palpation. The second patient had multiple additional lesions in the omentum that were not identified

by standard visual techniques, but only by fluorescence imaging, increasing the PCI from 4 to 6 (*Figure 1*). In the third and fourth patients, fluorescent positive lesions on the left upper peritoneum and peritoneum of the bladder increased the PCI from 9 to 10 and from 2 to 4 respectively. Both lesions were visible, but not considered malignant on initial inspection and palpation. In two patients, the PCI change due to fluorescence imaging was incorrect. A false-positive lesion on the liver capsule, detected by fluorescence imaging, led to an incorrect PCI increase from 4 to 5 and unnecessary resection of a superficial lesion on the liver capsule. The other patient, who received neoadjuvant chemotherapy according to the CAIRO-6 trial protocol, had a complete response. Six lesions were resected, which were all clinically suspect for malignancy; five of these lesions were fluorescent. Histopathological analysis confirmed that all lesions were benign, containing collagen-rich connective tissue, hypervascularization and an inflammatory reaction. One patient had a decrease in PCI owing to fluorescence imaging. This patient had a PCI of 5 and a FPCI of 4; however, after histopathological analysis the PCI was 3. Fluorescence imaging correctly identified two lesions (mesentery of the upper and lower ileum) as benign, but a false-positive lesion in the omentum eventually led to an incorrect FPCI. Both lesions on the mesentery of the ileum were still resected as they were clinically suspicious; bowel resection was not included.

A total of 103 lesions were excised from the 14 patients. Histopathology revealed that 66 of these lesions were malignant and 37 were benign. Of the 103 lesions, 79 were identified with fluorescence. Sixty-five of the 66 malignant lesions were fluorescent (true positive), resulting in a sensitivity of 98.5 per cent. No fluorescence was observed in 23 of the 37 benign lesions (true negative), resulting in a specificity of 62.2 per cent. This led to an accuracy of fluorescence imaging of 85.4 per cent. Nevertheless, 14 lesions showed a false-positive signal and one lesion was false negative, resulting in a positive predictive value of 82.3 per cent and a negative predictive value of 95.8 per cent (*Table 1*).

## DISCUSSION

SGM-101 had a high negative predictive value of 95.8 per cent and an accuracy of 85.4 per cent, which is in accordance with previous and concurrent studies with SGM-101, emphasizing that this technique is consistently reliable<sup>13</sup>. The selection of patients with peritoneal metastases of colorectal origin who might benefit from CRS-HIPEC is a major challenge. Several studies have demonstrated that the extent of peritoneal disease, best measured with the PCI, is one of the most important prognostic factors for increased local and distant recurrence

rates and diminished survival.<sup>7,8,18,19</sup> Completeness of cytoreductive surgery is another important prognostic factor for improved oncological outcomes.<sup>9,10,20</sup> In a retrospective analysis of 523 patients, Elias and colleagues showed that, besides lymph node status, surgical experience and adjuvant chemotherapy, PCI and the completion of cytoreduction were independent prognostic factors for disease-free survival.<sup>6</sup> With this in mind, it is apparent that adequate detection of peritoneal deposits is key to determining whether CRS-HIPEC is feasible and improves the completeness of cytoreduction. Even though a change in PCI might not fully reflect the benefit of tumor deposit detection with fluorescence imaging, because the additional information about, for example, an extralesion, might not alter the PCI, it is still beneficial for a more complete cytoreduction. The fact that this technique was able to detect additional lesions that were not considered to be malignant based on standard visual and tactile feedback is of great importance. The PCI increased accurately based on fluorescence imaging in almost one-third of the patients, which led to resection of lesions that would otherwise have been left behind. These results demonstrate the potential benefit of CEA-specific fluorescence imaging, as the detection of additional lesions with the help of this technique might result in more complete cytoreduction and subsequently improved oncological outcomes.

**REFERENCES**

- 1 van Gestel YR, de Hingh IH, van Herk-Sukel MP, et al. Patterns of metachronous metastases after curative treatment of colorectal cancer. *Cancer Epidemiol.* 2014;38(4):448-454.
- 2 Huguen N, van de Velde CJ, de Wilt JH, Nagtegaal ID. Metastatic pattern in colorectal cancer is strongly influenced by histological subtype. *Ann Oncol.* 2014;25(3):651-657.
- 3 Lemmens VE, Klaver YL, Verwaal VJ, Rutten HJ, Coebergh JW, de Hingh IH. Predictors and survival of synchronous peritoneal carcinomatosis of colorectal origin: a population-based study. *Int J Cancer.* 2011;128(11):2717-2725.
- 4 Razenberg LG, Lemmens VE, Verwaal VJ, et al. Challenging the dogma of colorectal peritoneal metastases as an untreatable condition: Results of a population-based study. *Eur J Cancer.* 2016;65:113-120.
- 5 Quere P, Facy O, Manfredi S, et al. Epidemiology, Management, and Survival of Peritoneal Carcinomatosis from Colorectal Cancer: A Population-Based Study. *Dis Colon Rectum.* 2015;58(8):743-752.
- 6 Elias D, Gilly F, Boutitie F, et al. Peritoneal colorectal carcinomatosis treated with surgery and perioperative intraperitoneal chemotherapy: retrospective analysis of 523 patients from a multicentric French study. *J Clin Oncol.* 2010;28(1):63-68.
- 7 Simkens GA, van Oudheusden TR, Nieboer D, et al. Development of a Prognostic Nomogram for Patients with Peritoneally Metastasized Colorectal Cancer Treated with Cytoreductive Surgery and HIPEC. *Ann Surg Oncol.* 2016;23(13):4214-4221.
- 8 Glehen O, Kwiatkowski F, Sugarbaker PH, et al. Cytoreductive surgery combined with perioperative intraperitoneal chemotherapy for the management of peritoneal carcinomatosis from colorectal cancer: a multi-institutional study. *J Clin Oncol.* 2004;22(16):3284-3292.
- 9 Verwaal VJ, van Tinteren H, van Ruth S, Zoetmulder FA. Predicting the survival of patients with peritoneal carcinomatosis of colorectal origin treated by aggressive cytoreduction and hyperthermic intraperitoneal chemotherapy. *Br J Surg.* 2004;91(6):739-746.
- 10 Esquivel J, Piso P, Verwaal V, et al. American Society of Peritoneal Surface Malignancies opinion statement on defining expectations from cytoreductive surgery and hyperthermic intraperitoneal chemotherapy in patients with colorectal cancer. *J Surg Oncol.* 2014;110(7):777-778.
- 11 Hoogstins CES, Boogerd LSF, Sibinga Mulder BG, et al. Image-Guided Surgery in Patients with Pancreatic Cancer: First Results of a Clinical Trial Using SGM-101, a Novel Carcinoembryonic Antigen-Targeting, Near-Infrared Fluorescent Agent. *Ann Surg Oncol.* 2018;25(11):3350-3357.
- 12 Harlaar NJ, Koller M, de Jongh SJ, et al. Molecular fluorescence-guided surgery of peritoneal carcinomatosis of colorectal origin: a single-centre feasibility study. *Lancet Gastroenterol Hepatol.* 2016;1(4):283-290.
- 13 Boogerd LSF, Hoogstins CES, Schaap DP, et al. Safety and effectiveness of SGM-101, a fluorescent antibody targeting carcinoembryonic antigen, for intraoperative detection of colorectal cancer: a dose-escalation pilot study. *Lancet Gastroenterol Hepatol.* 2018;3(3):181-191.
- 14 Tipirneni KE, Warram JM, Moore LS, et al. Oncologic Procedures Amenable to Fluorescence-guided Surgery. *Ann Surg.* 2017;266(1):36-47.
- 15 Tiernan JP, Perry SL, Verghese ET, et al. Carcinoembryonic antigen is the preferred biomarker for *in vivo* colorectal cancer targeting. *Br J Cancer.* 2013;108(3):662-667.
- 16 Hammarstrom S. The carcinoembryonic antigen (CEA) family: structures, suggested functions and expression in normal and malignant tissues. *Semin Cancer Biol.* 1999;9(2):67-81.
- 17 Boonstra MC, de Geus SW, Prevoo HA, et al. Selecting Targets for Tumor Imaging: An Overview of Cancer-Associated Membrane Proteins. *Biomark Cancer.* 2016;8:119-133.
- 18 PH. JPS. Clinical research methodologies in diagnosis and staging of patients with peritoneal carcinomatosis. *Peritoneal Carcinomatosis: Principles of Management.* . 1996:359-374.
- 19 da Silva RG, Sugarbaker PH. Analysis of prognostic factors in seventy patients having a complete cytoreduction plus perioperative intraperitoneal chemotherapy for carcinomatosis from colorectal cancer. *J Am Coll Surg.* 2006;203(6):878-886.
- 20 Shen P, Hawksworth J, Lovato J, et al. Cytoreductive surgery and intraperitoneal hyperthermic chemotherapy with mitomycin C for peritoneal carcinomatosis from nonappendiceal colorectal carcinoma. *Ann Surg Oncol.* 2004;11(2):178-186.

**FIGURE 1 Ex vivo fluorescence imaging of a lesion in the omentum.** *Ex vivo* A white light, B near-infrared (NIR) fluorescence and C merged white light and NIR fluorescence images of a lesion in the omentum detected *in vivo*, which was not suspicious clinically, resulting in a change in peritoneal carcinomatosis index from 4 to 6. Histopathological examination confirmed that this lesion was malignant.



**TABLE 1 Performance of fluorescence imaging for detection of lesions.**

	Malignant	Benign	Total	Sensitivity (%)	Specificity (%)	PPV (%)	NPV (%)	Accuracy (%)
<b>Fluorescence positive</b>	65 (TP)	14 (FP)	79					
<b>Fluorescence negative</b>	1 (FN)	23 (TN)	24					
<b>Total</b>	66	37	103	98.5 (65 of 66)	62.2 (23 of 37)	82.3 (65 of 79)	95.8 (23 of 24)	85.4 (88 of 103)

TP, true positive; FP, false positive; FN, false negative; TN, true negative; PPV, positive predictive value; NPV, negative predictive value.

Chapter VII

**THE QUANTIFICATION  
OF THE PHARMACOKINETIC  
AND PHARMACODYNAMIC  
PROPERTIES OF SGM-101 IN  
COLORECTAL AND PANCREATIC  
PATIENTS IN A PHASE I/II STUDY**

*Thesis chapter, not yet published*

KS de Valk<sup>1</sup>, MJ van Esdonk<sup>1</sup>, B Framery<sup>2</sup>, F Cailler<sup>2</sup>,  
AL Vahrmeijer<sup>3</sup>, J Burggraaf

1. Centre for Human Drug Research, Leiden, NL

2. SurgiMab, Montpellier, FR

3. Leiden University Medical Center, Leiden, NL



## ABSTRACT

This study quantified the pharmacokinetics (PK) of SGM-101 after a single intravenous dose of 5 mg, 7.5 mg, 10 mg, 12.5 mg or 15 mg and the pharmacodynamics (PD) on the tumor-to-background ratio (TBR) during surgery. The PK of SGM-101 was best described using a two-compartment model with linear elimination kinetics and a proportional residual error structure. Bodyweight was identified as a strong covariate on the central volume of distribution. The PK model was able to capture the general trend and the variability in the data over time for all dosing cohorts. A narrow concentration range in the SGM-101 concentrations at the time of surgery was observed, where an overlap in TBR was seen between the different dose levels. In all dosing cohorts, tumor fluorescence could be perceived.

## INTRODUCTION

Intraoperative fluorescence imaging or fluorescence-guided surgery (FGS) is an emerging surgical imaging technique that has the potential to revolutionize oncologic surgery.<sup>1</sup> Fluorescence imaging provides real-time intraoperative tumor visualization to assist surgeons in tumor resection and margin confirmation during surgery.<sup>1-4</sup> However, determining the optimal dose and timing of administration of a fluorescent agent for optimum intraoperative fluorescence remains challenging. This is mainly due to the high variability and complexity of tumors and the different factors that can influence fluorescence during a surgical procedure, such as the pharmacokinetic (PK) properties of a compound, the sensitivity of near-infrared (NIR) camera systems, the blood supply to the tumor, the occurrence of the enhanced permeability retention effect (EPR) and autofluorescence of surrounding tissue.

FGS has slowly been advancing and progressing in its implementation in standard of care. Numerous clinical trials are currently ongoing that are investigating different tumor-targeted fluorescent agents for the intraoperative visualization of various tumor types. SGM-101, a fluorescent anti-carcinoembryonic antigen (CEA) monoclonal antibody, is one of these tumor-targeted agents which has been studied in preclinical and phase I/II trials for the intraoperative assessment of primary, recurrent and metastasized colorectal and pancreatic cancer.<sup>2-6</sup> Since CEA is a tumor-specific marker highly overexpressed in a number of different epithelial cancers, including colorectal and pancreatic cancer, it is a promising target for tumor imaging.<sup>7</sup>

The phase I/II studies with SGM-101 have shown successful colorectal and pancreatic tumor exposure, where previous reports have described the efficacy of SGM-101 in terms of tumor detection and fluorescence detection.<sup>2-4</sup> The PK of SGM-101 have not previously been described and the relationship between SGM-101 concentrations and fluorescence remains unknown. The development and analysis of a population PK model can help in this phase of the study, since PK models are known to give a better understanding of an individual's response to a certain drug, in this case the distribution and clearance of SGM-101 in the tumor. Understanding the PK of SGM-101 can be of added value as it can result in improved assessments of the feasibility of the compound by implementing a more evidence-based optimal dosing regimen for subsequent clinical studies. Hence, the objective of this study was the quantification of the PK of SGM-101 after a single intravenous (IV) dose (5 mg, 7.5 mg, 10 mg, 12.5 mg or 15 mg) and the resulting tumor fluorescence during surgery, based on PK and pharmacodynamic (PD) samples from previously studied patient populations with SGM-101.

## METHODS

### Study design

SGM-101 PK results were available from two open-label exploratory studies with SGM-101, which were performed in France and the Netherlands.<sup>2-4</sup> The same assay was used in both studies, with a lower limit of quantification (LLQ) of 200 ng/ml and was carried out by Atlanbio/PhinC Development and EuroFins IADME BIOANALYSES, respectively. For each individual, dose level, time point and corresponding SGM-101 serum concentrations were available. The study performed in France was a phase I, first-in-human study, and included 18 patients with metastasized colorectal cancer. These patients were divided into 6 dosing cohorts (3 patients each cohort). In each cohort, 3 patients received a 30-minute infusion of a dose ranging from 5 mg, 7.5 mg, 10 mg, 12.5 mg to 15 mg. Cohorts 5 and 6 received the same dose (15 mg), with cohort 5 receiving the dose 24 h before surgery, such as cohort 1-4, and cohort 6 receiving the dose 48 h before surgery. The study performed in the Netherlands was a phase I/II study and included 67 patients with colorectal or pancreatic cancer. These patients were divided into 5 dosing cohorts (minimum of 3 patients per cohort), where patients received a 30-minute infusion of 5 mg, 7.5 mg, 10 mg, 12.5 mg or 15 mg, respectively. The timing of administration in these patients varied from 48 h to 144 h before surgery.

For the PK analysis, data was obtained from a total of 85 patients. Data was excluded from the analysis if all data of a subject was below the LLOQ.

### Population pharmacokinetic model development

One-, two-, and three-compartment models were investigated to quantify the PK of SGM-101. Both linear and non-linear elimination kinetics were explored. After structural model identification, inter-individual variability was included on the population parameters following a bottom-up stepwise inclusion procedure and was included in the model if a significant ( $p < 0.01$ ) improvement in model fit was observed. The inter-individual variability was log-transformed to prevent the estimation of negative individual estimates. A proportional, additive, or a combined proportional and additive residual error component was investigated.

Weight, body mass index, age and sex were the covariates that were included in the population PK model to explore their contribution on the identified inter-individual variability. Covariates were visualized and investigated with a Pearson correlation coefficient before formal inclusion in the PK model with a forward inclusion step ( $p < 0.01$ ) followed by backward exclusion ( $p < 0.001$ ).

Model performance was based on the numerical evaluation of the objective function value (OFV),  $-2 \times \text{Log likelihood}$ , the relative standard errors (RSEs), the condition number, and visual evaluation of the model was based on goodness-of-fit figures and a scatter visual predictive check (VPC) based on 1500 simulations incorporating inter-individual variability and residual variability.

### In and ex vivo tumor-to-background ratio

The PD data was extracted from the phase I/II study performed in the Netherlands, where the efficacy of SGM-101 was evaluated by measuring the fluorescence. Fluorescence was objectified by calculating the TBR in each lesion (*in vivo* and *ex vivo*). *In vivo* TBR was defined as the fluorescence of the lesion inside the patient prior to surgical resection. *Ex vivo* TBR was defined as the fluorescence of the lesion after resection on the back table. A total of 50 *in vivo* TBRS were obtained in the 5 mg ( $n=2$ ), 7.5 mg ( $n=2$ ), 10 mg ( $n=36$ ), 12.5 mg ( $n=4$ ) and 15 mg ( $n=6$ ) dose. For the *ex vivo* results, a total of 47 TBR results were obtained in the 5 mg ( $n=2$ ), 7.5 mg ( $n=2$ ), 10 mg ( $n=21$ ), 12.5 mg ( $n=8$ ) and 15 mg ( $n=14$ ) dose. Exploratory figures of the *in-* and *ex vivo* PD data were created to assess the relationship between SGM-101 concentrations and tumor-to-background ratio (TBR) versus the time after administration and between the different dosing cohorts. The developed population PK model was used to simulate individual PK at the time of surgery using the empirical Bayes estimates. A direct linear concentration-effect relationship was estimated on the available data to correlate the PK of SGM-101 with the available PD data.

### Software

Data was transformed and visualized in R v3.6.1.<sup>8</sup> Non-linear mixed effects modelling was performed in NONMEM v7.3.<sup>9</sup> Simulations were performed using mrg solve.<sup>10</sup>

## RESULTS

PK samples were collected in a total of 85 patients over two studies (55 men and 30 women). Five patients had all observations below the LLOQ, most likely due to pre-analytical issues, and were excluded. The remaining 80 patients (50 men and 30 women) were included, as these all presented at least one detectable concentration of SGM-101. These patients all received a single dose of SGM-101 approximately 24–144 hours (1–6 days) prior to the scheduled surgery; 5 mg ( $n=10$ ), 7.5 mg ( $n=8$ ), 10 mg ( $n=33$ ), 12.5 mg ( $n=14$ ) and 15 mg ( $n=15$ ) to enable fluorescence imaging of colorectal ( $n=66$ ) or pancreatic ( $n=14$ ) cancer during surgery. This resulted in a total of 468 post-dose PK samples available for model development. The subject characteristics of the analyzed patients are reported in *Table 1*.

The PK of SGM-101 was best described using a two-compartment model with linear elimination kinetics and a proportional residual error structure. Significant inter-individual variability was identified on the central volume of distribution and on the inter-compartmental clearance. A strong weight dependent central volume of distribution was identified, best described by a power relationship (normalized on 70 kg). Parameters were estimated with high parameter certainty ( $<50\%$ ) with a moderate RSE on clearance (48.8%). The condition number was acceptable with a value of 86. The parameter estimates of the developed PK model of SGM-101 are shown in *Table 2*. The PK model was able to capture the general trend and the variability in the data over time for all cohorts. The population and individual predictions were scattered closely around the line of unity and no bias over the different cohorts were identified (*Supplementary figure 1*).

The PK of SGM-101 over 120 h after a single dose was simulated for 1500 individuals with identical weight distributions as in the original study to evaluate model performance (*Figure 1*).

### Pharmacodynamics

A total of 97 TBR measurements were available for PD assessment, obtained in a total of 42 patients. The 97 measurements consisted of 50 *in vivo* measurements

and 47 *ex vivo* measurements. Simulated SGM-101 concentrations at the time of surgery identified a narrow concentration range, where an overlap in TBR was seen between the different dose levels, most likely due to the difference in the dosing-surgery time intervals between the cohorts. Higher doses did not show higher TBRs (Figure 2). Due to the similar PK of SGM-101 in the different dosing cohorts and variable TBRs, no PK/PD relationship could be defined. This was the case for both the *in vivo* and *ex vivo* TBRs. When the TBR was plotted against the time after dose (defined as the time between SGM-101 administration and imaging), no correlation could be observed.

## DISCUSSION

The developed PK model showed an accurate model prediction for SGM-101 in the 468 post-dose samples obtained in the 80 analyzed patients. The PK of SGM-101 was well characterized in the ascending doses ranging from 5 to 15 mg, administered as a 30-minute IV infusion. No concentration-effect relationship could be identified, as the explored dose levels showed similar SGM-101 concentrations, possibly due to variations in the interval between administration time and surgery between the cohorts. Yet, in patients who received SGM-101 in shorter administration time intervals (i.e. 24 and 48 hours) an increased background noise was observed during surgical procedures. This can be clarified by the higher blood SGM-101 concentrations found in the shorter administration time intervals, suggesting that an interval of less than 48h between dosing and surgery should be avoided. These higher blood concentrations can result in (too) strong background fluorescence, consequently resulting in insufficient malignant and benign tissue distinction, leading to inadequate TBRs. However, longer intervals between dosing and surgery (>120 h) may show similar results due to the slow elimination phase.

Five patients were excluded in the analysis as they all had PK data below the LLOQ. No clear reason could be identified for the discrepancy in the results in these subjects. All patients were administered SGM-101; one patient received 7.5 mg, one patient 10 mg and three patients received 15 mg SGM-101. One possible explanation could be that SGM-101 was (partly) administered subcutaneously in these patients, resulting in lower concentration levels. No particular reason for the other concentrations could be identified and are most likely caused by pre-analytical factors.

The PK parameters in the model were estimated with high accuracy, where one parameter (clearance) had a moderate RSE value of 48.78. The limited number of observations in the terminal elimination phase complicated the

estimation of this clearance parameter. Additional PK information on the concentration after 120 h is required to improve this estimation. Indeed, studies in rodents showed an elimination half-life of approximately 99-122 hrs, independent of gender. Experiments radioactive SGM-101 using mice with intra-peritoneal colorectal tumor model or in a transgenic mouse model expressing CEA indicated that the compound distributes rapidly to a variety of tissues, but normal tissue labeling was very low and decreased rapidly. At 24 hours after injection the only sites with a non-negligible presence of the injected dose were blood (5%) and tumor tissue (10-15 %). This is in keeping with the pharmacokinetics of monoclonal antibodies, although we were not able to identify and/or quantify of target mediated drug disposition, most likely due to the relative low doses that were employed. The low and transient exposure of normal tissues is a reassuring finding as it may indicate that the doses employed drug-drug interactions at the level of clearance or distribution are unlikely to occur. This is an important observation as surgery requires drugs, many patients with an oncologic disease are treated with neoadjuvant therapy (i.e. chemoradiotherapy) before or complimentary chemotherapy after surgery. The data presented here indicate that SGM-101, similar to other monoclonal antibodies has a low potential for drug-drug interactions.

A limitation of the study are the similar SGM-101 concentrations in the different dose levels. With the current PK model, no clear concentration-effect relationship can be perceived. Yet, previous reports have shown successful tumor fluorescence in patients, displaying a positive trend and feasibility of SGM-101. This suggests more data is required in a wide range of SGM-101 concentrations to better determine the correlation between SGM-101 and the fluorescence. This can be done by obtaining more blood samples after surgery, until discharge, to get a better picture of SGM-101 clearance. The concentration range investigated in this study (5 – 15 mg) showed adequate TBR's.

To the best of our knowledge, this is the first report that investigated the pharmacokinetic and pharmacodynamic properties of SGM-101 in patients. The developed PK model was able to simulate the area under the curve of SGM-101 profiles in the different dosing cohorts and has given us additional insight in the quantification of SGM-101 and fluorescence. This study successfully quantified the concentration range of SGM-101 per dose level, but also illuminated that longer observation periods are needed to allow better extrapolation of the most optimal dose and dosing-surgery interval of SGM-101.

## REFERENCES

- Vahrmeijer AL, Hutteman M, van der Vorst JR, van de Velde CJ, Frangioni JV. Image-guided cancer surgery using near-infrared fluorescence. *Nat Rev Clin Oncol*. 2013;10(9):507-518.
- Boogerd LSF, Hoogstins CES, Schaap DP, et al. Safety and effectiveness of SGM-101, a fluorescent antibody targeting carcinoembryonic antigen, for intraoperative detection of colorectal cancer: a dose-escalation pilot study. *Lancet Gastroenterol Hepatol*. 2018;3(3):181-191.
- Schaap DP, de Valk KS, Deken MM, et al. Carcinoembryonic antigen-specific, fluorescent image-guided cytoreductive surgery with hyperthermic intraperitoneal chemotherapy for metastatic colorectal cancer. *Br J Surg*. 2020;107(4):334-337.
- Hoogstins CES, Boogerd LSF, Sibinga Mulder BG, et al. Image-Guided Surgery in Patients with Pancreatic Cancer: First Results of a Clinical Trial Using SGM-101, a Novel Carcinoembryonic Antigen-Targeting, Near-Infrared Fluorescent Agent. *Ann Surg Oncol*. 2018;25(11):3350-3357.
- Gutowski M, Framery B, Boonstra MC, et al. SGM-101: An innovative near-infrared dye-antibody conjugate that targets CEA for fluorescence-guided surgery. *Surg Oncol*. 2017;26(2):153-162.
- Framery B, Gutowski M, Dumas K, et al. Toxicity and pharmacokinetic profile of SGM-101, a fluorescent anti-CEA chimeric antibody for fluorescence imaging of tumors in patients. *Toxicol Rep*. 2019;6:409-415.
- Boogerd LS, van der Valk MJ, Boonstra MC, et al. Biomarker expression in rectal cancer tissue before and after neoadjuvant therapy. *Onco Targets Ther*. 2018;11:1655-1664.
- Team RC. R: A language and environment for statistical computing. *R Foundation for Statistical Computing, Vienna, Austria*. 2019.
- Beal S, Sheiner LB, Boeckmann A, Bauer RJ. NONMEM User's Guides. *Icon Development Solutions, Ellicott City, MD, USA*. 2013.
- Baron KT. mrgsolve: Simulate from ODE-Based Models. *R package version 0.9.2* 2019.

**TABLE 1 Subject characteristics for the 80 subjects receiving SGM-101.**

Demographics				
SEX			AGE (YRS)	WEIGHT (KG)
Male	50	Mean	62.08	81.63
Female	30	SD	10.61	17.91
		Min	23	47
		Max	80	127

**TABLE 2 Pharmacokinetic model population parameter estimates of SGM-101.**

Label	Estimate	RSE%	Shrinkage
STRUCTURAL MODEL PARAMETERS			
Central volume of distribution (L)	5.23	3.40	
Peripheral volume of distribution (L)	26.2	18.15	
Inter-compartmental clearance (L/h)	0.158	14.43	
Clearance (L/h)	0.0296	48.78	
Weight exponent	0.586	19.69	
INTER-INDIVIDUAL VARIABILITY			
$\omega_2$ Central volume of distribution	0.055	18.45	4.7%
$\omega_2$ Inter-compartmental clearance	0.21	36.43	20.2%
Residual error $\sigma^2$ Proportional	0.017	14.40	14.4%

**FIGURE 1 Model-derived mean and 95% distribution in population (prediction interval).** The PK of SGM-101 over 120 h after a single dose was simulated for 1500 individuals with identical weight distributions as in the original study to evaluate model performance.

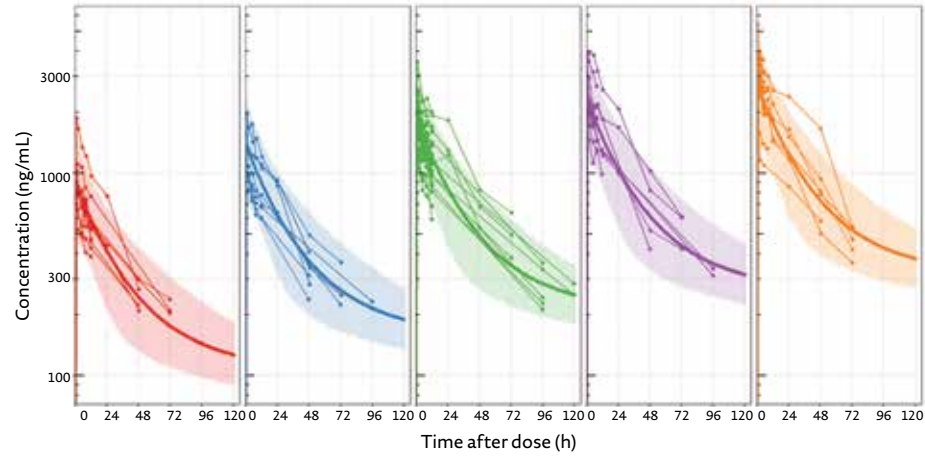
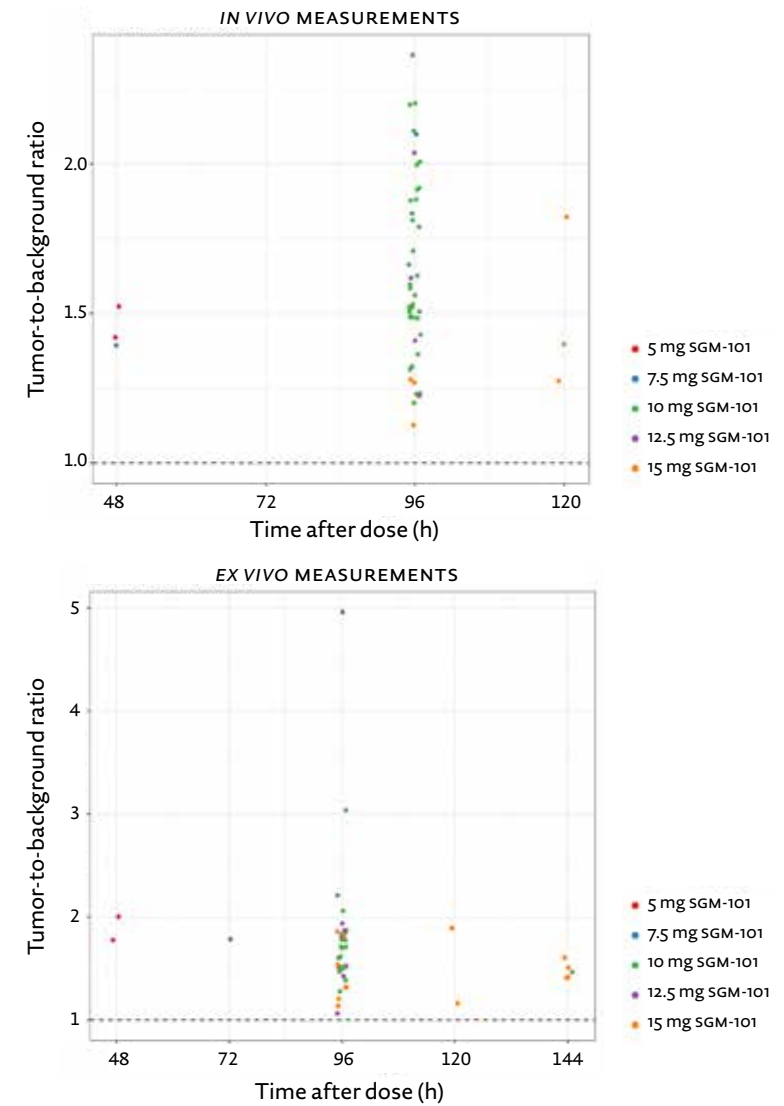
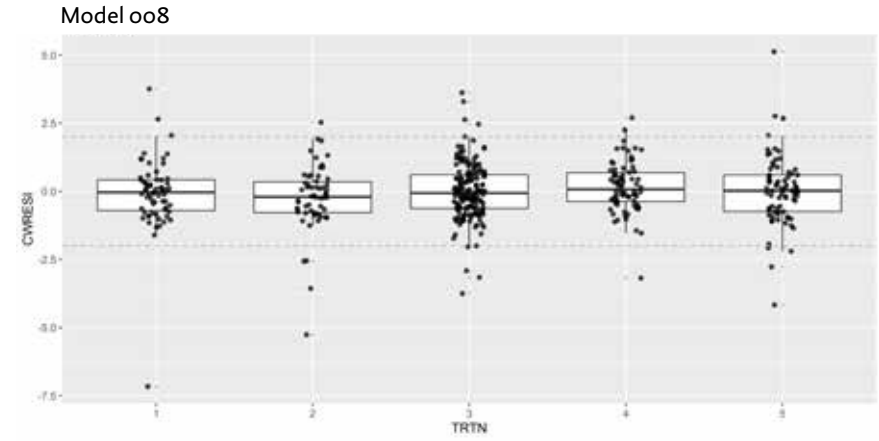
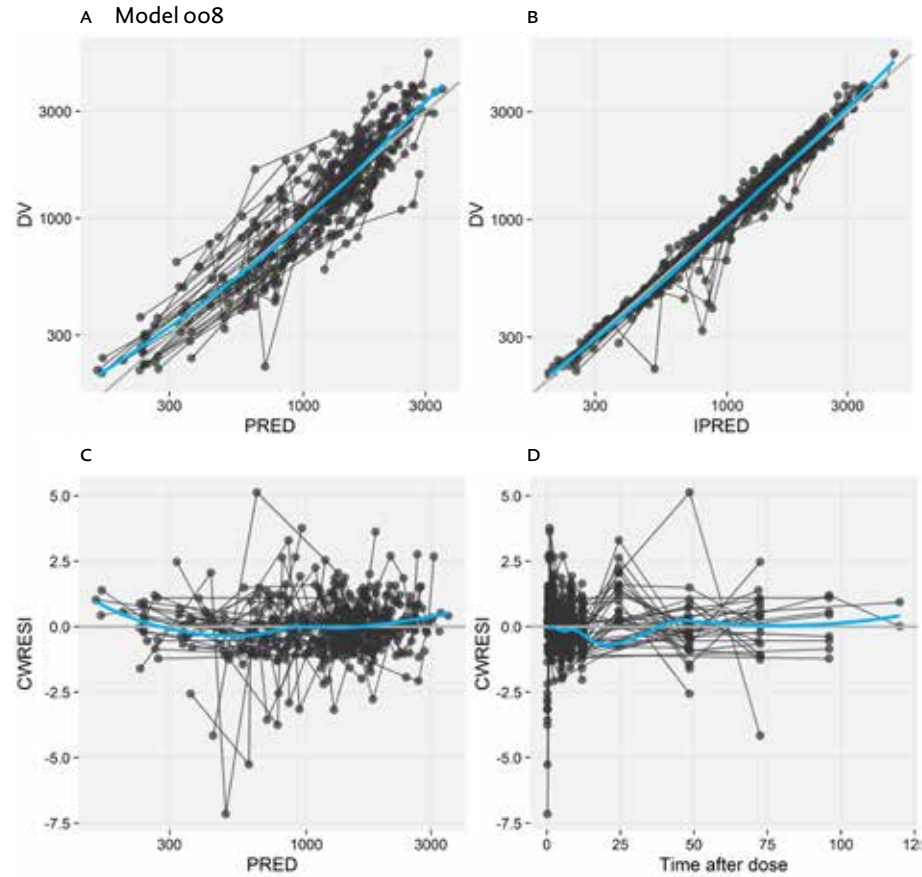


**FIGURE 2 Pharmacodynamics versus concentration SGM-101.** Simulated SGM-101 concentrations at the time of surgery identified a narrow concentration range, where an overlap in TBR was seen between the different dose levels. This was the case for both *in vivo* and *ex vivo* measurements. Higher doses did not lead to higher TBRs.




**SUPPLEMENTARY FIGURE 1 Population pharmacokinetic model Goodness-of-fit.** This figure demonstrates the PK model was able to capture the general trend and variability in the data over time for all cohorts. The population and individual predictions were scattered closely around the line of unity and no bias over the different cohorts were identified.



PART 3

**SUMMARY AND  
APPENDICES**



Chapter VIII

**SUMMARY AND  
GENERAL DISCUSSION**



## SUMMARY

Fluorescence guided surgery is a technique that has widely been implemented and investigated over the last decade, and has repetitively revealed to be a vital tool during surgery. However, the process of adopting this technique into standard of care along with developing and translating novel fluorescent agents into the clinic has proven to take time. Preclinical studies that have been validated several years ago have now slowly been making the transition into the surgical field to be appraised in patients.

This thesis mainly focused on the clinical translation of ZW800-1 and CRGD-ZW800-1 which were developed for the intraoperative imaging of the ureters and colon cancer, respectively. Furthermore, this thesis focused on the further appraisal of a previously studied tumor-targeted fluorescent antibody (SGM-101) for the intraoperative imaging of primary, recurrent and metastasized colorectal cancer.

### **PART I: Clinical translation of novel zwitterionic agents**

Over the last few years, significant progress has been made in the development of new agents for the fluorescence imaging of malignancies and vital structures. The first part of the thesis demonstrates the roadmap of translating fluorescent agents, from preclinical development and validation, into phase I/II clinical trials. It specifically focusses on the clinical translation of the zwitterionic fluorophore, ZW800-1, and its conjugation to a peptide, resulting in the tumor-targeted agent, CRGD-ZW800-1.

Chapter 2 introduces a general overview of the steps and processes involved in translating novel imaging agents into the clinic. Currently, multiple fluorophores and tumor-specific agents have entered clinical trials, where feasibility have been established for multiple cancer types. The clinical translation is an essential part in the evolution of fluorescence guided surgery. Most of the phase I/II clinical trials are primarily designed to demonstrate safety and feasibility of the agent, and often comprises of small subject populations. Phase I studies often include healthy volunteers and are planned into cohorts using commonly accepted number of subjects, usually consisting of 5-6 subjects per cohort. The sample size in early Phase II patient studies are often not based on statistical power considerations due to the exploratory nature of the study. Yet, despite the small subject numbers, these phase I/II studies consistently provide sufficient preliminary data regarding safety and feasibility of an agent for the design of subsequent larger studies. Nevertheless, at this point fluorescence guided surgery is gradually advancing into the next phase where multicenter phase III trials are being performed to:

- achieve wide-spread use of the technique and
- illustrate patient benefit in larger patient populations, which are important steps for regulatory bodies to approve novel agents and use in standard of care.

Chapter 3 is a great example of a study where the roadmap of clinically translating ZW800-1 is described and evaluated. ZW800-1 is a zwitterionic non-targeted fluorophore with an exclusive renal clearance and peak emission around 800 nm. Because of its extraordinary clearance pattern and established high quantum yield, it was opted as a suitable imaging agent for enhancing and visualizing the ureters during surgery. Preclinical animal studies recognized a high fluorescent signal in the ureters within minutes after intravenous administration of ZW800-1. Subsequently, the performed first-in human (phase I) and first-in-patient (phase II) studies demonstrated safety in doses up to 5 mg ZW800-1 and a promising pharmacokinetic profile. In patients undergoing laparoscopic lower abdominal surgery, a low dose of 1 mg or 2.5 mg ZW800-1 revealed to be useful in detecting the ureters during laparoscopic surgery. Within a few minutes after intravenous administration, intraoperative ureter detection was possible for at least one to three hours, depending on the dose given. Due to its pharmacokinetic properties and ultralow non-specific background binding, ZW800-1 allowed fast real-time anatomic and functional imaging of the ureters during laparoscopic abdominopelvic surgeries, and hence potentially decrease iatrogenic urethral injury. Another important advantage of this zwitterionic fluorophore is that it is optimally suitable for conjugation to numerous targeting moieties, such as ligands, peptides and antibodies, to create endless possibilities of targeted agents.

In Chapter 4, one of these conjugated agents is evaluated, where the peptide CRGD is conjugated to the fluorophore ZW800-1, resulting in the agent CRGD-ZW800-1. CRGD is a clinically well-known peptide that binds to integrins expressed on tumor cells and tumor-associated endothelium associated with neoangiogenesis, such as  $\alpha v \beta 6$ ,  $\alpha v \beta 3$  and  $\alpha v \beta 5$ . This chapter describes the development, preclinical validation and clinical translation of CRGD-ZW800-1 for the intraoperative fluorescence detection of colon cancer. CRGD-ZW800-1 was safe in both the phase I and II studies and revealed to be a viable tool for colon cancer detection during open and laparoscopic surgery. Visualization of colon cancer was possible during laparoscopic surgery after an intravenous bolus of 0.05 mg/kg, administered at least 2 hours prior to surgery. Simultaneous ureter imaging is also possible with this dosing interval (2-4 hours). However, longer intervals between injection and imaging (e.g. administering CRGD-ZW800-1

the day prior to surgery, approximately 18 hours prior to surgery) improved tumor fluorescence, most likely due to reduced background signals because of clearance. The study also showed that colon lymph node metastases were detectable with CRGD-ZW800-1 during *ex vivo* fluorescence analysis. Hence, CRGD-ZW800-1 is a promising agent for colon cancer imaging and can be implemented as a multipurpose agent, since different tumor types have ubiquitous overexpression of various  $\alpha v \beta$  integrins.

## **PART II: Fluorescence imaging with SGM-101**

The second part of the thesis specifically focused on the tumor-specific fluorescent antibody, SGM-101, which has previously been demonstrated to be an adequate agent for colorectal cancer imaging (Boogerd et al).

In Chapter 5, a dose-finding study is described where different doses and administration intervals of SGM-101 are evaluated to find the most optimal dosing regime for intraoperative fluorescence imaging of primary and recurrent colorectal cancer. The dose 10 mg SGM-101 administered four days prior to surgery, showed the highest tumor-to-background ratio (TBR) and effectiveness. Results showed a sensitivity of 96% and a negative predicate value of 94% for tumor detection. SGM-101 enabled fluorescence in primary and recurrent tumors, but it was also discovered that it did not show fluorescence in patients with a pathological complete response after neoadjuvant therapy, suggesting a great potential for surveillance programs. More importantly, SGM-101 was able to detect additional malignant lesions that were primarily invisible with the naked eye. These lesions were only detectable with fluorescence, resulting in additional resections or surgical plan alterations in 24% of the patients.

Following Chapter 5, Chapter 6 presents a multicentre pilot study investigating the role of SGM-101 during cytoreductive surgery and hyperthermic intraperitoneal chemotherapy (HIPEC) in peritoneally metastasized colorectal cancer. SGM-101 was able to correctly change the peritoneal carcinomatosis index (PCI) in four of the 14 included patients (28%) due to fluorescence imaging, resulting in completer cytoreductive surgery. The pilot study established that the use of fluorescence with SGM-101 was feasible in peritoneally metastasized colorectal cancer, allowing adequate intraoperative detection of small tumor deposits and alterations of the PCI. However, both studies (Chapter 5 and 6) exposed a relatively high false positive rate of SGM-101, which is a possible limitation of this agent. This limitation is most likely caused by the 700 nm peak emission of the agent, which is a well-known drawback as this goes together with increased background autofluorescence and decreased penetration depth. However, despite this, the results accentuated the potential of SGM-101 and designated a

fundamental base for the multinational phase III study, which enrolled the first patients in June 2019.

Chapter 7 presents a quantification of the pharmacokinetic (PK) and pharmacodynamic (PD) properties of SGM-101. The developed PK model was able to capture the general trend in data and revealed that longer intervals between administration and surgery (imaging) has its advantages, but also important limitations. The PK model showed narrow concentration ranges at the time of surgery of the different SGM-101 doses studied (5 mg, 7.5 mg, 10 mg, 12.5 mg, 15 mg), with an overlap in TBR between the different dose levels. In all dosing cohorts, tumor fluorescence could be perceived. Yet, for a better understanding of a possible PK/PD relationship, more blood samples are needed spread out over a longer period of time after administration.

## **DISCUSSION AND FUTURE PERSPECTIVES**

This thesis presents the different possibilities of fluorescence imaging during open and minimal invasive surgery with non-targeted and tumor-targeted agents. Fluorescence imaging is primarily employed to aid in the visualization of vital structures and the detection of primary, recurrent or metastasized malignancies.

Fluorescence guided surgery is a rapidly evolving technique, yet the mainstream of completed clinical trials consist of early phase I/II studies which primarily aimed at evaluating the safety and feasibility of an agent, as well as estimating the optimal imaging dose. The proof of principle of fluorescence imaging for real-time tumor detection has previously been demonstrated for different agents and cancer types, such as ovarian cancer, lung cancer, head-and-neck cancer, pancreatic cancer, colorectal cancer and liver and peritoneal metastases<sup>1-7</sup>. The application of fluorescence with a carcinoembryonic antigen (CEA)-specific agent, like SGM-101, can improve the detection of peritoneal lesions during cytoreductive surgery, which consequently can result in improved survival (this thesis). Multiple studies have also confirmed that fluorescence imaging can be helpful in visualizing vital structures, such as the biliary tract<sup>8</sup> and ureters (this thesis). Furthermore, the use of fluorescence on the back table has proven to be supportive in providing additional information on surgical resection margins (this thesis). Although all studies have shown promising results, it is important to substantiate results with larger pivotal studies. Nevertheless, this is also mandatory to further demonstrate the safety, effectiveness and validation of patient benefit to support a marketing application. Currently, SGM-101 is the only fluorescent agent discussed in this thesis that is currently being pursued in

a phase III multicenter trial in patients with primary, recurrent and metastatic colorectal cancer, to prove the added value in terms of resection margins and the detection of additional lesions.

The field of fluorescence guided surgery has undergone considerable advances in the development of commercially available NIR imaging systems and tumor-specific agents to improve the precision of tumor resections. In comparison to traditional imaging modalities, fluorescence imaging is unique in its ability to provide real-time feedback to the surgeon during surgery. Fluorescence imaging during oncologic resections usually consists of three components: intraoperative imaging before initial resection to detect the location and extent of the tumor, imaging of the surgical field after resection to detect any remaining fluorescence, and imaging on the back table to assess the specimens' dissection planes, thus margin discrimination. These three components steadily provide tremendous information during the surgical setting, where the decision making is crucial. Given the significant clinical implications of fluorescence imaging, general consensus on standardized protocols are needed to facilitate the design of suitable clinical trials and swift regulatory approval. It is important to design these trials in a manner where data on safety and efficacy can efficiently be obtained to prove patient benefit. Regulatory bodies do not specifically require direct measurement of survival endpoints to show benefit, but often want the studies to demonstrate that fluorescence imaging improves the detection of positive resection margins, since the correlation between tumor free margins and survival is already established. Yet, it is also important to assure standardization of NIR imaging systems, to make sure all available imaging systems are adequately sensitive and that fluorescence can accurately be quantified. This is considered important because this field requires the finest combination of both the NIR imaging device and fluorescent agent for optimal imaging.

On another note, it is important to realize that surgery has undergone multiple advancements in the past decades, where the use of minimal invasive surgery, such as robotic-assisted or laparoscopic surgery, has increased drastically. Minimal invasive surgery has proven to improve patient outcomes, but directly also created new challenges for the surgeon, such as the absence of tactile feedback and limitations in the field of view. During open surgery, surgeons have their visual and tactile feedback mechanism to distinguish between different types of tissue, where the consistency of tissue can give a surgeon a lot of information. Since the tactile feedback is absent during minimal invasive surgery, alternate techniques are expected to guide surgeons during resections. Therefore, fluorescence imaging has been gaining popularity for visual enhancement, as it can also simultaneously highlight vital structures adjacent to tumor tissue.

Such fluorescent agents, like CRGD-ZW800-1, have already been developed and clinically evaluated (this thesis). However, a combination of two different fluorophores or agents could also be a possibility, which is currently being assessed by our study group. Intraoperative guidance is essential to surgeons, since complete removal of tumor tissue and avoiding damage to essential structures are mandatory for prolonged survival and improved patient outcomes.

As presented by the studies in this thesis, intraoperative fluorescence imaging can revolutionize current surgical standards, since it leads to real-time feedback with a direct and immediate effect on patient care and decision-making. Despite remarkable developments in phase I/II clinical trials, the technique needs to be translated into broader and larger multicenter phase III studies for approval in standard of care. Our study group made a big leap in 2019 when we designed and commenced our first phase III clinical trial. This indicates that one of the major hurdles has been overcome, commencing a new influential era of fluorescence guided surgery. While this is one of the main steps for marketing approval and introduction to standard of care, it nonetheless remains important to design and perform solid early phase I/II trials to facilitate the design of future phase III studies. The future of fluorescence imaging seems promising, but for the growth of this technique, it is important to continuously demonstrate the benefit of fluorescence imaging in clinical trials and broaden its applicability for a wider implementation in standard of care.

## REFERENCES

- 1 Boogerd LSF, Hoogstins CES, Schaap DP, et al. Safety and effectiveness of SGM-101, a fluorescent antibody targeting carcinoembryonic antigen, for intraoperative detection of colorectal cancer: a dose-escalation pilot study. *Lancet Gastroenterol Hepatol.* 2018;3(3):181-191.
- 2 Hoogstins CES, Boogerd LSF, Sibinga Mulder BG, et al. Image-Guided Surgery in Patients with Pancreatic Cancer: First Results of a Clinical Trial Using SGM-101, a Novel Carcinoembryonic Antigen-Targeting, Near-Infrared Fluorescent Agent. *Ann Surg Oncol.* 2018;25(11):3350-3357.
- 3 Hoogstins CE, Tummers QR, Gaarenstroom KN, et al. A Novel Tumor-Specific Agent for Intraoperative Near-Infrared Fluorescence Imaging: A Translational Study in Healthy Volunteers and Patients with Ovarian Cancer. *Clin Cancer Res.* 2016;22(12):2929-2938.
- 4 Boogerd LS, Handgraaf HJ, Lam HD, et al. Laparoscopic detection and resection of occult liver tumors of multiple cancer types using real-time near-infrared fluorescence guidance. *Surg Endosc.* 2017;31(2):952-961.
- 5 Schaafsma BE, Mieog JS, Hutteman M, et al. The clinical use of indocyanine green as a near-infrared fluorescent contrast agent for image-guided oncologic surgery. *J Surg Oncol.* 2011;104(3):323-332.
- 6 Predina JD, Newton AD, Connolly C, et al. Identification of a Folate Receptor-Targeted Near-Infrared Molecular Contrast Agent to Localize Pulmonary Adenocarcinomas. *Mol Ther.* 2018;26(2):390-403.
- 7 Newton AD, Predina JD, Nie S, Low PS, Singhal S. Intraoperative fluorescence imaging in thoracic surgery. *J Surg Oncol.* 2018;118(2):344-355.
- 8 Ishizawa T, Bandai Y, Ijichi M, Kaneko J, Hasegawa K, Kokudo N. Fluorescent cholangiography illuminating the biliary tree during laparoscopic cholecystectomy. *Br J Surg.* 2010;97(9):1369-1377.

## Chapter IX

### **NEDERLANDSE SAMENVATTING**

## SAMENVATTING

Fluorescentie geleide chirurgie is een techniek die de afgelopen jaren op grote schaal is geïmplementeerd en onderzocht, waarbij herhaaldelijk is gebleken dat het tijdens de operatie een goed hulpmiddel is. Het is een techniek die wordt toegepast om op een selectieve manier belangrijke anatomische structuren en tumorweefsel te kunnen laten oplichten tijdens de operatie. Het standaard kunnen toepassen van deze techniek in de zorg en het verder ontwikkelen van nieuwe fluorescente middelen kost echter veel tijd. Preklinische studies, inclusief dierproeven, die enkele jaren geleden zijn uitgevoerd en gevalideerd, hebben nu pas de overgang gemaakt naar de kliniek om bij patiënten geëvalueerd te worden. Dit proefschrift heeft zich met name gericht op de klinische translatie van ZW800-1 en CRGD-ZW800-1, die respectievelijk ontwikkeld zijn voor de intra-operatieve beeldvorming van de ureters en colorectaal carcinoom. Verder richtte dit proefschrift zich op de verdere beoordeling van een eerder bestudeerd tumor-specifiek fluorescent antilichaam (SGM-101) voor de beeldvorming van primair, recidief en gemetastaseerd colorectaal carcinoom.

### DEEL I: Klinische translatie van nieuwe middelen

De afgelopen jaren is er aanzienlijk vooruitgang geboekt in de ontwikkeling van nieuwe middelen voor fluorescentie geleide chirurgie. Het eerste deel van het proefschrift presenteert het proces van het klinisch translateren van nieuwe middelen, vanaf preklinische ontwikkeling en validatie tot aan klinische fase I/II onderzoeken. Het richt zich in het bijzonder op de klinische translatie van de zwitterionische fluorofoor, ZW800-1, en de conjugatie ervan met een peptide, resulterend in het tumor-gerichte middel, CRGD-ZW800-1.

Hoofdstuk 2 introduceert een algemeen overzicht van de stappen en processen die betrokken zijn bij het translatie proces naar de kliniek. Momenteel worden meerdere fluoroforen en tumor-specifieke middelen in klinische onderzoeken onderzocht om de veiligheid en haalbaarheid in verschillende tumorsoorten te evalueren. Het klinisch translatie proces is een essentieel onderdeel in de evolutie van fluorescentie geleide chirurgie. De meeste klinische fase I/II onderzoeken zijn voornamelijk ontworpen om de veiligheid en haalbaarheid van een middel aan te tonen, en bestaan vaak uit een klein aantal proefpersonen. Fase I studies worden vaak bij gezonde vrijwilligers uitgevoerd, met ongeveer 5-6 proefpersonen per cohort. In de opeenvolgende fase II studies, wordt een studie vaak opgezet met een exploratief karakter waarbij de patiënten populaties vaak niet worden gebaseerd op statistiek maar meestal een 3+3 design wordt gebruikt. Ondanks de kleine aantal proefpersonen, leveren de fase I/II

onderzoeken structureel voldoende informatie over de veiligheid en haalbaarheid van een middel voor het opzetten van grotere vervolgstudies. Desalniettemin vordert de fluorescentie geleide chirurgie geleidelijk naar de volgende fase, waarin multicenter fase III onderzoeken worden uitgevoerd om 1) een mondiaal gebruik van de techniek te bewerkstelligen en 2) het voordeel voor de patiënt aan te tonen in een grotere patiëntenpopulatie, wat een belangrijke stap is voor de bevoegde instanties om nieuwe fluorescente middelen te kunnen goedkeuren en gebruiken in standaardzorg.

Hoofdstuk 3 is een goed voorbeeld van een studie waarin het stappenplan van de klinische translatie van ZW800-1 wordt beschreven en geëvalueerd. ZW800-1 is een zwitterionisch niet-specifiek fluorofoor met een exclusieve renale klaring en een piekemissie rond de 800 nm. Vanwege de klaring door de nier en hoog fluorescentie signaal, werd het uitgekozen als een geschikt middel voor het visualiseren van de ureters tijdens laparoscopische chirurgie. Dierproeven lieten een intensief fluorescent signaal zien in de ureters enkele minuten na intraveneuze toediening van ZW800-1. Vervolgens hebben de uitgevoerde fase I (gezonde vrijwilligers) en fase II (patiënten) studies laten zien dat doseringen tot 5 mg ZW800-1 goed werden verdragen en werd daarnaast een optimaal farmacokinetisch profiel gezien met snelle renale klaring. Bij patiënten die een laparoscopisch abdominale ingreep ondergingen, bleek een lage dosering van 1 mg of 2,5 mg ZW800-1 voldoende te zijn voor het detecteren van de ureters tijdens de operatie. Enkele minuten na intraveneuze toediening was het mogelijk om intra-operatief de ureters te detecteren gedurende een periode van ten minste 1 tot 3 uur, afhankelijk van de gegeven dosering. Vanwege de farmacokinetische eigenschappen en niet-specifieke achtergrondbinding, zorgde ZW800-1 voor een snelle ('real-time') anatomische en functionele informatie over de ureters tijdens laparoscopische chirurgie, waarmee iatrogen letsel potentieel kan worden verminderd. Een ander belangrijk voordeel van dit fluorofoor is dat het optimaal geschikt is voor conjugatie aan bijvoorbeeld liganden, peptiden en antilichamen, om eindeloze mogelijkheden te creëren van tumor-gerichte middelen.

In Hoofdstuk 4 wordt een van deze geconjugeerde middelen geëvalueerd, waarbij het peptide CRGD geconjugeerd is aan ZW800-1, resulterend in het middel CRGD-ZW800-1. CRGD is een klinisch bekend peptide dat aan integrines bindt die tot expressie komen op tumorcellen en tumor-geassocieerd endotheel, zoals  $\alpha v \beta 6$ ,  $\alpha v \beta 3$  en  $\alpha v \beta 5$ . Dit hoofdstuk beschrijft de ontwikkeling, preklinische validatie en klinische translatie van CRGD-ZW800-1 voor de intra-operatieve detectie van colon carcinoom. CRGD-ZW800-1 was veilig in zowel de fase I en II studies en bleek een goed hulpmiddel te zijn voor de detectie van colon carcinoom tijdens open en laparoscopische colon chirurgie. Visualisatie van colon carci-

noom tijdens laparoscopie was mogelijk na een intraveneuze bolusinjectie van 0.05 mg/kg, ten minste 2 uur voor de operatie. Tevens is simultane beeldvorming van de ureters mogelijk binnen dit tijdsinterval (2-4 uur). Langere intervallen tussen injectie en beeldvorming (bijvoorbeeld toediening van CRGD-ZW800-1 de dag voor de operatie, ongeveer 18 uur van tevoren) liet een verbeterd fluorescentie signaal zien in de tumor, waarschijnlijk als gevolg van verminderd achtergrondsignaal door de klaring. De studie liet ook zien dat lymfeklier metastasen detecteerbaar zijn met CRGD-ZW800-1 tijdens *ex vivo* fluorescentieanalyse. Dit maakt CRGD-ZW800-1 een veelbelovend middel voor de intra-operatieve beeldvorming van colon carcinoom en kan worden geïmplementeerd als een multifunctioneel middel, aangezien verschillende tumortypen een over expressie hebben van verschillende  $\alpha\beta$  integrines.

## DEEL II: Fluorescentie beeldvorming met SGM-101

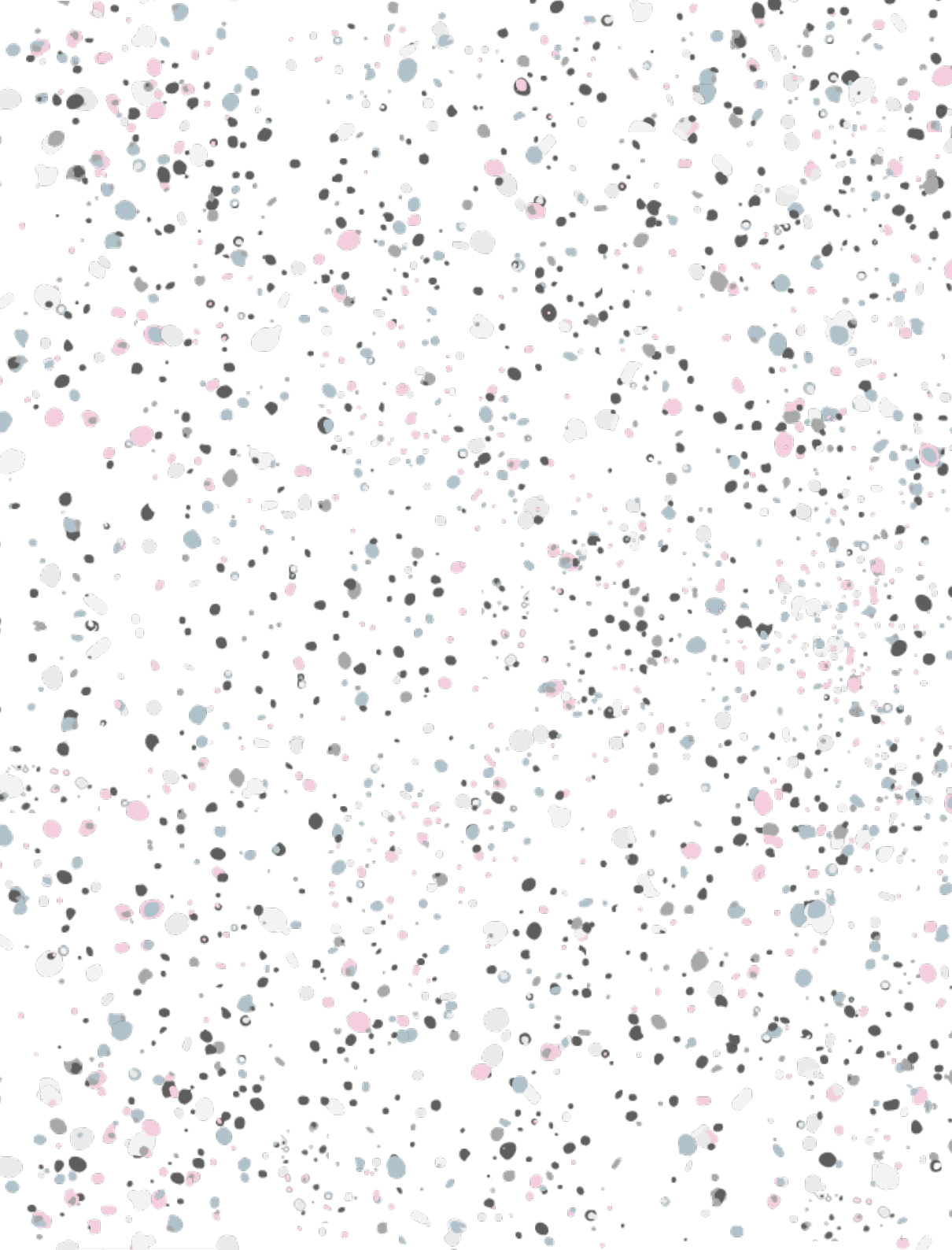
Het tweede deel van het proefschrift richt zich op het tumor-specifiek fluorescent antilichaam, SGM-101, waarvan eerder is aangetoond dat het potentieel een middel is voor beeldvorming van colorectaal carcinoom (Boogerd et al).

In Hoofdstuk 5 wordt een dosisbepalingsstudie beschreven waarin verschillende doseringen en toedieningsintervallen van SGM-101 zijn geëvalueerd om het meest optimale doseringsregime te vinden voor de intra-operatieve beeldvorming van primair en recidief colorectaal carcinoom. De dosering van 10 mg SGM-101, toegediend vier dagen voor de operatie, toonde de hoogste 'tumor-to-background ratio' (TBR) en effectiviteit aan. De resultaten lieten een sensitiviteit van 96% zien en een negatief voorspellende waarde van 94% voor tumordetectie. SGM-101 maakte fluorescentie mogelijk in primair en recidiverende colorectaal tumoren, maar liet ook zien dat er geen fluorescentie zichtbaar was in patiënten met een pathologisch compleet respons na neoadjuvante chemoradiotherapie. De studie liet een ander belangrijk voordeel zien van SGM-101, dat het namelijk extra maligne laesies kon detecteren die onzichtbaar waren met het blote oog. Deze laesies waren alleen detecteerbaar met fluorescentie, en heeft bij 24% van de patiënten tot een extra resectie of veranderingen in het chirurgisch plan geleid.

Aansluitend aan Hoofdstuk 5, beschrijft Hoofdstuk 6 een pilotstudie die de rol van SGM-101 onderzoekt tijdens cytoreductieve chirurgie en hyperthermische intraperitoneale chemotherapie (HIPEC) bij peritoneaal gemetastaseerd colorectaal carcinoom. SGM-101 was in staat om de peritoneale carcinoom-index (PCI) correct te veranderen bij vier van de 14 geïncludeerde patiënten (28%) ten gevolge van fluorescentie, wat heeft geresulteerd in completere cytoreductieve chirurgie. De pilotstudie heeft laten zien dat het gebruik van

fluorescentie met SGM-101 haalbaar is bij peritoneaal gemetastaseerd colorectaal carcinoom, met adequate intra-operatieve detectie van kleine tumordeposities en veranderingen van de PCI. In beide onderzoeken (hoofdstuk 5 en 6) werd echter relatief veel vals positieven gevonden, wat een mogelijke beperking is van SGM-101. De beperking is zeer waarschijnlijk te wijten aan de piekemissie van het middel bij 700 nm. Rond deze golflengte is er een grote kans op autofluorescentie waardoor er hoger signaal ontstaat van de achtergrond en verder is bij deze golflengte een verminderde diepte penetratie. Desondanks laten de resultaten van beide studies de voordelen van SGM-101 zien en vormden ze een fundamentele basis voor de internationale fase III studie, welke in juni 2019 de eerste patiënten heeft geïncludeerd.

Hoofdstuk 7 beschrijft de farmacokinetische (PK) eigenschappen van SGM-101 door gebruik te maken van een populatiemodel. Met deze aanpak is het mogelijk om de gegevens van alle deelnemers die ooit SGM-101 ontvingen te combineren en integraal te analyseren. De analyse toonde aan dat langere intervallen tussen toediening en operatie (beeldvorming) voordelen hebben, maar ook belangrijke beperkingen. Het PK model liet zien dat op het moment van de operatie een nauw concentratiebereik is van de bestudeerde SGM-101 doseringen (5 mg, 7.5 mg, 10 mg, 12.5 mg, 15 mg) met een overlap in TBR. Met alle doseringen was tumor fluorescentie waargenomen. Echter, voor een betere evaluatie van de PK zijn meer bloedmonsters nodig, verspreid over een langere periode na toediening. Idealiter zou ook meer gedetailleerde informatie beschikbaar moeten zijn over de betekenis van *in vitro* maten zoals de bindingsconstante van SGM-101 aan gezond en tumorweefsel om beter inzicht te krijgen in de onderliggende factoren die de TBR bepalen.



## CURRICULUM VITAE

Kim Samita de Valk was born on November 9th 1989 in Bangkok, Thailand. Due to her father's work she lived and grew up in Thailand, Venezuela, the Netherlands and the United States of America (USA). In 2008, she graduated with an International Baccalaureate (IB) diploma from the Washington International School, in Washington D.C, USA. After graduating high school in the United States, she moved back to the Netherlands to study Medicine at the Erasmus University in Rotterdam. In 2015, she successfully achieved her medical degree (MD) and started working as a surgical resident at IJsselland Hospital in Capelle a/d IJssel. After one year of surgical work experience, she started a PhD trajectory at the Image-Guided Surgery group under supervision of dr. A.L. Vahrmeijer (co-promotor) and Prof.dr. J. Burggraaf (promotor) at the Department of Surgery at Leiden University Medical Center (LUMC) and the Centre for Human Drug Research (CHDR). Her research aimed at clinically translating novel fluorescent agents for the intraoperative imaging of vital structures, such as the ureters, and gastrointestinal tumors, with colorectal cancer in specific. Due to the unique collaboration between the LUMC and CHDR, she performed several phase I studies in healthy volunteers at CHDR and phase II studies in (oncologic) patients at hospitals such as LUMC and Catherina Hospital in Eindhoven. After finishing her PhD trajectory, Kim shortly went back to work as a surgical resident at Haaglanden Medical Center in The Hague, before deciding to pursue a clinical career in urology. Currently, Kim is working as a urology resident at the urology department at the Erasmus Medical Center in Rotterdam.

## LIST OF PUBLICATIONS

**de Valk KS**, Deken MM, Schaap DP, Meijer RP, Boogerd LS, Hoogstins CE, van der Valk MJ, Kamerling IM, Bhairosingh SS, Framery B, Hilling DE, Peeters KC, Holman FA, Kusters M, Rutten HJ, Cailler F, Burggraaf J, Vahrmeijer AL. *Dose-finding study of a CEA-targeting agent, SGM-101, for intraoperative fluorescence imaging of colorectal cancer*. *Ann Surg Oncol*. 2021 Mar;28(3):1832-1844.

Meijer RP, **de Valk KS**, Deken MM, Boogerd LS, Hoogstins CE, Bhairosingh SS, Swijnenburg RJ, Bonsing BA, Framery B, Sarasqueta AF, Putter H, Hilling DE, Burggraaf J, Cailler F, Mieog JS, Vahrmeijer AL. *Intraoperative detection of colorectal and pancreatic liver metastases using SGM-101, a fluorescent antibody targeting CEA*. *Eur J Surg Oncol*. 2021 Mar;47(3 Pt B):667-673.

Faber RA, Verbeek FP, **de Valk KS**, Vahrmeijer AL, Mieog JS. *A Systematic Review of Clinically Available and Experimental Dyes for Intraoperative Near-Infrared Fluorescence Imaging of the Ureters During Laparoscopic Surgery*. *Laparosc Surg*. 2021;5:4.

Deken MM, van Doorn HC, Verver D, Boogerd LS, **de Valk KS**, Rietbergen DD, van Poelgeest MI, de Kroon CD, Beltman JJ, van Leeuwen FW, Bosse T, Putter H, Braak JP, de Geus-Oei LF, van de Velde CJ, Burggraaf J, Vahrmeijer AL, Gaarenstroom KN. *Near-infrared fluorescence imaging compared to standard sentinel lymph node detection with blue dye in patients with vulvar cancer – a randomized controlled trial*. *Gynecol Oncol*. 2020 Dec;159(3):672-680.

**de Valk KS**, Deken MM, Handgraaf HJ, Bhairosingh SS, Bijlstra OD, van Esdonk M, Terwisscha van Scheltinga AG, Valentijn AR, March TL, Vuijk J, Peeters KC, Holman FA, Hilling DE, Mieog JS, Frangioni JV, Burggraaf J, Vahrmeijer AL. *First-in-Human Experience with cRGD-ZW800-1 a Zwitterionic Integrin-Targeted Near-Infrared Fluorescent Agent in Colon Carcinoma*. *Clin Canc Res*. 2020 Aug 1;26(15):3990-3998.

Schaap DP\*, **de Valk KS\***, Deken MM, Meijer RP, Burggraaf J, Vahrmeijer AL, Kusters M. *Carcinoembryonic antigen-specific, fluorescent image-guided cytoreductive hyperthermic intraperitoneal chemotherapy for metastatic colorectal cancer*. *Br J Surg*. 2020 Mar;107(4):334-337.

Meijer RP, **de Valk KS**, Framery B, Gutowski M, Pelegrin A, Cailler F, Hilling DE, Vahrmeijer AL. *The clinical translation of a near-infrared fluorophore for fluorescence guided surgery: SGM-101 from the lab to a phase III trial*. *Proceedings Volume 11222, Molecular-Guided Surgery: Molecules, Devices, and Applications vi*. 2020 Feb 19.

**de Valk KS\***, Handgraaf HJ\*, Deken MM, Sibinga Mulder BG, Valentijn AR, Terwisscha van Scheltinga AG, Kuil J, van Esdonk M, Vuijk J, Bevers RF, Peeters KC, Holman FA, Frangioni JV, Burggraaf J, Vahrmeijer AL. *A Zwitterionic near-infrared fluorophore for real-time ureter identification during laparoscopic abdominopelvic surgery*. *Nat Commun*. 2019 Jul 16;10(1):3118.

**de Valk KS**, Vahrmeijer AL. *The Clinical translation of novel near-infrared fluorophores for fluorescence guided surgery*. *Proceedings volume 10862, Molecular-Guided Surgery: Molecules, Devices and Applications V*. 2019 Mar 7.

Dulfer RR\*, **de Valk KS\***, Gilissen F, van Ginhoven TM, Smit PC. *Introduction of daycare thyroid surgery in a Dutch non-academic hospital*. *Neth J Med*. 2016 Nov;74(9):395-400.





